Investigation into key molecular pathways in the pathogenesis of cutaneous melanoma

Ewan R. S. Brown

Thesis presented for the degree of PhD

The University of Edinburgh

2009

Table of contents

Declaration

I hereby declare that this thesis has been composed by me and it has not been accepted in any previous applications for a degree at this time or at any other university. The work described has been performed by me, except where expressly indicated otherwise. All sources of information have been specifically acknowledged. The experiments were designed in collaboration with my supervisor Prof. David W. Melton.

Acknowledgements

I am extremely grateful to Prof. David Melton and Prof. John Smyth for support and guidance over the past three years. I would also like to thank Tamasin Doig, Val Doherty, Gillian Smith, Niall Anderson and John Bartlett (and his lab) for lending their expertise and enthusiasm to the tissue microarray project. I owe a big thanks to all those in the Melton lab past and present, particularly Jim Selfridge, Ann-Marie Ritchie, Jennifer Doig, Oliver Maddocks and Liang Song for their help. Finally, I am indebted to my family and especially to Jill for her continued support.

Abstract

An improved understanding of the molecular pathogenesis of melanoma is required in order to develop more effective prevention strategies, define new prognostic markers and to identify new molecular targets for therapy.

The melanocortin-1 receptor (MC1R) plays a key role in pigment production and is a major determinant of skin phototype and sensitivity to UV irradiation. The postulated role of MC1R in protecting melanocytes from apoptosis in response to UV irradiation led to our hypothesis that manipulation of the MC1R may affect growth of melanoma cell lines and sensitivity to DNA damage. A panel of melanoma cell lines were characterised with respect to MC1R sequence, MC1R mRNA expression, presence of BRAF mutations and sensitivity of cell lines to DNA damage-induced apoptosis. Manipulation of MC1R using MC1R ligand, MC1R antibody or MC1R siRNA had no major effect on proliferation or DNA damage-induced apoptosis.

In order to compare the characteristics of melanoma cells in culture with the melanomas from which they were derived, a novel melanoma cell line was established from fresh human metastatic melanoma tissue fragments removed during surgery. The cell line (Edmel 3) was found to retain the morphological characteristics of the tumour from which it was derived (i.e. mixed spindle/epithelioid cells). Subpopulations of cells of different morphology could not be subcloned from the parent cell line. Compared to established cell lines response to DNA damage was delayed and growth as xenografts was considerably slower.

A series of tissue microarrays which included 51 benign naevi, 27 dysplastic naevi, 54 in-situ melanomas, 312 primary melanomas and 64 metastatic melanomas were constructed in order to provide an efficient method of evaluating the expression of proteins at various stages of melanoma progression. A significant fall in B-catenin, bcl-2 and galectin-3 expression between primary and metastatic melanomas and a rise in B-catenin and galectin-3 expression between naevi and dysplastic naevi were found. Correlation of protein expression with clinicopathologic data confirmed that low nuclear galectin-3 expression was associated with poor survival. These findings suggest that nuclear galectin-3 is a novel prognostic marker in primary melanoma.

Abbreviations

AJCC	American joint committee on cancer
APS	ammonium persulfate
cAMP	cyclic adenosine monophosphate
cDNA	complementary DNA
CRUK	Cancer Research UK
Ct	cycle threshold
DAB	diaminobenzidene
DMEM	Dulbecco's Modified Eagle Medium
DMSO	dimethyl sulphoxide
dNTPs	deoxyribonucleoside triphosphates
ECL	enhanced chemiluminescence
EDTA	ethylenediamenetetraacetic acid
FACS	fluorescence activated cell sorting
FCS	foetal calf serum
GAPDH	glyceraldehyde-3-phosphate dehydrogenase
GFP	green fluorescent protein
IBMX	isobutylmethylxanthine
IHC	immunohistochemistry
LMM	lentigo maligna melanoma
MC1R	melanocortin-1-receptor
α-MSH	alpha-melanocyte stimulating hormone
NDP-α-MSH	[NIe4,D-Phe7] alpha-melanocyte stimulating hormone
NEAA	non-essential amino acids
o/n	overnight

PAGE	polyacrylamide gel electrophoresis
PBS	phosphate buffered saline
PCR	polymerase chain reaction
PMSF	phenylmethanesulphonylfluoride
RFLP	restriction fragment length polymorphism
RGP	radial growth phase
RT	reverse transcriptase
SD	standard deviation
SDS	sodium dodecyl sulphate
SEM	standard error of the mean
siRNA	short interfering ribonucleic acid
Taq	thermophilus aquaticus
TEMED	tetramethylethylenediamine
TMA	tissue microarray
TNM	tumour, node, metastases
VGP	vertical growth phase
UVC	ultra violet C
v/v	volume against volume
w/v	weight against volume

Chapter 1 Introduction

1.1 General introduction

Melanoma is the most lethal form of skin cancer and an increasingly common disease worldwide (Tsao et al, 2004). It is a tumour of melanocytes which are cells of neural-crest lineage that are located and evenly distributed in the basal epidermal layer of human skin. Owing to its propensity for vertical growth with deep invasion, many melanomas metastasize. Although the majority of patients with early-stage melanoma enjoy long-term survival following simple surgical excision, patients with metastatic disease have a dismal prognosis. Melanoma is characterised by high resistance to chemotherapy and to date no therapeutic regime has been shown to improve the survival of patients with advanced melanoma in randomized trials (Eggermont and Kirkwood 2004).

Genetic, epidemiological and genomic investigations have uncovered a spectrum of mutations that are associated with melanoma and have identified how some mutations are related to melanoma susceptibility and progression (Rodolfo et al, 2004). There is optimisim that the increased understanding of the genetic changes underlying melanoma development may lead to the development of more effective prevention strategies, the establishment of new classification systems, the identification of new prognostic markers and the establishment of new molecular targets for therapy.

The work presented in this thesis aims to investigate a number of key pathways in the molecular pathogenesis of melanoma. Chapter 3 investigates a key melanoma susceptibility gene, the melanocortin-1 receptor in melanoma, chapter 4 describes the establishment and charcterisation of a novel melanoma cell line and chapter 5 describes the investigation of melanoma progression and prognosis using tissue microarrays.

1.2 Melanocyte function

Melanocytes are specialist pigment cells that are found predominantly in the skin and eyes where they produce melanins, the pigments responsible for skin and hair colour. Cutaneous melanocytes originate from highly motile neural-crest progenitors that migrate to the skin during embryonic development. In the skin, melanocytes reside in the basal layer of the epidermis and in the hair follicles (Figure 1.1).

Melanin production occurs predominantly in a lysosome-like structure known as the melanosome. The two main types of melanin are brown black eumelanin (main type in dark skin and hair) and the red-yellow pheomelanin (main type in red hair and freckled individuals). Both types of melanin derive from a common tyrosinase-dependant pathway with the same precursor, tyrosine. The absence or severe dysfunction of tyrosinase and other key pigment enzymes results in oculocutaneous albinism which presents with intact melanocytes but inability to make pigment (Oetting et al, 2003). Pheomelanin is more photolabile than eumelanin and can produce amongst its by-products, hydrogen peroxide, superoxide and hydroxyl radicals, all known as triggers of oxidative stress (Hill et al, 2000). Individual melanocytes can produce both types of melanin with the ratio dependant on the expression of pigment enzymes and the availability of tyrosine and sulphydral-containing reducing agents in the cell (Land et al, 2000).

Melanin is distributed to surrounding keratinocytes through melanocytic dendritic processes. The formation, maturation and trafficking of melanosomes is crucial to pigmentation and defects in this process can lead to depigmented disorders such as Hermansky-Pudlak Syndrome (Wei 2006). It is commonly believed that melanin is crucial for absorption of free radicals that have been generated within the cytoplasm by UV, and it acts as a direct shield from UV and visible light radiation (Lin and Fisher, 2007).

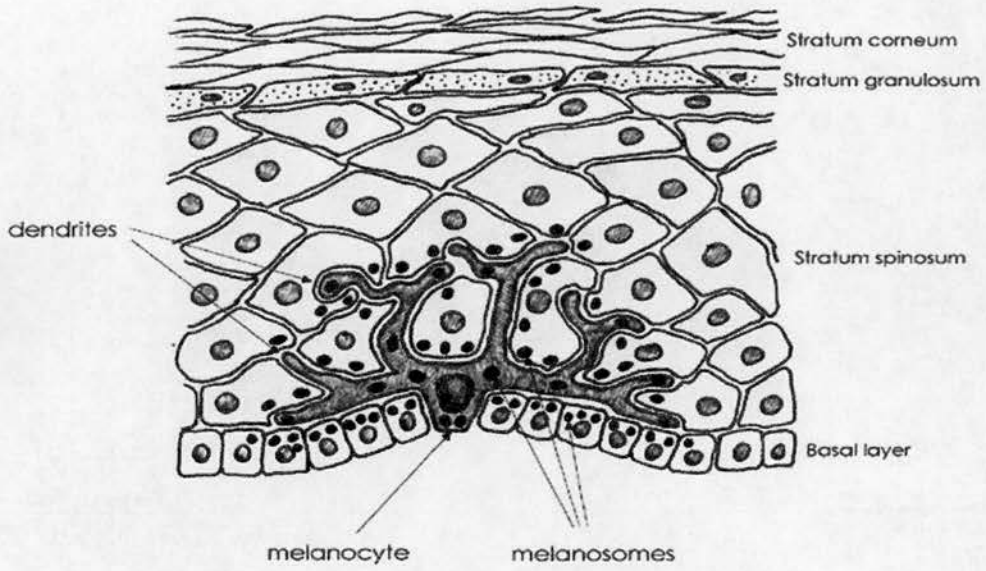

Figure 1.1. Schematic diagram showing the cellular architecture of the epidermis and the relationship between melanocytes and keratinocytes. From Rees 2004.

Ultraviolet radiation causes genetic changes in the skin, impairs cutaneous immune function, increases the local production of growth factors, and induces the formation of DNA-damaging reactive oxygen species that affect keratinocytes and melanocytes (Meyskens et al, 2004). The tanning response is a defensive measure in which melanocytes synthesize melanin and transfer it to keratinocytes where it absorbs and dissipates ultraviolet energy. It is one of the most striking examples of enviormental adaptation in humans and involves a complex interaction between melanocytes and keratinocytes.

Pigmentary response of the skin to UV is determined to a large extent by the amount, type, and arrangement of melanin (Prota 2000). It is now known that keratinocytes secrete various factors in response to UV irradiation that regulate melanocyte survival, differentiation, proliferation and motility, stimulating melanocytes to produce melanin (Eves et al, 2005). The precise underlying mechanism of UV-

induced pigmentation (suntanning) is only now beginning to be established with a recent study suggesting that p53 may play a central role (Cui et al, 2007).

1.3 Melanoma epidemiology, aetiology and prevention

Cutaneous melanoma is the eighth most common cancer in the UK (Cancer Research UK 2006) and is the second commonest in young people (aged 20-39). Scotland has the highest rate of melanoma of any country in the UK and the last 20 years has seen a doubling of melanoma cases (Figure 1.2 A). The commonest site of melanoma is on the legs in females and on the trunk in males (Figure 1.2 B,C). A further 73% rise in Scottish melanoma cases is predicted over the next 10-15 years, the largest increase for any solid tumour (Doherty 2006)).

The highest incidence of melanoma is in parts of the world where fair skinned individuals have high UV exposure such as Queensland, Australia (AIHW 2003). Age-standardised incidence (per 100,000 population) is 41 and 31 for males and females respectively compared to 21.4 and 13.8 in the US and 9.7 and 11.2 in the UK. The basis for the dramatic rise in incidence of melanoma is incompletely understood although the localized degradation of the ozone layer, the increase in solar exposure as a recreational activity, and the immigration of fair-skinned populations into equatorial latitudes each appear to play some causative role (Berwick and Halpern 1997).

The mean age of presentation with melanoma is approximately 55 years (NCI 2008). The principal risk factors for cutaneous melanoma are thought to represent the interplay between genetic factors and exposure to sunlight (Jhappan et al, 2003) and include family history, presence of multiple naevi, geographical location, hair and skin colour and history and pattern of sun exposure.

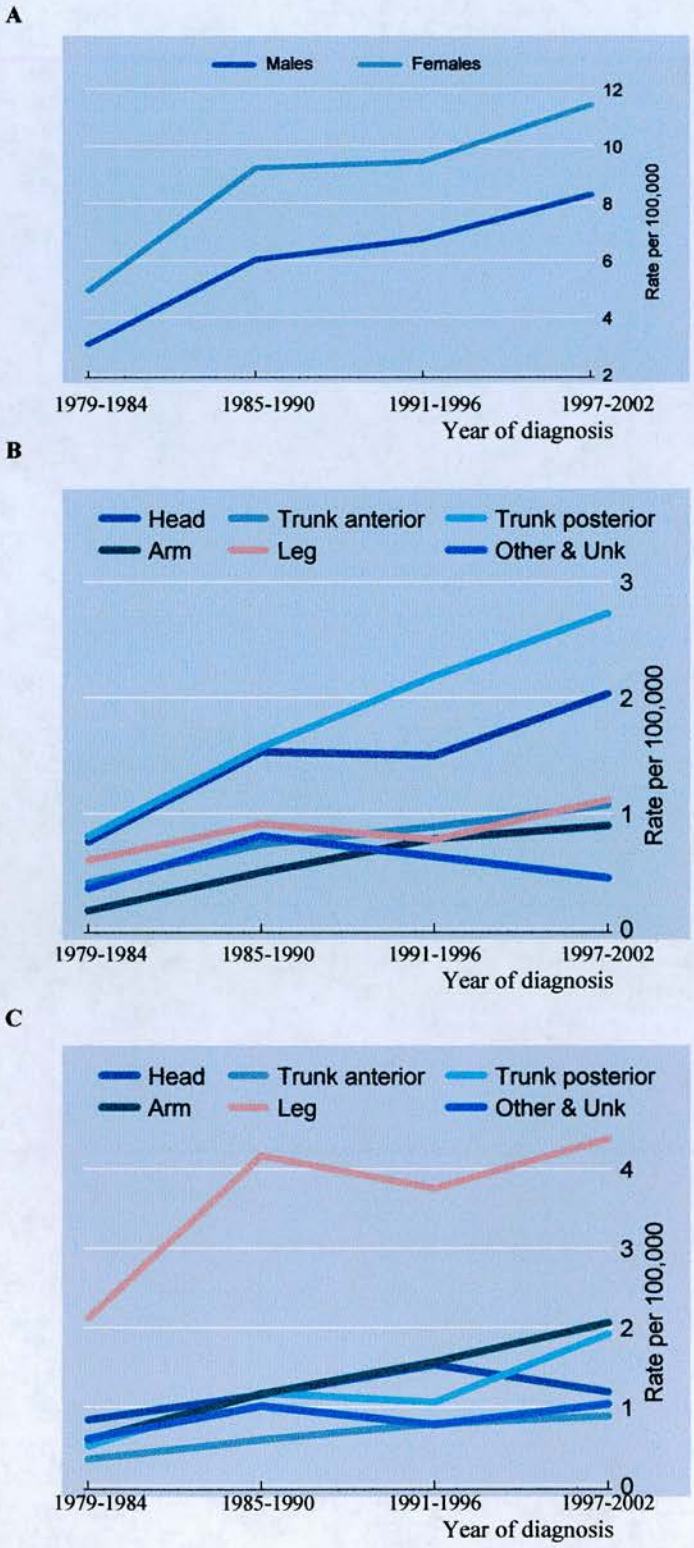

Figure 1.2. Incidence of cutaneous melanoma in South-East Scotland. Incidence rates are shown for 5 year cohorts from 1979-2002. Total population is 1.2 million. **(A)** Overall incidence in Females versus Males. **(B)** Incidence by body site in Males. **(C)** Incidence by body site in Females. Adapted from Doherty 2006. Unk = unknown.

The risk of an individual developing a melanoma is greatly increased if there is a family history of the disease. Only very occasionally, however, is melanoma due to the presence of identifiable heritable mutations in highly penetrant genes (see section on genetic susceptibility to melanoma for further discussion). Melanoma risk is highest in those with fair skin and inability to tan, particularly in those with red hair (Marrett et al, 1992). Freckling and blue eyes also confer a modest increase in risk for melanoma development (Bliss et al, 1995). Some inherited variants of the melanocortin-1 receptor confer increased UV sensitivity and a twofold to fourfold elevation in melanoma risk (Hayward 2003).

The presence of multiple naevi in an individual, whether atypical or not, is a strong marker for melanoma risk irrespective of family history (Berwick and Halpern 1997). A meta-analysis of observational studies found that an individual who has more than 100 common naevi or more than two atypical naevi has a fivefold to 20-fold increased risk of melanoma (Gandini et al, 2005).

Whereas squamous and basal carcinomas appear to be linked to total lifetime sun exposure, melanoma development is most closely associated with intense, intermittent exposure (Armstrong and Kricker, 2001). UV causes many types of mutation, but cytosine-thymine (C-T) and CC-TT are regarded as UV signature mutations. These mutations will however only be seen in melanoma if C residues occur in functionally critical areas of the genome (Povey et al, 2007). The nucleotide excision repair (NER) pathway deals with the main types of UV-induced DNA damage (cyclobutane pyrimidine dimmers and 6-4 photoproducts) and inefficient repair of DNA photoproducts is associated with melanoma risk (Mitchell 1991). This is exemplified by the disease xeroderma pigmentosum (XP), which is characterised by mutations in specific genes involved in the nucleotide excision repair (NER) pathway and is associated with an elevated risk of both melanoma and non-melanoma skin cancer (Kraemer et al, 1994).

Additional evidence for a role of UV induced DNA damage in development of melanoma comes from a number of epidemiological studies; high levels of sunlight in childhood are a strong determinant of melanoma risk (Whiteman et al, 2001); melanoma patients are inefficient in repairing UV induced DNA damage (Wei et al, 2003); and mutations in the melanoma susceptibility gene CDKN2A (which encodes p16 and ARF proteins) reduce the ability of cells to process UV-induced DNA damage, independent of cell cycle effects (Sarkar-Agrawal et al, 2004). Epidemiologic observations suggest that chronic or low-grade exposures to UV induce protection against DNA damage whereas intense, intermittent exposures cause genetic damage (Gilchrest et al, 1999). Although UV irradiation is the key environmental risk factor for melanoma not all melanomas arise on sun-exposed sites and not all mutations identified in melanoma have a UV signature (Thomas et al, 2006). This raises the issue of the importance of other forms of DNA damage and repair pathways in melanoma.

The association of melanoma with use of sun beds is controversial. Some studies have not found sunbed use to be a significant risk whereas others have found small increases in risk (Holly et al, 1995; Westerdahl et al, 1994; Autier 2005).

Primary prevention campaigns aimed at reducing people's exposure to sun were introduced in Australia in the 1980s and adopted elsewhere. There is however no direct evidence that reducing sun exposure has had an effect on melanoma incidence and there has been some recent concern that drastic reduction in sun exposure in temperate climates may have a negative impact on health because of low Vitamin D levels (Bataille et al, 2008). Secondary prevention and screening strategies have not yet been formally assessed although some centres suggest that patients at increased risk of melanoma should be offered screeing by a dermatologist (Newton Bishop et al, 2007).

1.4 Melanoma diagnosis and staging

UK guidance suggests that lesions suspected to be melanoma should be excised completely with a clinical margin of 2mm of normal skin and a cuff of fat (Roberts et al, 2002)). This allows confirmation of the diagnosis by examination of the whole lesion. The Royal College of Pathologists has produced a minimum dataset which defines the histological features of a melanoma that should be included in the histopathology report (Royal College of Pathologists, 2002).

Cutaneous melanomas are usually divided into four clinico-pathologic subtypes (Fecher et al, 2007). Acral melanoma tends to be found on the palms of the hands, the soles of the feet and in the nail bed and is not associated with UV exposure. Acral accounts for about 50% of melanoma in non-Caucasian populations. Lentigo maligna is generally flat in appearance and occurs on sun-exposed regions in the elderly. It is therefore associated with lifetime chronic sun exposure. Nodular melanoma typically consists of raised nodules without a significant flat portion. Superficial spreading melanoma (SSM) is by far the most common form of melanoma. It is usually flat with an intra-epithelial component, particularly at the edges, and is linked to episodes of severe sunburn, especially at an early age. Although this classification is commonly used it has little prognostic or therapeutic significance (Balch et al, 1992).

Several clinical and histological parameters that have been shown to influence the prognosis of cutaneous melanoma have been identified (Balch 2000). The clinical parameters include anatomical site, gender and age. Tumours located on the trunk, head or neck tend to be thicker and carry poorer prognoses than those on the extremeties. Survival rates are generally higher for Females than Males and higher in the young than in the elderly. The histological parameters that influence prognosis include depth of invasion, and ulceration. Depth of invasion (Clark level) and tumour thickness (Breslow) are the most important variables in melanoma prognosis. Applied mathematical models have revealed a linear correlation between patient

survival and tumour thickness. Ulceration is found in 20-25% of all melanomas and is especially common in Male patients. Data on several of these clinical and histological parameters have been used to classify patients into groups of similar prognosis, a process known as staging (Table 1.1).

Stages I and II are melanomas that are localized to the skin at varying depths of invasion; stage III includes patients with regional recurrence and nodal spread of disease, and stage IV patients have distant metastatic spread of melanoma. Although staging patients is helpful for clinical purposes the parameters are frequently unreliable; some deep melanomas lack metastatic potential, whereas some thin melanomas have an aggressive course and are able to disseminate. Additional prognostic factors are therefore required.

1.5 Melanoma therapy

The most important determinant of melanoma outcome is early diagnosis which allows treatment to be undertaken at a stage when cure is readily achievable. Most melanomas can be identified by clinical examination with several features being suggestive of a diagnosis of melanoma. These include asymmetry of a lesion, border irregularity, colour change and diameter greater than 6mm i.e. the so-called ABCD system of diagnosis (Friedman et al, 1985). In addition, clinical suspicion should be aroused by any significant change in an existing naevus or skin lesion. It should be noted that approximately 1.6-10% (Thompson et al, 2005) of all melanomas are non-pigmented and as a result amelanotic melanomas are often mistaken for basal cell and squamous cell carcinomas or even benign inflammatory lesions. Nodular melanomas are more likely than other types of melanoma to be amelanotic

Stage	TNM Classification	Histological/Clinical Features	5 Year Survival
0	Tis0 N0 M0	Intraepithelial/in-situ melanoma	100%
IA	T1a N0 M0	<1mm without ulceration and level II/III	>95%
IB	T1b N0 M0	<1mm with ulceration and level III/IV	
	T2a N0 M0	1.01-2cm without ulceration	89-91%
IIA	T2b N0 M0	1.01-2cm with ulceration and level	
	T3a N0 M0	2.01-4cm without ulceration	77-79%
IIB	T3b N0 M0	2.01-4cm with ulceration	
	T4a N0 M0	>4mm without ulceration	63-67%
IIC	T4b N0 M0	>4mm with ulceration	45%
IIIA	T1-4a N1a M0	1 nodal micrometastases, nonulcerated 1°	
	T1-4a N2a M0	2-3 microscopic nodes, nonulcerated 1°	63-69%
IIIB	T1-4b N1a M0	1 nodal micrometastases, ulcerated 1°	46-53%
	T1-4b N2a M0	2-3 microscopic nodes, ulcerated 1°	
	T1-4a N1b M0	1 nodal macrometastases, nonulcerated 1°	
	T1-4a N2b M0	2-3 macroscopic nodes, ulcerated 1°	
	T1-4a/b N2c M0	In-transit mets and/or satellite lesions	30-50%
IIIC	T1-4b N2a M0	1 macroscopic regional node, ulcerated 1°	
	T1-4a/b N2a M0	2-3 metastatic nodes, ulcerated 1°	
	Any T N3 M0	4 or more metastatic nodes	24-29%
IV	Any T any N M1a	Skin, or nodal mets with normal LDH	
	Any T any N M1b	Lung mets with normal LDH	
	Any T any N M1c	Mets with elevated LDH or visceral mets	7-19%

Table 1.1. AJCC 2002 Revised Melanoma Staging. The table shows the 5 year survival for patients with different stages of melanoma determined by Breslow thickness, presence of ulceration, nodal involvement or presence of metastatic disease. TNM stands for tumour, nodes, metastases. LDH = lactate dehydrogenase. Other prognostic factors that are not included in the AJCC staging system include sex, site and presence of mitoses.

(Chamberlain et al, 2003).

The standard approach to management of primary melanoma is excisional biopsy of the lesion followed by detailed pathology review. On the basis of the pathology report a planned re-excision is normally undertaken with a wide margin of between 1 and 3cm depending on the Breslow thickness of the primary lesion. Sentinel node biopsy, a minimally invasive procedure that provides accurate assessment of regional node status (Morton et al, 1992), is often offered for patients with melanomas of greater than 1mm Breslow. Although this procedure provides prognostic information it is still unclear whether completion nodal dissection in patients with a positive sentinel node provides a significant survival advantage.

More than 80% of patients with melanoma will die from other causes (Beddingfield 2003). However those patients at intermediate or high risk of recurrence would potentially benefit from eradication of micrometastatic disease through the use of effective systemic adjuvant therapy. Although numerous trials of adjuvant therapies have been carried out in melanoma patients using chemotherapy, vaccines, biological agents and combinations of these, the only drug that has been shown reproducibly to have some impact on patient outcome in large randomised trials is high dose intravenous interferon-alpha (Hersey et al, 2003). A pooled analysis of trials at median follow-up times of 2.1-12.6 years showed significant improvement in relapse-free survival for patients treated with high-dose interferon-alpha of about 10% at 5 years but no clear benefit in terms of overall survival, compared with patients randomly allocated to observation or vaccine therapy (Kirkwood et al, 2004). The most recent analysis of the interferon-alpha data however has suggested a proportional benefit in overall survival of 3% at five years (Wheatley K, 2007). At present high dose interferon is not regarded as standard adjuvant therapy in the UK although it is widely used in parts of North America.

For patients with metastatic melanoma, no randomised controlled trials have shown a significant survival advantage with the use of any specific drug or combination of drugs (Brown and Kirkwood, 2003). Among cytotoxic agents dacarbazine is widely regarded as the benchmark and although it has been said to produce a response rate in 15-20% with a median duration of response of 4 months (Eggermont and Kirkwood, 2004) the most recent data from a study of 771 patients showed a response rate in the dacarbazine arm of only 7.5% (Bedikian et al, 2006). A variety of regimens combining dacarbazine with other cytotoxic agents, tamoxifen, or interferon-alfa have shown promising response rates in single-institution phase 2 trials but no survival advantage has been shown in randomised phase 3 studies (Tsao et al, 2004). The cytokine interleukin 2 has approval for use in the US for treating metastatic melanoma on the basis of durable responses in some patients. The overall response rate however is low (16%) and as systemic toxicity is high its use is restricted to selected patients in specialist centres. Surgery is used for treatment of local recurrences and for metastatic disease in regional lymph nodes and can also be valuable for patients with surgically resectable disease in up to 3 visceral sites.

1.6.1 Genetic susceptibility to melanoma

Linkage-analysis studies of families with a high incidence of melanoma culminated in the identification of two susceptibility genes – CDKN2A and CDK4. About 10% of all melanoma cases are familial and between 25-40% of inherited cases of melanoma carry mutations in the CDKN2A locus (Kamb et al, 1994) (which encodes p16INK4A and p14ARF) and CDK4 (Zuo et al, 1996). INK4 is a CDK inhibitor that binds to and inhibits CDK4 (and CDK6), which otherwise phosphorylates pRb and induces G1-S phase progression. ARF acts through a distinct pathway involving stabilisation of p53 through abrogation of murine double minute-2-induced p53 degradation. More recently a pigmentation-associated predisposition to melanoma has been identified with the discovery of polymorphisms of the melanocortin-1 receptor (MC1R) which are associated with red hair, fair skin, sun sensitivity and freckling phenotype.

1.6.2 The melanocortin-1 receptor

The melanocortin-1 receptor (MC1R) is a member of the G-protein coupled receptor (GPCR) superfamily which is formed by over 1000 members and accounts for more than 1% of the mammalian genome. GPCRs play a central role in allowing cells to communicate with their environment and mediate the responses to a wide variety of stimuli including light, taste molecules, neurotransmitters and hormones (Fredholm et al, 2007). GPCRs regulate the activity of metabolic enzymes and pathways, ion channels, membrane transporters and the function of the transcriptional, motility and secretory machineries. Recent evidence has suggested a role for MC1R in response to pain (Mogil et al, 2005) but it is best known for its central position in melanocyte cell biology (Cone et al, 1996, Sturm 2002). It plays a key role in pigment production and is a major determinant of skin phototype and sensitivity to UV light induced damage.

MC1R belongs to a five member sub-family of GPCRs termed MC1R to MC5R (Reviewed in Getting 2006): MC2R is expressed in the adrenal cortex and has a role in steroidogenesis; MC3R is expressed in brain and heart tissue and is involved in energy metabolism and in control of inflammation; MC4R is expressed in the brain and has a role in energy homeostasis and pain; and MC5R is expressed in lymphocytes and exocrine glands and has immunoregulatroy functions. MC1R is expressed predominantly on melanocytes and melanoma cells but is also found in a variety of other cell types found in skin including keratinocytes, fibroblasts and T lymphocytes as well as in other organs including the testis and the brain (Adachi et al, 1999, Bhardwaj et al, 1997, Bohm et al, 1999, Salzar-Onfray et al, 2002, Stander et al, 2002, Xia et al, 1995).

The MC1R physiologic agonists belong to a group of small peptide hormones (melanocortins) which are derived from the precursor proopiomelanocortin (POMC) and expressed in the pituitary and peripheral locations including the skin (Eves et al, 2005). POMC protein contains 3 main domains: the central highly conserved $ACTH_{1-39}$ sequence, with α-MSH at its N-terminus; the C-terminal B-lipotropin, which can be cleaved to generate β-endorphin; and the N-terminus region which contains γ-MSH (Castro and Morrison, 1997). Preferential natural agonists of MC1R are α-melanocyte stimulating hormone (α-MSH) and adrenocorticotropic hormone (ACTH). α-MSH, a tridecapeptide (Ac-Ser-Tyr-Ser-Met-Glu-His-Phe-Arg-Trp-Gly-Lys-Pro-Val-NH2), was discovered primarily for its function in pigmentation although recent research has suggested a role in other biological activities including learning and memory, cardiovascular function, reproduction, and feeding behaviour (Bertolinin and Gessa, 1981, Eves et al, 2005, Getting, 2006, Voisey et al, 2003, Wikberg et al, 2000).

α-MSH is produced primarily by keratinocytes in response to UV. Binding of α-MSH to a site on the extracellular domain of MC1R on melanocytes is transduced by the receptor into an increase in intracellular cAMP levels (Barsh et al, 2000,

D'Orazio et al, 2006). α-MSH signalling is involved in the developmental migration of melanocyte precursors (melanoblasts) from the neural crest to the skin and in melanocyte motility (Mayer, 1973, Hirobe, 1992). It also provides a potent signal for melanocyte proliferation and stimulates melanin synthesis (Lin and Fisher, 2007). Activation of MC1R by α-MSH results in increased activity of tyrosinase, a key enzyme catalysing the rate limiting step in melanin synthesis. This signal leads to not only an increase in the amount of pigment produced but also an increase in the ratio of black and strongly protective eumelanins to yellowish and poorly protective pheomelanins (Lin and Fisher, 2007). *In vitro*, the effects of α-MSH can be mimicked by a number of drugs including forskolin, IBMX and cholera toxin, indicating that α-MSH functions mainly through elevating cAMP levels in the cell (Eves et al, 2005). Although cAMP triggers numerous downstream effects, one important target is the MITF gene, which is transcriptionally upregulated by cAMP signalling in a melanocyte-restricted fashion (Garraway et al, 2005). It is now recognised that MITF is a regulator of pigmentation as well as a key transcription factor involved in survival pathways both during development and during neoplastic growth of melanoma (Levy et al, 2006). cAMP has also been shown to inhibit the phosphatidylinositol 3-kinase/AKT pathway and to stimulate the MAPK pathway through B-Raf activation and may therefore influence both differentiation and survival of melanocytes (Dumaz et al, 2006). Although it appears that the principal role of MC1R is in mediating the response of the melanocytes to UV radiation it may also play a central role in other aspects of skin biology including the acute inflammatory response (Eves et al, 2005).

1.6.3 MC1R in melanoma susceptibility

MC1R is an integral membrane protein of 317 amino acids and contains an extra-cellular N-terminus, seven transmembrane fragments and an intracellular C-terminal extension. It is encoded for within a single exon of the MC1R gene on chromosome 16q24.3 (Mountjoy et al, 1992). The elucidation of the role of human MC1R in pigmentation followed the identification of the MC1R locus underpinning a series of

mutations in mice at the classical coat-colour locus extension (Robbins et al, 1993). Point mutations within MC1R that confer constitutive activity result in a dominant black phenotype in mice whereas loss-of-function alleles result in a yellow coat (Cone et al, 1996). In the MC1R loss-of-function mouse, expression of the wild-type MC1R allele results in over-rescue (yellow to black) (Healy et al, 2006). These observations led to the hypothesis that part of the variation of normal human pigmentation within and between populations may arise from polymorphisms in the human MC1R gene.

The human MC1R gene is highly polymorphic and many of the natural variants are functionally relevant (Wong and Rees 2005). In man, more than 60 natural variants of MC1R have been reported. Several variants are associated with fair skin, red hair colour, freckles and increased skin cancer risk. The best characterised variants are the red hair colour (RHC) alleles Arg151Cys, Arg160Trp and Asp294His. Analysis of functional effects of cloned RHC variants in heterologous cell lines suggested they were loss of function since the receptors were severely compromised in their ability to stimulate cAMP production (not due to altered affinity of agonist). However the 3 common RHC alleles could rescue to varying degrees eumelanin production in MC1R deficient transgenic mice suggesting that they were not complete loss of function and that they may possess different levels of activity (Reviewed in Healy 2004).

Within human melanocytes the MC1R genotype provides the first level of regulation of MC1R signalling. MC1R activity can also be modulated by several mechanisms including changes in gene expression, mRNA stability and/or translation efficiency or the rate of post-translational processing of the receptor protein and its traffic through the secretory pathway (Rouzaud et al, 2003). Once in the plasma membrane, MC1R activity is primarily controlled by the interaction of the receptor with the activatory melanocortins.

In view of the known higher risk of melanoma development in individuals with certain pigmentary characteristics including fair skin type, red hair, inability to tan and freckling it is perhaps not surprising that a number of case-controlled studies have shown an association between MC1R variants and melanoma (Sturm 2002). These alleles are in fact associated with increased risk of melanoma and nonmelanoma skin cancer (Box et al, 2001) as well as with increased penetrance and reduced age of onset in familial melanoma in CDKN2A mutation carriers (Goldstein et al, 2005). It is widely thought that the lack of photoprotective eumelanin in the skin of people with MC1R variants explains the reason for the elevated melanoma risk. It is also possible that the relatively higher levels of phaeomelanin may contribute to the increased risk of melanoma due to the association of phaeomelanin with the generation of increased free radicals following exposure to UV (Menon et al, 1983).

1.6.4 MC1R and non-pigmentary pathways

Studies on sporadic melanoma have suggested that the elevated risk of developing melanoma remains raised even after controlling for skin type and hair colour in the analysis (Box et al, 2001). Although this may be partly due to the difficulty in accurately defining pigmentation phenotype it has been interpreted by some authors as indicating that the risk of development of melanoma as a result of MC1R variants arises secondary to the effects of variants on non-pigmentary pathways. Two recent studies have provided evidence that signalling through the MC1R receptor may influence risk of melanoma development through an effect on DNA repair. This effect appears to be independent of pigmentary response.

The first study investigated the effects of α-MSH and endothelin-1 on DNA repair following UV radiation in cultured human melanocytes (Kadekaro et al, 2005). It was found that α-MSH rescued human melanocytes from UV radiation induced apoptosis and reduced DNA photoproducts and oxidative stress. Notably, loss-of-

function mutations in the MC1R abolished the anti-apoptotic effect of α-MSH. This study suggested that the survival effects of α-MSH were mediated independent of regulation of melanocyte proliferation and melanogenesis.

A second study investigated the effects of α-MSH on apoptosis and DNA repair following UV radiation in normal human melanocytes (Bohm et al, 2005). It was found that α-MSH markedly reduced the formation of UVB radiation-induced DNA damage as demonstrated by reduced amounts of cyclobutane pyrimidine dimers, ultimately leading to reduced apoptosis. The effect was not related to alterations in cell cycle distribution nor via changing the expression of apoptosis-related proteins. Although this study suggested that α-MSH causes a reduction in UVB radiation-mediated DNA damage via activation of the nucleotide excision repair pathway it is also possible that the effect of α-MSH is due to reduced formation of reactive oxygen species. This requires further investigation.

It has therefore been proposed that loss-of-function mutations in the MC1R gene may not only affect constitutive pigmentation but they may also predispose human melanocytes to the DNA damaging effects of UV radiation which may increase melanoma risk (Figure 1.3). The proposed role of the α-MSH/MC1R pathway in protecting melanocytes from apoptosis may be of importance in the understanding of melanoma pathogenesis and for the development of preventative and therapeutic measures.

1.6.5 MC1R as a therapeutic target in melanoma

Although the α-MSH/MC1R/cAMP signalling pathway has an undisputed role in promoting pigmentation, data relating cAMP to melanoma progression appear contradictory. A limited number of *in vitro* studies have investigated the influence of MC1R genotype on melanoma cell behaviour. When the wild-type MC1R is

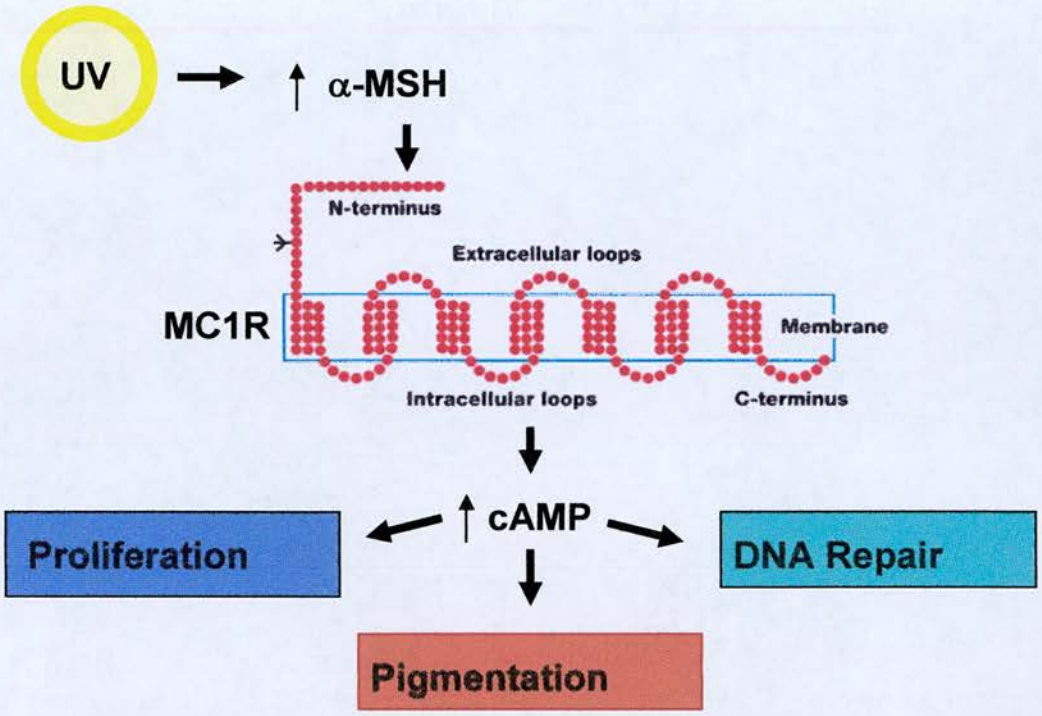

Figure 1.3. Schematic diagram displaying the relationship of UV exposure to signalling through MC1R. Possible downstream effects of stimulation of the MC1R by α-MSH via elevated intracellular cAMP are shown.

transfected into the amelanotic murine melanoma cell line B16G4F they remain amelanotic which allows a unique opportunity to investigate the non-pigmentary consequences of MC1R variants in the absence of confounding by effects of these variants on pigmentation. In cell growth assays, α-MSH suppressed proliferation of wild-type MC1R transfectants, but no suppression of growth was observed following addition of ligand to cells with variant MC1R (Arg151Cys, Arg160Trp and Asp294His) (Robinson et al, 2002). In addition, binding of the melanoma cells to fibronectin was inhibited by α-MSH in the wild-type transfected cells but this effect was not seen in the variant MC1R lines. Taken together these data suggest that compromised cAMP signalling could favour melanoma progression and that α-MSH may have an inhibitory effect in early melanoma development. The lack of these

inhibitory effects in individuals with variant MC1R may permit melanomas to arise more readily.

In contrast, α-MSH and cAMP have been found to increase c-met expression in melanoma cells which increases melanoma metastatic potential (Beuret et al, 2007). Also, the CREB/ATF family of transcription factors that function downstream of the cAMP pathway have been reported to act as survival factors and contribute to the malignant phenotype (Eves et al, 2002). Whether the α-MSH/MC1R/cAMP signal is pro-survival or growth inhibitory may be dictated by the cellular context, the extracellular signals, the microenvironment or the mutational status of the melanoma.

The possibility of using MC1R as a target for antibody or T cell based immunotherapy is dependant on how selectively this receptor is expressed in melanoma versus normal tissues. Analysis of MC1R expression by Western blot, immunohistochemistry and flow cytometry confirmed that MC1R is expressed at high levels in the majority of melanoma cell lines and in fresh primary and metastatic melanomas and at low levels in certain normal tissues (Salazar-Onfray et al, 2002). A number of studies have now been carried out to explore the use of MSH conjugated to radioisotope to target the MC1R (Raposinho et al, 2008).

MC1R is involved in many of the processes that distinguish melanoma from other tumour types; extreme migratory ability of normal precursors, pigment production and resistance to apoptosis. The MC1R pathway therefore represents a suitable candidate for further evaluation in the search for improved understanding of melanoma tumourigenesis and the development of novel therapeutics and is the subject of the first part of this thesis.

1.7.1 Genetics changes in melanoma progression

The Clark model of the progression of melanoma emphasizes the stepwise transformation of melanocytes to melanoma (Clark and Elder, 1984). This model describes histopathological changes that occur along 5 steps in melanomagenesis; benign naevus, dysplastic naevus, radial-growth phase (RGP) melanoma, vertical-growth phase (VGP) melanoma and metastatic melanoma (Figure 1.4). Naevi are benign, senescent neoplasias that consist of aberrant proliferation of melanocytes in the basal epidermis. Although naevi show varying degrees of dysplasia they only rarely transform to invasive melanomas (Lin and Fisher 2007). RGP melanoma is an intra-epidermal lesion that can involve some local microinvasion of the dermis. The change from RGP to VGP melanoma is a key switch as cells acquire metastatic potential and can spread either through lymphatics or directly by the bloodstream to distant sites giving rise to life-threatening disease. The proportion of melanomas that arise from naevi as opposed to those that arise de novo without any obvious precursor lesion remains controversial (Ackermann, 2000).

The biological changes occurring in melanoma progression are likely to arise from a complex interaction between malignant cells and host factors. Key changes that are acquired in metastatic progression consist of uncontrolled autocrine growth, resistance to apoptosis and the achievement of invasive properties including adhesive, motility, proteolytic and angiogenic capacities (Hsu et al, 2002). It is hoped that an increased understanding of the key steps involved in melanoma progression will lead to the identification of new therapeutic targets.

The specific molecular changes and the mechanisms underlying melanoma progression are now beginning to be unravelled by genomic and proteomic approaches (Reviewed in Miller 2006). Mutations in critical growth regulatory genes, the production of autocrine growth factors and loss of adhesion receptors all contribute to disrupted intracellular signalling in melanocytes allowing them to escape their tight regulation by keratinocytes. Consequently melanocytes can

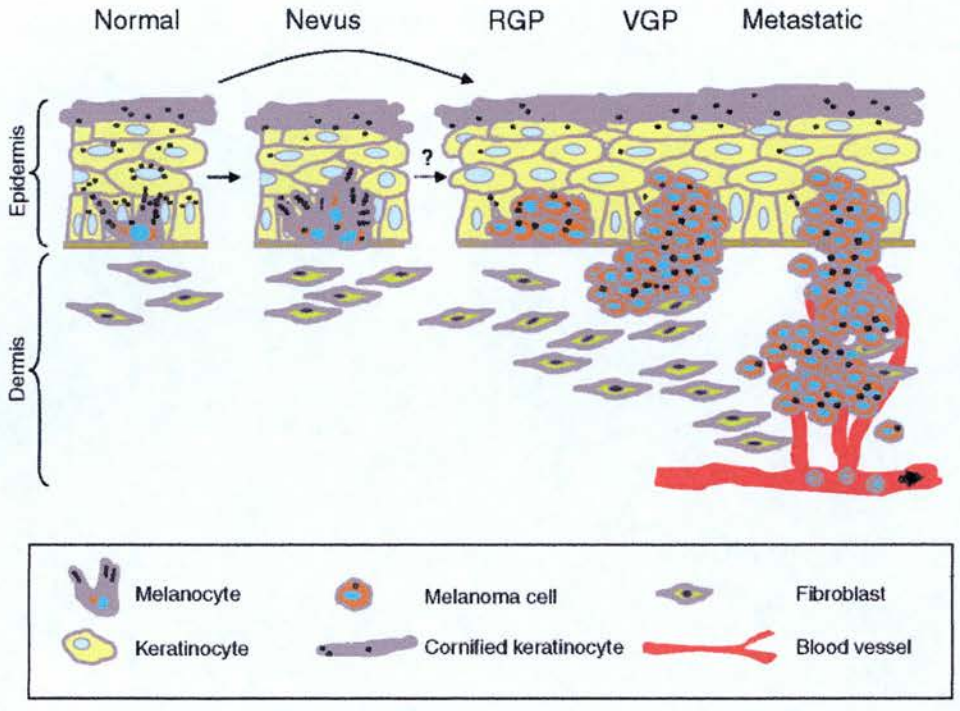

Figure 1.4. Schematic diagram displaying the spatial relationship of melanocytes to the rest of the cells in the skin during the various proposed steps of melanoma progression. Adapted from Gaggioli and Sahai 2002.

proliferate and spread, leading to formation of a naevus. The acquisition of invasive behaviour is the key transition in the progression of benign melanocytes to life threatening melanoma. Underlying the invasive behaviour is increased motility caused by changes in cytoskeletel organisation and altered contacts with the extracellular matrix (Rodolfo et al, 2004). Changes in the interactions of melanoma cells with keratinocytes and fibroblasts enable them to survive and proliferate outside their normal epidermal location. Although the pattern of genetic change in melanoma is diverse they have convergent effects on key biochemical pathways (Hayward 2003) including the Raf/MAPK, PI3K/AKT/PTEN, Rb and WNT pathways and the pathways of apoptosis. Proteins involved in tumour/stroma interaction also have a key role in melanoma progression.

1.7.2 The MAP kinase pathway in melanoma progression

The multikinase MAP kinase cascade is a critical growth signalling pathway that is among the most common sites of mutation in human cancers. The initiator protein in the pathway, RAS, can be activated by growth factors and can signal through many downstream proteins, including the RAF family of proteins. Mutations in RAS are frequent in human cancers, including approximately 15% of melanomas and they are almost always reciprocal to mutations in BRAF (Davies et al, 2002, Akslen et al, 2005). BRAF mutations play an important role in the initiation and /or progression of melanoma via sustained BRAF-mitogen-activated protein kinase kinase-extracellular signal regulated kinase (BRAF-MEK-ERK) activation. The BRAF gene is mutated in approximately 70% of primary melanomas (Rodolfo et al, 2004). 80-90% of these mutations involve a T1799A transversion in exon 15 that results in the substitution of a glutamate for a valine at position V600E (Panka et al, 2006). The V600E mutant B-Raf possesses the hallmarks of an oncogene: (1) the kinase activity of B-Raf V600E is 10 times greater than wild-type B-Raf, (2) it constitutively stimulates ERK activity *in vivo* independent of RAS, and (3) it potently transforms NIH3T3 cells (Karasasides et al, 2004).

Although UV irradiation appears to induce BRAF mutations, V600E requires a GTG to GAG change, a mutation that does not conform to a typical UVB-damaged DNA signature (Thomas et al, 2006). The mechanism by which UV induces BRAF mutations in melanoma is uncertain. One possibility is that the mutations are not induced directly by UV irradiation but are a secondary consequence of exposure. Melanin production results in the accumulation of highly toxic oxidising agents and so its increased synthesis following UV exposure could cause further DNA damage in the melanocytes. It is also possible that the inflammatory response that accompanies sunburn could contribute.

Recent studies have shown that the presence of a mutation in BRAF does not correlate with activation of ERK in melanocytic naevi (Uribe et al, 2006). Thus, BRAF mutations do not seem to be sufficient to produce MAPK activation in melanocytic naevi. This suggests that other events are needed to induce MAPK activation such as BRAF overexpression, inhibition of MAPK phosphatases or suppression of RAF kinase inhibitors.

1.7.3 The importance of apoptosis in melanoma progression

Melanocytes have an important role as the photoprotectors of the skin and have a high inherent resistance to apoptosis (Soengas and Lowe 2003). They can survive considerable genotoxic stress in order to secrete melanin that protects neighbouring cells from further damage. The extreme resistance of melanoma to chemotherapeutic drugs and the generally low apoptotic indices in melanoma has prompted an extensive search for cell death factors altered during melanoma progression.

The dependence of melanocytes on Bcl-2 for survival is illustrated by the depigmentation and loss of melanocytes of mice deficient for Bcl-2 (Hodgkinson et al, 1993). The importance of Bcl-2 on melanoma however is less clear. Some reports suggest that high Bcl-2 is associated with poor survival of metastatic melanoma patients whereas others suggest a downregulation of Bcl-2 during melanoma progression and argue against the use of Bcl-2 as a prognostic factor (Reviewed in Serrone and Hersey 1999). Suppression of Bcl-2 using antisense technologies induces death of melanoma cells and potentiates the effects of chemotherapy (Jansen et al, 1998).

Other proteins involved in apoptosis have also been implicated in melanoma pathogenesis. PUMA belongs to the Bcl-2 family of apoptotic regulators and overexpression is an independent predictor of survival (Karst et al, 2005). Conversely, loss of expression of Bcl-2 proteins, Bax and Bak are associated with

worse long-term prognosis in primary melanoma (Fecker et al, 2006). The X-linked inhibitor of apoptosis (XIAP) is associated with chemoresistance in many cancers and expression is higher in melanomas (particularly in early stage disease) than naevi (Kluger et al, 2006). Survivin is a member of the inhibitors of apoptosis family (IAP) that is overexpressed in invasive and metastatic melanomas (Soengas et al, 2003). Although inactivating mutations of the tumour suppressor p53 are uncommon the p53 pathway is frequently downregulated in melanoma. Mechanisms include ARF deletion or overexpression of MDM2 which occurs in approximately 50% of melanomas (Polska et al, 2001). Finally, Apaf-1, an effector of apoptosis, is inactivated in approximately 40% of melanomas (Soengas et al, 2001).

1.7.4 Other important pathways in melanoma progression

A number of other proteins have been implicated in melanoma pathogenesis. E-Cadherin, N-Cadherin and P-Cadherin are adhesion molecules that all have key roles in the development and progression of melanocytic tumours (Bachmann et al, 2005). The cytoplasmic domain of E-cadherin links to the cytoskeleton through interactions with B-Catenin. Lack of B-Catenin nuclear staining is related to tumour thickness and associated with poor prognosis (Bachmann et al, 2005).

Galectin-3 is a member of the B-galactoside-binding gene family that has been implicated in a variety of biological functions including tumour cell adhesion, proliferation, differentiation, angiogenesis, cancer progression and metastasis (Nakahara et al, 2005). It is expressed broadly in normal and tumour cells and although predominantly localized in the cytoplasm may translocate to the nucleus. Although it has been reported for some time as having an important role in cancer progression a recent study has suggested an important role for galectin-3 in melanoma progression; primary and metastatic melanomas expressed galectin-3 at a significantly higher level than naevi in both cytoplasm and nuclei and there was a

trend towards worse survival for those patients showing higher levels of cytoplasmic than nuclear galectin-3 expression. (Prieto et al, 2006).

1.8 Molecular classification of melanoma

Epidemiologic and molecular studies suggest that different types of melanoma can be distinguished on sun-exposed skin versus non-sun-exposed skin. Array-base comparative genomic hybridisation, DNA sequencing and immunohistochemistry was used to determine genome-wide changes in DNA copy number and BRAF/N-RAS mutational status in 126 primary melanomas (Curtin et al, 2005). Tumours were classified into 4 types on the basis of location and history of UV exposure defined by presence or absence of solar elastosis: acral, mucosal, and cutaneous melanomas with chronic sun-damage (CSD) or without chronic sun-damaged skin. Most non-CSD melanomas had BRAF or NRAS mutations. Those without mutations had increased copies of CDK4 or CCND1. The incidence of BRAF and N-RAS mutations in CSD melanomas was much lower. Deletion of CDNK2A was common in mucosal and acral melanomas. Of all histopathologic subtypes acral and mucosal melanomas had the greatest number of genomic events. These findings provide genetic support for the existence of distinct molecular pathways to melanoma, also known as the 'divergent pathway hypothesis'.

A recent study identified an important link between germline mutations in MC1R and BRAF mutations (Landi et al, 2006). In a study of 200 cases of primary melanoma MC1R variant alleles were found to be associated with melanoma risk specifically in patients with melanomas in non-CSD skin. This risk appeared to be associated with tumours harbouring BRAF mutations suggesting that germline events may influence genetic events leading to tumourigenesis in response to environmental exposure. Whether the MC1R-BRAF link is a consequence of a direct effect of impaired MC1R on BRAF or is due to alterations in other pathways is unclear. The proposed link between these distinct molecular pathways has previously been suggested by studies in melanocytes where crosstalk between cAMP and BRAF/CRAF signalling was investigated (Dumaz 2006). Further investigation into

whether different UV exposures lead to biologically distinct melanomas is not only critical to understanding the role of UV in melanomagenesis it may ultimately allow the development of separate targeted therapeutic strategies for patients with all types of melanoma.

1.9 Prognostic markers in melanoma

A number of approaches to investigate novel prognostic markers in melanoma have been used. One method used to identify novel candidate proteins involved in melanoma prognosis is gene expression profiling. Gene expression microarray on frozen samples of melanoma has identified characteristic gene expression differences distinguishing different classes of metastatic melanoma from one another and from primary and premalignant lesions. These studies have been limited by unavailability of fresh primary material which is usually fixed in its entirety for diagnostic purposes. One recent study analysed gene expression in 83 frozen primary melanoma samples collected over a 20 year period (Winnepenninckx et al, 2006). 254 genes were identified that were associated with a good prognosis. However, when this set of genes were used to classify a validation set, only 11 out of 17 patients had clinical outcome predicted correctly. Indeed, mathematical modelling predicts that gene expression profiles of several thousand patients are needed to generate a robust gene set for predicting cancer outcome (Dai et al, 2005). Obtaining such large numbers of frozen primary melanomas is impossible, making it necessary to explore other ways to investigate gene expression changes in melanoma.

A number of studies have used immunohistochemistry to investigate the prognostic role of key proteins in melanoma pathogenesis. The advantage of this approach is that fixed samples can be used and therefore many more samples are accessible. Immunohistochemistry studies that have used tissue microarrays to identify novel prognostic markers in melanoma are discussed in more detail in Chapter 5.

1.10 The future

Given the poor response that is seen to chemotherapy in melanoma there is a great deal of interest in the development of new agents. In particular the key pathways that are central to melanoma pathogenesis and responsible for the resistance to existing chemotherapy drugs are the subjects of intense investigation to assess their potential as therapeutic targets (Thompson et al, 2005). A number of exciting drugs that target key proteins involved in growth signalling, apoptosis and angiogenesis are currently under clinical development.

The MAPK pathway is an attractive target for therapeutic intervention in melanoma due to its central role in the regulation of proliferation, invasion, and survival and the recent development of drugs that inhibit the various kinases and GTPases that comprise the pathway (Panka et al, 2006). Sorafenib, a multitargeted oral kinase inhibitor, is currently approved for use in the US for patients with renal cell and hepatocellular carcinomas (Eisen et al, 2006). It is a moderately potent inhibitor of B-Raf but it also inhibits several other receptor tyrosine kinases involved in tumour progression including vascular endothelial growth factor receptor (VEGF) -2 and -3 and platelet derived growth factor receptor (PDGF). As a single agent Sorafenib has shown very modest activity with patients with melanoma and although early studies looking at combinations with chemotherapy looked promising, randomised studies have been negative (Bayer et al, 2006). Newer more selective B-Raf inhibitors are currently undergoing preclinical testing whilst drugs that inhibit other targets in the MAPK pathway such as MEK are undergoing assessment in clinical trials.

Oblimersen is an anti-sense oligonucleotide to the anti-apoptotic molecule Bcl-2 which is over expressed in many melanomas. This drug has been shown to sensitise melanoma cells to chemotherapy in preclinical studies (Jansen et al, 2004) and in Phase III testing of oblimersen plus dacarbazine versus dacarbazine alone has shown a positive impact on progression free survival (Bedikian et al, 2006).

One of the most intriguing areas of development has seen a therapy that is established in other cancer types emerge as a potentially useful treatment for patients with melanoma. Aberrations in KIT are found at relatively high frequency in melanomas arising on sun-damaged skin or in acral or mucosal areas (Curtin et al, 2006). Clinical trials are underway to establish whether patients with melanomas who have a c-kit mutation gain any benefit from imatinib, the tyrosine kinase inhibitor targeting ABL, PDGF-R and KIT that is already proven to be highly effective in patients with chronic myeloid leukaemia (CML) or gastrointestinal stromal tumour (GIST) (de Kogel and Schellens, 2007).

Other molecular targeted therapies undergoing clinical investigation in melanoma are shown in Table 1.2. One of the attractions of these new therapies is that the understanding of the pathways that the agents target may allow the use of molecular markers to predict response. Such a strategy is already in use in the selection of patient groups with higher chances or response to therapies that target Her-2, or EGFR in patients with breast or lung cancer respectively. It remains to be seen whether any of these therapies emerge as effective treatments for melanoma as single agents or whether strategies such as combining targeted therapy to more than one signalling pathway or tailoring treatment to the particular genetic subtype of melanoma prove to be more effective.

Molecular Target	Mechanism of Action	Agent	Clinical Trial in Melanoma
Bcl-2	Antisense	Oblimersen	Phase III
RAS	Farnesyltransferase inhibitor	Tipifarnib	Phase I/II - combination with sorafenib
BRAF	Tyrosine kinase inhibitor	Sorafenib	Phase III - combination with chemo
MEK	Tyrosine kinase inhibitor	PD0325901	Phase I/II - single agent
HSP90	Disrupts HSP90 complexes	17-AAG	Phase II - single agent
VEGF	VEGF inhibitor	Bevacizumab	Phase II - combination with chemo
Multi-kinase	Tyrosine kinase inhibitor	Sunitinib	Phase II - combination with chemo
Integrins	$\alpha v\beta 3$ integrin inhibitor	MEDI-522	Phase I/II - single agent
Cell cycle	CDK inhibitor	Flavopiridol	Phase I
PI3K/AKT	AKT inhibitor	Perifosine	Phase II - single agent
Proteasome	Proteasome inhibitor	Bortezomib	Phase I - combination with chemo
c-kit	Tyrosine kinase inhibitor	Imatinib	Phase II – single agent
mTOR	mTOR inhibitor	Temsirolimus	Phase II – single agent

Table 1.2. Table of selected molecular targets with examples of agents in clinical development for treatment of patients with melanoma (taken from www.clinicaltrials.gov, www.cancer.gov and www.asco.org).

1.11 Summary and Aims

Given the rising incidence of melanoma and the poor outcome for patients with metastatic disease there is a great need to improve our understanding of the molecular basis of melanoma pathogenesis in order to develop more effective prevention strategies, refine classification systems, define new prognostic markers and to identify new molecular targets for therapy. The aim of the work presented in this thesis was to conduct a number of studies that would add to our understanding of several aspects of melanoma biology.

The postulated role of MC1R in protecting melanocytes from apoptosis in response to UV irradiation led to our hypothesis that manipulation of the MC1R may affect growth of melanoma cell lines and sensitivity to DNA damage. The aims of the work in chapter 3 were: firstly, to establish whether melanoma cell growth can be adversely affected by manipulation of the melanocortin receptor (MC1R); secondly, whether manipulation of MC1R results in increased sensitivity to DNA damage induced apoptosis; and thirdly, whether RHC (red hair colour) MC1R alleles result in diminished DNA repair capacity and increased sensitivity to DNA damage.

Given the limitations of long established cell lines it was thought that it may be beneficial to establish novel melanoma cell lines. The aim of the work in chapter 4 was to establish and characterise novel melanoma cell lines from fresh human melanoma tissue fragments removed during surgery. The characterisation included basic morphology and growth characteristics, immunohistochemistry, response to DNA damage, ability to form xenografts in SCID mice and correlation of the findings with the clinical samples from which the cells were derived.

The investigation of melanoma progression and prognosis at the mRNA level has been limited by the unavailability of fresh melanoma tissue. Studies using

immunohistochemistry on fixed tissue has the advantage of opening up access to large numbers of samples, often with correlative clinical data. The aims of the work in chapter 5 were to firstly, develop a tissue microarray that includes all stages of melanoma development, secondly, investigate changes in the expression of key proteins during melanoma progression and thirdly, identify novel prognostic markers in primary melanomas. The 3 proteins chosen for assessment were B-catenin, bcl-2 and galectin-3.

Chapter 2 Materials and Methods

2.1 Materials

General laboratory chemicals were purchased from Sigma, unless otherwise indicated. All PCR primers were purchased from Sigma and cell culture medium was obtained from Gibco. All materials were stored at room temperature (r/t) unless stated otherwise.

2.1.1 DNA manipulation reagents

Church buffer: 0.25M sodium phosphate, 1mM EDTA, 7% (w/v) SDS.

DNA isolation buffer: 10mM Tris HCl pH8.0, 400mM NaCl, 3mM EDTA, 1% (w/v) SDS. Stored at 4°C.

Lysis buffer: 10mM Tris HCl pH8.3, 140mM NaCl, 3mM KCl, 12% (w/v) sucrose, 1mM EDTA, 1% (v/v) Triton X-100.

Proteinase K stock solution: 2mg/ml proteinase K, 100mM EDTA pH7.5, 2% (w/v) SDS. Stored at –20°C.

SSC (x20): 3M NaCl, 300mM tri-sodium citrate dihydrate pH7.0

TAE electrophoresis buffer**:** 40mM Tris-acetate, 1mM EDTA.

TBE electrophoresis buffer: 90mM Tris-HCl, 90mM boric acid, 2mM EDTA, pH8.3.

TE pH7.4 or 7.5: 10mM Tris HCl pH7.4 or 7.5, 1mM EDTA.

2.1.2 RNA manipulation reagents

Denaturation buffer: 0.5M NaOH, 1.5M NaCl.

5× MOPS buffer: 200mM MOPS, 50mM NaOAc, 5mM EDTA. pH adjusted to 7.0 with NaOH.

RNA loading buffer: 50% (v/v) glycerol, 1mM EDTA pH8.0, 0.4% (w/v) bromophenol blue, 1mg/ml ethidium bromide. Stored at −20°C.

RNA sample buffer: 10ml deionised formamide, 3.5ml 37% formaldehyde, 2ml 5× MOPS buffer. Stored at −20°C.

2.1.3 Protein manipulation reagents

Bacterial lysis buffer: 50mM sodium phosphate buffer pH8.0, 300mM NaCl, 10% (v/v) glycerol, 15mM β-mercaptoethanol, 0.5mM PMSF, complete protease inhibitors. β-mercaptoethanol, PMSF and complete protease inhibitors were added immediately prior to use. Stored at 4°C.

Complete protease inhibitors: A cocktail of several serine and cysteine protease inhibitors in tablet form (does not contain metalloproteases; Roche). Stored at −20°C.

ECL solution 1: 100mM Tris HCl pH8.5, 0.396mM p-coumaric acid, 2.5mM luminol. Stored at 4°C protected from light.

ECL solution 2: 100mM Tris HCl pH8.5, 5.632mM H_2O_2. Stored at 4°C.

PBS: 140mM NaCl, 3mM KCl, 2mM KH_2PO_4, 10mM Na_2HPO_4.

Protein loading buffer (2X): 1.5M Tris (pH 6.8), 30% glycerol, 20 % SDS, 2M β-mercaptoethanol, 0.0018% bromophenol blue.

RIPA buffer: 150mM NaCl, 1% NP-40, 0.5% sodium deoxycholate, 0.1% SDS, 50mM Tris HCl pH8.0.

SDS PAGE loading buffer (2×): 100mM Tris HCl pH6.8, 4% (w/v) SDS, 20% (v/v) glycerol, 200mM DTT, 0.2% (w/v) bromophenol blue. Stored at −20°C.

SDS PAGE separating gel: 8-15% (w/v) 29:1 acrylamide:bis-acrylamide, 0.1% (w/v) SDS, 390mM Tris HCl pH8.8, 0.08% (v/v) TEMED, 0.1% (w/v) APS. Prepared immediately prior to use.

SDS PAGE stacking gel: 5% (w/v) 29:1 acrylamide:bis-acrylamide, 0.1% (w/v) SDS, 129mM Tris HCl pH6.8, 0.1% (v/v) TEMED, 0.1% (w/v) APS. Prepared immediately prior to use.

Semi-dry transfer buffer: 48mM Tris, 39mM glycine, 0.037% (w/v) SDS, 20% (v/v) methanol. The final pH should be 9.0-9.4.

TBST: 20mM Tris pH8.0, 100mM NaCl, 0.05% (v/v) Tween 20.

Tris-glycine electrophoresis buffer: 25mM Tris, 250mM glycine, 0.1% (w/v) SDS.

2.1.4 Other reagents

Citric acid solution (antigen retrieval): 0.1M Citric acid, pH 6.0.

Stock Solution (FACS): 2000mg trisodium citrate, 121mg Tris, 1044mg spermine tetrahydrochloride, 2ml Nonidet P40 made up to 2000ml with distilled water, pH 7.6.

Solution A (FACS): 15mg trypsin dissolved in 500ml Stock Solution, pH 7.6.

Solution B (FACS): 250mg trypsin inhibitor, 50mg ribonuclease A made up to 500ml with Stock Solution, pH 7.6.

Solution C (FACS): 208mg propidium iodide, 500mg spermine tetrahydrochloridemade made up to 500ml with Stock Solution, pH 7.6.

Solution P1: 25mM Tris-HCl pH8, 10mM EDTA, 50mM glucose.

Solution P2: 200mM NaOH, 1% (w/v) SDS.

2.1.5 Mammalian cells

A375, C32, G361 and WM115 human melanoma cell lines were obtained from the European Collection of Cell Cultures (ECACC). HBL was obtained from Gentaur (Brussels, Belgium). PEA1, PEO1 and PEO14 ovarian cancer cell lines were donated

by Grant Sellar, Cancer Research Centre, The University of Edinburgh. All cell lines were free from mycoplasma and were maintained in DMEM (Gibco, Paisley, UK) supplemented with 10% fetal calf serum, 1mM sodium pyruvate and 1x non-essential amino acids at 37°C in 5% CO_2 unless stated otherwise.

2.1.6 Mammalian cell culture media and related reagents

DMEM: 500ml DMEM (Cambrex), 10 or 15% (v/v) FBS, 50U/ml penicillin, 50µg/ml streptomycin, 4mM L-glutamine, 1 x NEAA. Stored at 4°C.

PBS: 140mM NaCl, 3mM KCl, 2mM KH_2PO_4, 10mM Na_2HPO_4.

RPMI: 500ml RPMI, 10% FBS, 50U/ml penicillin, 50µg/ml streptomycin, 4mM L-glutamine, 1 x NEAA. Stored at 4°C.

Trypsin-EDTA: 10× trypsin-EDTA (Cambrex) diluted in PBS to 0.25% (w/v) trypsin, 1mM EDTA. Stored at −20°C.

2.1.7 Bacterial strains

DH5α: grown on/in LB medium at 37°C.

2.1.8 Bacterial cell culture media and related reagents

Ampicillin stock solution: 50mg/ml ampicillin in dH_2O. 0.2µm filter sterilised and stored at −20°C. Added to LB medium to 100µg/ml.

Blue/white selection LB agar plates: 40µl 100mM IPTG, and 40µl 40mg/ml X-gal, was spread over LB agar plates containing the appropriate antibiotic(s). The plates were dried at r/t before being used the same day.

Choramphenicol stock solution: 34mg/ml chloramphenicol in 96% (v/v) ethanol. Stored at −20°C protected from light. Added to LB medium to 34μg/ml.

Competent cell buffer A: 100mM RbCl, 50mM $MnCl_2$, 30mM KOAc, 10mM $CaCl_2$, 15% (v/v) glycerol. The pH was adjusted to 5.8. 0.2μm filter sterilised and stored at 4°C.

Competent cell buffer B: 10mM MOPS, 10mM RbCl, 75mM $CaCl_2$, 15% (v/v) glycerol. The pH was adjusted to 6.8. 0.2μm filter sterilised and stored at 4°C.

IPTG stock solution: 1M IPTG in dH_2O. 0.2μm filter sterilised and stored at −20°C.

Kanamycin stock solution: 10mg/ml kanamycin in dH_2O. 0.2μm filter sterilised and stored at −20°C. Added to LB medium to 40μg/ml.

Miniprep solution 1: 25mM Tris HCl pH8.0, 10mM EDTA, 50mM glucose. Stored at 4°C.

Miniprep solution 2: 200mM NaOH, 1% (w/v) SDS. Prepared immediately prior to use.

X-gal stock solution: 40mg/ml X-gal in dimethylformamide (DMF). Stored at −20°C protected from light.

2.1.9 Oligonucleotides

Custom oligonucleotides were purchased from Sigma-Genosys. Lyophilised oligonucleotides were resuspended in dH_2O to 100pmol/μl. PCR stocks were diluted in dH_2O to 25pmol/μl, and DNA sequencing stocks were diluted in dH_2O to 1pmol/μl. Resuspended oligonucleotides were stored at −20°C.

PCR primers

Name	Sequence (5′-3′)	Description
MC1R(F)	ATGAACTAAGCAGGACACC TGGAG	MC1R forward primer
MC1R(R)	GGGACCAGGGAGGTAAGGA ACTGC	MC1R reverse primer
BRAF Bts1 (F)	GGTGATTTTGGTCTAGCTGC A	BRAF forward primer 1 (Bts1 assay)
BRAF (F)	TCATAATGCTTGCTCTGATA GG	BRAF forward primer 2 (Bts1 assay)
BRAF (R)	GGCCAAAAATTTAATCAGTG GA	BRAF reverse primer 1 (Bts1 assay)
BRAF Xba1 (F)	TAAAAATAGGTGATTTTGGT CTAGCTCTAG	BRAF forward primer 1 (Xba1 assay)
BRAF Xba1 (R)	ACTATGAAAATACTATAGTT GAGA	BRAF reverse primer 1 (Xba1 assay)
BRAF (R2)	TGGATCCAGACAACTGTTCA AA	BRAF reverse primer 2 (Xba1 assay)
BRAF (R3)	CCTCAATTCTTACCATCCAC A	BRAF reverse primer 3 (Xba1 assay)
BRAF (R4)	GGCCCAAAAATTTAATCAGT GGGAAAAATAG	BRAF forward primer 4 (Xba1 assay)

Real-time PCR primers

Name	Sequence (5′-3′)	Description
MC1R (RT) F	TGTCGTCTTCAGCACGCTCTT	MC1R forward primer
MC1R (RT) R	ACGTACAGCACGGCCATGA	MC1R reverse primer
B-actin F	ATCCCCCAAAGTTCACAATG	B-actin forward primer
B-actin R	GTGGCTTTTAGGATGGCAAG	B-actin reverse primer

2.1.10 Plasmids

Name	Source
pGEM®-T Easy	Promega

2.1.11 Antibodies

Antibody	Antigen retrieval	Dilution	System
B-catenin (Dako M3539)	Pressure cooker EDTA	1:80	Envision
Bcl-2 (Dako M0887)	Pressure cooker EDTA	1:50	Envision
E-cadherin (Dako M3612)	Pressure cooker EDTA	1:25	Envision
Galectin-3 (Cedarlane 8942F)	Pressure cooker EDTA	1:150	Biosystems
Ki67 (Dako M7240)	Pressure cooker citrate	1:200	Envision
S100 (Dako Z0311)	Pressure cooker citrate	1:1000	Envision

2.2 Methods

2.2.1 Preparation of genomic DNA from cell lines

Genomic DNA was extracted from melanoma and ovarian cancer cells using the same method. Cells were harvested by trypsinisation and pelleted by centrifugation at 1,300 rpm for 5 minutes. The pellet was resuspended in PBS and digested overnight at 37°C in 750µl DNA isolation buffer supplemented with proteinase K to a final concentration of 280µg/ml. The supernatant was extracted twice with 750µl PCA (25 parts redistilled phenol, 24 parts chloroform, 1 part isoamyl alcohol) and vigorous shaking and subsequently with 750µl CA (24 parts chloroform, 1 part isoamyl alcohol) to remove traces of phenol. The DNA was precipitated for 10 minutes at room temperature by addition of 750µl of isopropanol. Following 10 minutes centrifugation, the nucleic acid pellet was washed twice with 70% ethanol, dried, resuspended in 200µl sterile distilled water and stored either at 4°C in the short term or -20°C for longer periods.

2.2.2 Preparation of genomic DNA from melanoma tissue samples

Melanoma tissue cores were de-paraffinised with xylene (1ml). Following centrifugation, the supernatant was discarded and the samples were then washed with 100% ethanol and allowed to dry. DNA was isolated from the deparaffinised tissue using the QIAquick DNA isolation kit (QIAGEN). In brief, samples were resuspended in buffer ATL (15µl) and proteinase K (10µl), mixed thouroughly and incubated at 56°C overnight. 25µl of buffer ATL and 50 µl of buffer AL followed by 50µl of ethanol were added and after incubation at room temperature for 5 minutes the samples were added to QIAamp MiniElute columns and centrifuged at 6000g for 60 seconds. 500µl of buffer AW1 was added to the columns and they were centrifuged again at 6000g for 60 seconds. This process was repeated with buffer

AW2. 25µl of water was added to the column and DNA was eluted by centrifugation at 20000g for 60 seconds.

2.2.3 Measurement of DNA concentration

RNAse treated DNA samples were diluted in 1ml of distilled water and the absorbency at 260 and 280nm measured in a spectrophotometer. Double stranded DNA of concentration 50µg/ml has an $OD_{260nm} = 1.0$.

2.2.4 Electrophoresis of DNA in agarose gels

DNA fragments were separated on 0.8-3% (w/v) agarose gels containing 0.5µg/ml ethidium bromide and 1X TBE. DNA samples were mixed with 1/5 volume of 5X sample buffer prior to loading. Electrophoresis was carried out at 30-100V in 1X TBE buffer. DNA was visualised by UV illumination and Hyperladder I^{TM} was used as a size marker.

2.2.5 Purification of DNA from agarose gels

DNA fragments required for cloning were resolved by agarose gel electrophoresis and were purified using the QIAquick gel extraction kit (QIAGEN) according to the manufacturer's instructions.

2.2.6 Transfer of DNA from agarose gels to membranes (Southern Blotting)

An appropriate restriction enzyme (Pst1) was used to cut 10 µg of DNA and the resulting fragments were separated by agarose gel electrophoresis. The gel was then

soaked in denaturation buffer for 30 minutes and the DNA was transferred onto a Genescreen Plus nylon membrane (New England Nuclear) by capillary action. Denaturation buffer was employed as the transfer medium. A wick was made from wet blotting paper, placed on a platform with both ends submerged in a denaturation buffer reservoir. The gel was laid on top of the wick and a sheet of nylon membrane was placed on top and overlaid by three sheets of moistened blotting paper and a stack of dry paper towels. Transfer was allowed to proceed for 12-24 hours after which time the membrane was neutralised in neutralising buffer for 30 minutes and air-dried.

2.2.7 Labelling DNA by random priming with nonamer primers (Megaprime™ DNA labelling system)

Radioactively labelled DNA was obtained using a randomly primed DNA labelling method. The Megaprime method (Amersham) is based on the hybridisation of a mixture of many different nonamer nucleotides to the DNA which allows small amounts of DNA to be labelled to high specific activities. The complementary strand is synthesised from the 3'OH termini of the primer using Klenow polymerase, simultaneously incorporating radiolabelled dCTP into the newly synthesised DNA strand. Approximately 10ng of DNA was dissolved in 28µl of sterile distilled water and denatured by boiling for 5 minutes. 10µl of labelling buffer, 50µCi of α-^{32}PdCTP and 2 units of Klenow polymerase were added, and the mixture was incubated at 37°C for 15 minutes.

2.2.8 Separation of unincorporated radionucleotides

Unincorporated nucleotides were separated from the labelled DNA by chromatography on a NICK R Column (Pharmacia). The column was first

equilibrated with TE and the labelling reaction was then added. 400µl of TE was added and the labelled DNA was eluted by the addition of a further 400µl TE.

2.2.9 Hybridisation

Membranes onto which DNA or RNA had been transferred were first blocked by prehybridising in 30ml of modified Church buffer for 2 hours at 65°C. Hybridisation was performed by addition of denatured radiolabelled probe to the prehybridisatioon mixture and incubation for a further 12-24 hours at 65°C (or 60°C for RNA). Following hybridisation, non-specifically bound DNA molecules were removed by washing with 2X SSC at room temperature. The membrane was then immersed in 2X SSC, 1% (w/v) SDS for 30 minutes at 65°C. The membrane was then sealed in a plastic bag to prevent drying out and radioactive DNA molecules bound to the membrane were then visualised by autoradiography or phosphorimagery.

2.2.10 Removal of probes

Southern filters were boiled three times for 10 minutes with gentle shaking in 0.1X SSC, 1% (w/v) SDS. Northern filters were washed five times for 3 minutes in hot 0.1X SSC, 0.01% (w/v) SDS. The blots were then autoradiographed to confirm that dehybridisation was complete. Filters were then dried and the hybridisation could be repeated as above.

2.2.11 Autoradiography

In order to visualise radioactive molecules hybridised to membranes autoradiography was performed using Hyperfilm™ MP autoradiography film in a cassette conataining intensifying screens (Cronex Lightning Plus, Du Pont). Cassettes were stored at -

70°C during exposure to slow the reversal of activated bromide crystals to their stable form and give an enhanced signal.

2.2.12 DNA ligation

DNA ligation reactions were performed in a 20µl volume, and contained 5 Weiss units T4 DNA ligase, Rapid ligation buffer (both Fermentas Life Science) and 50ng vector DNA. A 3:1 molar ratio of insert DNA to vector DNA was present in each reaction. DNA ligation reactions were incubated for 1h at r/t, then 5µl was transformed into a 200µl aliquot of competent bacterial cells.

2.2.13 Restriction digestion

Restriction digests contained 4U restriction enzyme (New England BioLabs)/µg DNA and the appropriate reaction buffer, and were supplemented with 100µg/ml BSA if required. Restriction digests were incubated at the appropriate temperature for the restriction enzyme (usually 37°C) for a minimum of 2h.

2.2.14 Polymerase chain reaction

The polymerase chain reaction (PCR) was used to amplify specific DNA molecules from a DNA template. Routine PCRs were prepared in a 50µl volume containing Taq PCR buffer (Promega), 2.5mM $MgCl_2$, 1U Taq DNA polymerase (Promega), 0.5pmol/µl forward and reverse primers, 0.25mM dNTPs and 1µl genomic DNA template. A negative control that contained no template DNA was also prepared.

The PCR cycling conditions were as follows: initial DNA denaturation at 94°C for 3 min, then 30-38 cycles of DNA denaturation at 95°C for 60s, primer annealing at 50-65°C for 60s, and DNA polymerase extension at 72°C for 1min/kb PCR product. The

primer annealing temperature was based on primer-specific recommendations from the oligonucleotide supplier and empirical observations. After PCR cycling, the PCRs were incubated at 72°C for 10min in order to extend any remaining incomplete PCR products. 5µl of each PCR was analysed by agarose gel electrophoresis.

2.2.15 DNA sequencing

Prior to sequencing, plasmid DNA was purified using a QIAGEN plasmid preparation kit and PCR products were purified using a QIAquick PCR purification kit (Qiagen) according to the manufacturer's instructions. DNA sequencing was performed using the BigDye Terminator v3.1 Cycle Sequencing kit (ABI). DNA sequencing reactions contained 2µl BigDye Terminator v3.1, 3.2pmol primer and 50-300ng DNA template in a 10µl volume, and were incubated under the following conditions: initial DNA denaturation at 96°C for 1min, then 25 cycles of DNA denaturation at 96°C for 10s, primer annealing at 50°C for 5s, and extension at 60°C for 4min. Sequencing reactions were cleaned up and were run on an ABI 3730 capillary sequencer by the School of Biological Sciences Sequencing Service. DNA sequence data was analysed using Lasergene software (DNA Star).

2.2.16 Preparation of RNA (RNA-Bee method)

Total RNA was extracted from cultured mammalian cells using the commercially available reagent RNAzol^{TM}B. Cultured cells were lysed directly in the culture dish by the addition of RNAzol^{TM}B (0.2ml per 10^6 cells) and the RNA was solubilised by pipetting the lysate several times. The RNA was extracted by the addition of 0.2 ml chloroform per 1ml RNAzol^{TM}B followed by vigorous shaking of the mixture for 30 seconds. The suspension was then centrifuged at 12000g for 15 minutes at 4^{o}C. The aqueous phase was transferred to a fresh tube and an equal volume of isopropanol was added. RNA was allowed to precipitate at room temperature for 10 minutes and

then pelleted by centrifugation at 12000g for 5 minutes. The RNA pellet was then washed in 70% ethanol and centrifuged at 7500g for 5 minutes. The pellet was allowed to air dry before being resuspended in 50µl of sterile distilled water for storage at -70°C.

2.2.17 Measurement of RNA concentration

The OD_{260nm} and OD_{280nm} of RNA samples were measured in a spectrophotometer. An OD_{260nm} of 1 = 40µg/ml ssRNA, and an OD_{260nm}:OD_{280nm} ratio of 1.8-2.0 indicates the absence of residual protein or phenol from the RNA sample. An OD_{260nm}:OD_{280nm} ratio of <1.8 suggests the presence of contaminants in the RNA sample.

2.2.18 Electrophoresis of RNA in agarose gels

The separation of RNA on the basis of molecular weight was achieved by the electrophoresis of RNA denatured in a formaldehyde-formamide sample buffer in non-denaturing TAE agarose gels. RNA samples were electrophoresed on denaturing 1.4% (w/v) agarose gels containing 0.5µg/ml ethidium bromide, 1X MOPS and 0.66M formaldehyde. 20µg of total RNA in 20µl of sterile distilled water was added to an equal volume of formamide sample buffer and ¼ volume of 5X sample buffer. Samples were heated for 5 minutes at 65°C and snap chilled on ice immediately prior to loading. Electrophoresis was carried out in a 1X MOPS buffer system at 100V for 3-4 hours.

2.19 Transfer of RNA from agarose gels to membranes (Northern Blotting)

Following electrophoresis the gel was soaked in 10X SSC with gentle agitation for 20 minutes. This procedure was repeated once prior to transfer. The method used for transfer was as described for DNA except that 10X SSC was used as the transfer medium. On completion of transfer the membrane was rinsed in 2X SSC and baked for 2 hours at 80°C.

2.2.20 Reverse transcription of RNA

Total RNA samples were treated with DNase 1 to ensure removal of contaminating DNA prior to reverse transcription using a DNA-free Kit (Ambion) according to manufacturer's instructions. cDNA was prepared from RNA using the Retroscript Kit (Ambion) following manufacturer's instructions. In brief, 2µg of total RNA was mixed with 2µl of random decamers, mixed and then denatured at 70°C for 3 minutes. 2µl 10 x RT buffer, 4µl dNTPs, 1µl RNase inhibitor, and 1µl reverse transcriptase enzyme were then added, incubated at 42°C for 1 hour and then heated to 92°C for 10 minutes to inactivate the RT.

2.2.21 Real-time PCR

Real-time PCR was used to quantify the abundance of various cDNAs of interest using SYBR Green I detection chemistry and a MyCyclerTM Real-Time PCR detection system (Bio-Rad). SYBR Green I is a fluorescent molecule that can bind to dsDNA and then absorb light with a wavelength of 498nm and emit light with a wavelength of 522nm. This enables the amplification of a PCR product to be measured continuously over time. Real-time PCR reactions were prepared in a 20µl volume using iQ SYBR Green I Supermix (BioRad). This supermix contains PCR buffer, hot-start iTaq DNA polymerase, dNTPs and SYBR Green I dye. Prior to PCR

cycling, a cDNA template and forward and reverse primers specific to a particular gene were added (2.5µl cDNA and a final primer concentration of 0.5pmol/µl). Each cDNA sample was assayed in triplicate with two primer pairs; one pair was specific to the gene of interest (MC1R), and the other pair was specific to the reference gene (B-actin). To evaluate the primers used and the efficiency of the real-time PCR, a dilution series of a cDNA sample was also analysed in duplicate with each primer pair (the magnitude of the dilution used depended on the expected differences in the abundance of the amplified cDNA). Finally, a duplicated negative control that contained no template cDNA was included.

The PCR cycling conditions were as follows: 95°C for 3min (initial DNA denaturation and iTaq DNA polymerase activation), then 40 cycles of DNA denaturation at 95°C for 45s and primer annealing at 55-60°C for 45s. The primer annealing temperature was based on primer-specific recommendations from the oligonucleotide supplier and empirical observations. A DNA polymerase extension step at 72°C was not required as the amplicons are short enough to be copied as the thermal cycler increases in temperature from the primer annealing temperature to the DNA denaturation temperature (95°C). When PCR cycling was complete, melt curve analysis was performed. DNA was denatured at 95°C for 1min and annealed at 35°C for 10s. The temperature was then increased to 95°C in 120 steps, each consisting of a 10s incubation at a temperature 0.5°C higher than the preceding step. The continuous measurement of fluorescence throughout the melt curve cycle allows the determination of the T_m of the ds DNA molecule(s) present.

The dilution series of a cDNA sample with a specific primer pair allows the calculation of two values: the correlation coefficient and the PCR efficiency, which in turn allow the evaluation of the primer pair and the efficiency of the real-time PCR. The correlation coefficient is a measure of the correlation between the amount of cDNA template present and the amplification of the cDNA dilution series. The PCR efficiency is a measure of the amount of DNA that is copied per cycle. The melt curve is used to verify that the PCR amplifies a single dsDNA product. Different amplicons have different melt curves because of different lengths and different base compositions. The melt curve can be used to determine whether primer dimers are

present because primer dimers are usually shorter than the PCR product and subsequently have a lower T_m.

The relative abundance of MC1R cDNA and B-actin cDNA was calculated using the standard curve method. A standard curve was constructed from mRNA of known concentration and then used as a reference standard for extrapolating quantitative information for the mRNA targets of unknown concentration.

2.2.22 siRNA nucleofection

SMARTpool siRNA oligos contain four highly functional duplexes that target different regions of the target gene. They were resuspended in 1X siRNA Buffer (Dharmacon, Inc.) to 20μM (stock). The stock solutions were stored in small aliquots at -20°C. A nucleofector (Amaxa Biosystems) was used for transfections into G361 cells. Cells were plated into 6-well plates 3 days prior to transfection. When they reached 70-80% confluency the cells were trypsinised and counted using a Coulter counter (Beckman Coulter). $1x10^6$ cells were then centrifuged at 1000xg for 5 minutes and the pellet resuspended in 100μl of the appropriate nucleofector solution (Amaxa Biosystems). pmaxGFP Vector (2μg) or 100nM siRNA solution (0.25ml of siRNA stock solution) was added to each and the solution was transferred to a cuvette. Cells were then electroporated in the nucleofector. A number of different nucleofector solutions and nucleofection programmes were tested in order to establish optimum nucleofection conditions (see Chapter 4). The cuvette was removed from the machine immediately following electroporation and 500μl of warmed medium was added to the cell. The cells were then transferred into a six well plate containing 1 ml of medium using the pipettes provided. Controls included cells with no siRNA/vector or cells with siRNA/vector but no electroporation.

2.2.23 Assessment of transfection efficiency

Twenty-four hours after nucleofection with pmaxGFP vectorm, media from the G361 cultures was collected. Cells were then trypsinised and resuspended in PBS. The trypsinised cells and the media taken off before trypsinisation were combined, pelleted by centrifugation and then resuspended in 190µl binding buffer and 10µl propidium iodide solution. Transfection efficiency was assessed using flow cytometry which detected cells that contained GFP (transfected cells) as well as cells which took up propidium iodide (non-viable cells).

2.2.24 Isolation of protein lysates from mammalian cells

Cells were trypsinised, washed with PBS and then pelleted by centrifugation. Cell pellets were resuspended in 50-100µl RIPA lysis buffer and maintained on ice for 15 minutes. Complete Protease Inhibitor Cocktail (Roche) was added to protect protein against protein degradation. Cell lysates were passed up and down a small bore syringe needle repeatedly to break up DNA. Samples were centrifuged x 15 minutes at 13,200 rpm at 4°C and the supernatant was collected.

2.2.25 Measurement of protein concentration

Protein concentrations were measured using the Bio-Rad Protein assay. This assay is based on protein binding by Coomassie Brilliant Blue G-250 in an acidic solution, and the associated change in the absorbance maximum from 465nm to 595nm. Protein samples were incubated with a 1:5 dilution of the dye reagent for 10min, then the OD_{595} was measured in a spectrophotometer. 0.5, 1, 2, 5, 10 and 20µg bovine serum albumin (BSA) were used to prepare a standard curve each time the assay was performed. The concentrations of the protein samples of interest were determined by

substitution of the measured OD_{595} values into the equation that describes the BSA standard curve.

2.2.26 SDS polyacrylamide gel electrophoresis

The separation of proteins on the basis of molecular weight was achieved by denaturing SDS polyacrylamide gel electrophoresis (SDS PAGE), using the vertical electrophoresis Mini-PROTEAN 3 and PROTEAN II systems (both Bio-Rad). The polyacrylamide separating gels were between 8% and 15% (w/v) depending on the molecular weight of the protein(s) of interest. 5% (w/v) polyacrylamide stacking gels were used. Protein samples (in SDS PAGE loading buffer) and pre-stained protein marker, broad range (6-175kD; New England BioLabs) were incubated at 100°C for 5min, before being loaded into the wells of the stacking gel. 30 micrograms of total protein was loaded per gel track. SDS PAGE gels were run at constant current (mini-PROTEAN 3 gels were run at 17.5mA, and PROTEAN II gels were run at 25mA) in Tris-glycine electrophoresis buffer.

2.2.27 Western Immunoblotting

Proteins were transferred onto an Immobilon-P PVDF transfer membrane (Millipore, Billerica, Massachusetts) according to the method of Towbin 1979, using a Mini Trans-Blot system (Biorad) at 100V, constant voltage at 4°C. Non-specific binding sites on the western blot were blocked by incubation in 5% (w/v) commercial dried milk powder in TBST (10mM Tris-HCl, 0.15M NaCl, 0.05% (wt/vol) Tween 20, pH8.0) for 1 hour at room temperature followed by incubation with primary antibody TBST. Blots were then incubated with horseradish-peroxidase-conjugated secondary antibody diluted in TBST for 1 h at room temperature. Immunoreactive bands were visualized using chemiluminescence (ECL plus, Amersham Biosciences, Buckinghamshire, UK).

2.2.28 Production of MC1R probe

The pGEM®-T Easy vector System was used to clone the MC1R PCR product. 2µl of MC1R PCR product was incubated with 5µl 2x rapid ligation buffer, 1µl pGEM®-T Easy vector and 1µl of T4DNA ligase in 10µl of dH_20 at room temperature for 1 hour. 2µl of the ligation reaction was then added to 50µl of DH5α cells. This was incubated on ice for 30 minutes and then placed at 37°C for 20 seconds. 400µl of pre-warmed L-broth was then added and cells were incubated at 37°C for 1 hour with vigorous shaking. 20µl of cells were then spread on pre-warmed agar plates with ampicillin selection and incubated overnight at 37°C. 30µl of X-Gal was spread over the surface of the plate to enable blue-white colour selection of colonies containing recombinant plasmids. White colonies were grown overnight at 37°C in 5ml L-broth supplemented with ampicillin to a final concentration of 50µg/l. 1.5ml of the culture was transferred to a microfuge tube and the cells pelleted by centrifugation for 1 minute. The pellet was resuspended in 100µl of solution P1 and the cells lysed by addition of 200µl of solution P2. 150µl of 3M sodium acetate pH5 was then added and the precipitated chromosomal DNA, SDS and protein was sedimented by centrifugation for 5 minutes. The supernatant was transferred to a new tube and the plasmid DNA was precipitated by addition of 0.5 ml isopropanol on ice for 10 minutes. Following centrifugation for a further 10 minutes the pellet was washed with 70% ethanol and then dissolved in 50µl of dH_20. Samples that contained vector which had incorporated the MC1R sequence were recognised by production of a 1.2kb band following restriction digestion with EcoR1.

2.2.29 Bacterial growth conditions

Bacterial cells were recovered from frozen glycerol stocks by scraping the surface of the frozen stock with a sterile loop, and then streaking the loop across an LB agar plate containing the appropriate antibiotic(s). Plates were incubated inverted at 37°C

o/n. Liquid bacterial cultures were grown in LB broth containing the appropriate antibiotic(s). A single bacterial colony was inoculated into a small volume of LB broth (usually 5ml) and the culture was incubated at 37°C with shaking at 200rpm o/n.

2.2.30 Preparation of competent bacteria

A 5ml o/n bacterial culture in LB broth was prepared, and was diluted into 500ml LB broth the following morning (a culture flask with a volume of at least 4× the volume of the culture was used). The culture was then incubated at 37°C with shaking until an OD_{650nm} of 0.5 was reached. The bacterial cells were incubated on ice for 10min, then pelleted by centrifugation at 2,400rpm for 15min at 4°C. The cell pellet was resuspended in 165ml ice cold Competent cell buffer A, and the resuspended cells were incubated on ice for 45min before being pelleted again. The cell pellet was resuspended in 40ml ice cold Competent cell buffer B, and the resuspended cells were incubated on ice for 15min. 200µl aliquots of the competent cells were flash frozen in liquid N_2 and were stored at −70°C. The transformation efficiency of the competent bacterial cells was tested by the transformation of defined amounts of plasmid DNA (transformation efficiencies of $>10^6$ colonies/µg DNA were considered to be successful).

2.2.31 Transformation of bacteria by heat shock

Aliquots of competent bacterial cells were thawed on ice. 10-100ng of plasmid DNA, or 5µl of a ligation reaction, was added to a tube of competent bacterial cells, and the tube was mixed gently. A positive control consisting of plasmid DNA of known quality, and a negative control consisting of dH_2O alone, was also included in each group of bacterial transformations. The mixture of cells and DNA was incubated on ice for 30min, before being heat shocked in a 42°C water bath for 1min30s and

incubated on ice for 2min. 1ml LB broth was added and the transformations were incubated at 37°C for 1h with shaking. This incubation allows plasmid-encoded genes that confer antibiotic resistance to be expressed. Aliquots of the transformations were then plated out onto LB agar plates containing the appropriate antibiotic(s). When a high transformation efficiency was expected, e.g. when miniprepped plasmid DNA was transformed, 25µl of the transformation was plated out. However, when a low transformation efficiency was expected, e.g. when a DNA ligation reaction was transformed, the whole transformation was plated out. The plates were inverted and incubated at 37°C o/n.

2.2.32 Isolation of plasmid DNA from bacteria

E. coli strain DH5α was routinely used for cloning and plasmid isolation. This strain has a mutation in the *recA* gene, which encodes a protein involved in DNA recombination. The absence of the recA protein therefore increases the stability of plasmid inserts within the host cells. DH5α also has a mutation in the *endA* endonuclease gene, allowing the isolation of high quality plasmid DNA. Finally, DH5a also has a mutation in *hsdR*; this inactivates the *Eco*K I endonuclease and thereby prevents the cleavage of plasmid DNA by the *Eco*K I restriction and modification system.

The following protocol describes a cost-effective method to isolate crude plasmid DNA that is suitable for use in restriction digest-based screening of DNA constructs. 2ml o/n bacterial culture in LB broth was centrifuged at 6,000rpm for 1min, and the cell pellet was resuspended in 100µl Miniprep solution 1 with 100µg/ml RNase A. The cells were then lysed under alkaline conditions by the addition of 200µl Miniprep solution 2, and the mixture was neutralised with 150µl 5M KOAc pH4.8. The cellular debris, cell wall-bound chromosomal DNA and the denatured proteins were pelleted by centrifugation at 14,000rpm for 5min. The plasmid DNA was recovered from the supernatant by ethanol precipitation, and was resuspended in

50µl TE pH7.4. 3µl plasmid DNA prepared according to this protocol was used in analytical restriction digests. Plasmid DNA was stored at −20°C.

When plasmids were required for DNA sequencing, or when larger quantities of plasmid were needed, plasmid DNA was isolated using QIAGEN Mini, Midi and Maxi prep kits according to the manufacturer's instructions.

2.2.33 Mammalian cell growth conditions

Prior to defrosting mammalian cells, the appropriate cell culture medium was pre-warmed to 37°C. The stock of frozen cells was quickly thawed in a 37°C water bath. 5ml medium was added drop-wise to the cells, and the cell suspension was incubated at r/t for 2min. A further 10ml medium was added drop-wise, then the cells were pelleted by centrifugation at 1,300rpm for 3min. A single cell suspension was prepared in fresh medium and transferred to a cell culture plate (10ml medium/10cm diameter plate). The volume of medium and the diameter of the plate used were determined by the amount of cells in the stock. Plates were incubated at 37°C in 5% CO_2.

When the cells were confluent, the plate was washed with PBS before being incubated with trypsin-EDTA (1ml/10cm diameter plate) for 3-5min. Trypsin is a serine protease that can mediate the detachment of cells from the cell culture plate surface. After cell dissociation from the surface, fresh medium (10ml/10cm diameter plate) was added, and a single cell suspension was prepared. The cells were pelleted by centrifugation at 1,300rpm for 3min and were resuspended in fresh medium. The required volume of the cell suspension was transferred into a new cell culture plate with an appropriate volume of additional medium. As commonly used mammalian adherent cell lines divide approximately once every 24h, and cells were routinely passaged to 12.5-25% confluency, passaging was carried out once every 2-4d.

2.2.34 Cryopreservation of cell lines

When preparing a stock of frozen cells, cells were trypsinised and spun down as described above. The cell pellet was then resuspended in cell culture medium containing 10% (v/v) DMSO (cells from a 10cm diameter plate were resuspended in 1ml total volume). The presence of DMSO increases the survival of cells during freezing and thawing by minimising the formation of ice crystals within the cells. The cell stocks were stored at −20°C for 1h, then at −70°C o/n, before being transferred to a liquid N_2 cryostore for indefinite storage.

2.2.35 Primary Culture

Following surgery, a small portion of tissue that was macroscopically consistent with melanoma was cut from the main surgical specimen and placed in a sterile container on wet ice for immediate transfer to the laboratory. The size of the tissue was typically around $5mm^3$. Following mincing and trypsinisation the tissue was plated in t25 culture flasks and then observed over a period of several weeks. Variations from standard culture conditions are described in Chapter 4.

2.2.36 Counting of cells

Cells were diluted 1:100 in isotone and counted using the Coulter Counter Z series (Beckman Coulter).

2.2.37 Cell survival assays

Cells were plated onto 30mm dishes in duplicate at a density of $2.5x10^5$ cells per dish (or $7.5x10^4$ cells per dish for ovarian cell lines) and after 24 hours the medium was

aspirated. For UV survival assays 0.2ml of PBS was added and the dishes were UV irradiated at the doses described using a UV lamp (254nm). Immediately after UV irradiation normal medium was replaced. For cisplatin survival assays medium was aspirated after 24 hours and replaced with medium containing cisplatin at the doses described. After 24 hours the cisplatin-containing medium was removed and replaced with normal medium. For α-MSH survival assays medium was aspirated after 24 hours and replaced with medium containing α-MSH at doses of 1pM to 1 μM. This medium was replenished every 48-72 hours. All dishes were incubated for a further five days or until the control dishes were confluent. For MC1R antibody assays media was aspirated after 24 hours and replaced with medium containing MC1R antibody at doses of 10ng/ml to 10μg/ml. This medium was replenished every 48 hours. All dishes were incubated for a further five days or until the control dishes were confluent. The cells were fixed with Carnoy fixative (3:1 methanol: glacial acetic acid) and stained with Crystal Violet. Cell survival was then determined by extracting the dye from the stained cells using 70% ethanol and measuring optical density at 575nm. Each UV, cisplatin, α-MSH or MC1R antibody dosage was performed in duplicate and survival determined relative to untreated control dishes.

2.2.38 Proliferation assay

Cells were plated at a density of 2×10^3 cells per well in a 12 well dish in DMEM supplemented with antibiotics, NEAA, glutamate and FCS. Every 48 hours duplicate dishes were trypsinised and counted using a Coulter counter.

2.2.39 Microscopy

Cultured cells were viewed using a Leitz Labovert FS phase contrast microscope. Cells or tissue sections stained by immunohistochemistry were viewed by light microscopy on an Olympus BX51 using DP software (Olympus).

2.2.40 Generation of xenografts

Cells were grown in standard culture dishes and then trypsinised and counted. 10^7 cells were resuspended in 0.1ml DMEM media with or without matrigel and injected subcutaneously into the flanks of SCID mice. 5 mice were used for each cell line and each mouse had an injection on either flank (one with and one without matrigel). Growth was monitored over a 16 week period.

2.2.41 Determination of apoptosis by Annexin V staining

In early stages of apoptosis, phosphatidylserine (PS) is translocated from the inner part of the membrane to the outer layer and thus becomes exposed at the external surface of the cell. Annexin V is a phospholipid-binding protein with high affinity for PS and is therefore suitable for detecting apoptotic cells.

Cells were plated onto 60mm dishes at a density of $3x10^5$ cells (melanoma) or $2.5x10^5$ cells (ovarian cell lines) per dish. After twenty-four hours cells were treated with UV (0, 10 or 30 J/m^2) or cisplatin (5 or 20μM). For assays involving the use of α-MSH cells were pre-incubated with α-MSH for 24 hours prior to UV or cisplatin exposure. Twenty-four hours after treatment medium from each dish was collected and cells were trypsinised. Cells were then pelleted and resuspended in 0.5ml PBS. Following further centrifugation cells were resuspended in 195μl binding buffer (10mM Hepes/NaOH, pH7.4, 140mM NaCl, 2.5mM $CaCl_2$) and stained with AnnexinV-FITC (5μl). After sitting at room temperature for 10 minutes cells were pelleted and resuspended in 190μl binding buffer and 10μl propidium iodide (20μg/l stock). Immediately after staining, samples were analysed by flow cytometry (Beckman Coulter Inc, Miami, Florida) using Expo^{TM}32 ADC software.

2.2.42 DNA content assay

Cells were plated and treated as per the method above. Twenty-four hours after UV irradiation (or cisplatin treatment) medium and cells were harvested as above and then resuspended in 100µl citrate buffer. Cells were treated with 425µl trypsin (30µg/l) and 325µl trypsin inhibitor (0.5mg/ml) was then added after ten minutes. After a further 10 minutes 250µl propidium iodide (0.42mg/ml) was added and samples were analysed by flow cytometry (Beckman Coulter Inc, Miami, Florida) using Expo^{TM}32 ADC software.

2.2.43 Immunocytochemistry of mammalian cells

For immunocytochemistry studies cells were grown on cover slips in 12 well plates. Media was aspirated from cells and they were then washed with PBS prior to being fixed in 4% formaldehyde for 5 minutes. They were then rinsed with PBS then incubated with 0.1% Triton in order to permeabilise the cells. Hydrogen peroxidase activity was blocked by incubation in 5% hydrogen peroxide for 5 minutes. Cells were incubated in blocking serum for 10 minutes prior to incubation with primary antibody. Cells were then incubated in secondary antibody followed by Strep ABC using the Vectastain kit (Vector Labs.). This procedure employs biotinylated antibody and a preformed Avidin: Biotinylated enzyme complex. Detection was by means of DAB staining for 2 minutes. Between each step cells were rinsed with PBS. Cells were dehydrated in graduated ethanol and then xylene and mounting onto glass slides using Pertex mounting medium. Controls without primary antibody and without secondary were used for each experiment.

2.2.44 Patient Samples

Formalin-fixed, paraffin-embedded melanoma and naevi specimens were obtained with local ethics committee approval from the pathology department, Royal Infirmary, Edinburgh. A full description of the patients and samples used is given in chapter 5.

2.2.45 Construction of TMAs

A full description of construction of the tissue microarrays is given in chapter 5.

2.2.46 Immunohistochemistry

Formalin-fixed, paraffin embedded sections of melanoma, naevi or tissue microarray sections were deparaffinised in xylene, and rehydrated in graduated alcohol, to water. Antigen retrieval was by microwave pressure cooking in Tris/EDTA buffer (pH8.0) or citric acid (pH6.0) for 20 mins. Slides were incubated in hydrogen peroxide for five minutes in order to block endogenous peroxidase activity. Sections were incubated with primary antibody in dilution buffer (DAKO ChemMate Ab diluent). Slides were then rinsed in TBS and incubated for 30 mins in secondary antibody (DAKO REAL Envision Horseradish peroxidase Rabbit/Mouse). After rinsing in TBS, sections were incubated in DAB for 10 minutes, counterstained, dehydrated and mounted. For automated staining the Bond^{TM} automated immunohistochemistry system was used as per the manufacturer's instructions. For each staining run a negative, no-antibody control was included. Stained sections were examined without knowledge of the outcome of individual cases.

2.2.47 Immunohistochemistry scoring system

Protein expression was assessed by staining intensity, frequency and location. The intensity of the staining was scored according to a 4 point scale: 0 = no staining, 1 = weak, 2 = moderate, 3 = strong. The frequency of cells staining at each of the 4 intensities was then multiplied by the intensity score to give an overall staining 'histoscore' up to 300. Slides were examined by 2 independent observers, including a histopathologist, without knowledge of the outcome of individual cases. Where examination of the staining pattern indicates localisation to different cellular compartments, samples were scored separately for nuclear, cytoplasmic or membranous staining.

2.2.48 Statistics

Power calculations were performed in order to ensure sufficient numbers of patients were included in the study to detect differences in protein expression between groups. Each calculation estimated the minimum effect size required to achieve an 80% power with a significance level of 0.005 (to allow for the number of simultaneously-tested proteins in each analysis, but slightly less conservatively than with a Bonferroni correction). The numbers of samples to be included on the TMAs were assumed to be 400 primary melanomas and 50 of each other category (naevi, dysplastic naevi, in-situ melanomas and metastatic melanomas). The following conclusions were made:

1 It would be possible to detect a reduction in strong expression prevalence of 28% or more in primary melanoma patients or 38% or more in any of the other groups (assuming strong expression is found in 60-75% of metastatic melanoma patients).

2 It would be possible to detect a difference of 20% or more between those individuals with *thin* (frequency 0.6) or *thick* (frequency 0.4) primary

tumours (assuming the *thick* tumour group has a strong expression prevalence of 50-60%).

If differences in overall survival for the 400 primary melanoma patients are examined by log-rank test, a decrease of 11% in 5 year survival in the *strong* expression group would be detectable (assuming that roughly equivalent numbers of patients have *low* or *strong* expression, that the *low* group have 5 year survival of around 85% and that at least 78 mortality events occur in both groups). Similarly, a reduction from 95% to 78% in 5 year survival would be detectable for the *strong* expression group (assuming at least 21 mortality events occur). Melanoma mortality figures in Scotland meet these requirements.

The Kaplan-Meier method and the log-rank test were used to evaluate correlations between protein staining and patient survival. Cox proportional hazards models were used to develop a multifactorial survival model for primary melanoma in terms of both conventional risk factors and protein expression.

2.2.49 Solar elastosis scoring

Solar elastosis scoring was adapted from a previously described method (Landi 2006). The breakdown of the scores are as follows:

1: no elastotic fibres, 2: rare elastotic fibres, 3: scarcely scattered elastotic fibres between collagen bundles, 4: scattered elastotic fibres between collagen bundles, 5: densely scattered elastotic fibres between collagen bundles, 6: densely scattered elastotic fibres between collagen bundles with occasional bushels, 7: densely scattered elastotic fibres between collagen bundles with some bushels, 8: densely scattered elastotic fibres between collagen bundles mostly as bushels, 9: focal formation of amorphous deposits of blue-gray material with lost fibre architecture 10: moderate formation amorphous deposits of blue-gray material with lost fibre architecture 11: large formation of amorphous deposits of blue-gray material with lost fibre architecture.

Chapter 3

Investigation of the role of the melanocortin-1 receptor in cutaneous melanoma

3.1 Introduction

The melanocortin-1 receptor (MC1R) plays a key role in pigment production and is a major determinant of skin phototype and sensitivity to UV light (Cone et al, 1996). α-MSH is the principal ligand of the MC1R and is produced in the skin in response to UV (Schauer 1994). Binding of α-MSH to MC1R activates the pigmentary machinery which results in pigment-containing melanosomes being passed onto neighbouring keratinocytes where it can protect them from UV-induced damage (Lin and Fisher, 2007). Recent studies have shown that manipulation of the MC1R pathway can result in artificial tanning and protection from DNA damage in mice (D'Orazio et al, 2006)).

The discovery of polymorphisms of MC1R established a genetic basis for differences in skin (and hair) colour and melanoma susceptibility and helped open up the understanding of the interaction between genes and the environment (Rana 1999). MC1R polymorphisms are particularly prevalent in Caucasian populations of Northern Europe and several studies have shown a clear link between red hair colour (RHC) alleles and the development of melanoma (Sturm 2002). The presence of RHC MC1R polymorphisms give an estimated relative risk of 2 for development of melanoma (Palmer et al, 2000). Functional studies have suggested that the increased risk may not only be attributed to impaired pigmentary response (due to impaired cAMP signalling in response to α-MSH) but may also be due in part to the effect of MC1R polymorphisms on non-pigmentary pathways.

A proposed non-pigmentary mechanism for increased melanoma risk is a reduction in repair capacity in melanocytes that have polymorphisms in MC1R (Bohm et al, 2005, Kadekaro et al, 2005). A high repair capacity and resistance to apoptosis are characteristics of melanocytes that allows them to survive the DNA-damaging effects of UV radiation (Jhappan et al, 2003). This resistance to apoptosis is also apparent in melanomas which are largely insensitive to the effects of DNA damaging

chemotherapy agents (Eggermont and Kirkwood 2004). An increased understanding of the pathways that influence apoptosis in melanocytic lesions will be important in trying to find more suitable therapies for this disease. The postulated role of MC1R in protecting melanocytes from apoptosis in response to UV irradiation has led to our hypothesis that manipulation of the MC1R may affect growth of melanoma cell lines and sensitivity to DNA damage. If it was confirmed that reduced MC1R expression resulted in increased sensitivity to DNA damage this would represent a novel therapeutic approach for augmenting the effects of standard chemotherapeutic agents in the treatment of cutaneous melanoma. This would be of relevance to patients with normal MC1R as well as those with RHC alleles in which residual function of the MC1R pathway may be retained despite impaired signalling (Sanchez Mas et al, 2002, Schioth et al, 1999, Scott et al, 2002).

The methods chosen in this chapter for measurement of apoptosis in melanoma cell lines in response to DNA damage were the annexin V/propidium iodide assay and the DNA content assay. In early stages of apoptosis there is translocation of phosphatidylserine (PS) from the inner part of the plasma membrane to the outer layer so that PS becomes exposed at the external surface of the cell. Annexin V is a phospholipid-binding protein with high affinity for PS and is used as a sensitive probe for PS exposure and hence detection of cells in early apoptosis. In late apoptosis the cell membrane becomes permeable and as a result propidium iodide can enter the cells and bind to DNA where it can be detected by fluorescence. The DNA content assay relies on the amount of DNA per cell varying according to stage of the cell cycle. In normal profiles of diploid cells most cells are in G1 or G2/M. Any cells detected in the sub-G1 area of a DNA content profile are usually apoptotic or necrotic. Both methods of measuring apoptosis use a flow cytometer.

The aims of the work in this chapter were: firstly, to establish whether melanoma cell growth can be adversely affected by manipulation of the melanocortin receptor (MC1R); secondly, whether manipulation of MC1R results in increased sensitivity to DNA damage induced apoptosis; and thirdly, whether RHC (red hair colour)

MC1R alleles result in diminished DNA repair capacity and increased sensitivity to DNA damage. In the first part of the chapter a panel of melanoma cell lines were characterised with respect to MC1R sequence, MC1R mRNA expression, presence of BRAF mutations and sensitivity of cell lines to DNA damage-induced apoptosis. In the latter part of the chapter the role of the MC1R was investigated by adding α-MSH or MC1R antibody to the culture medium or by reducing MC1R expression by using siRNA.

3.2 Results

3.2.1 Detection of MC1R polymorphisms in melanoma cell lines

The melanoma cell lines chosen for these studies (A375, C32, G361, HBL, Wm115) were established lines that were obtained from cell line banks. All cell lines were originally isolated from metastases from cutaneous melanomas. They were largely non-pigmented although G361 retained its ability to produce pigment for several passages in culture and HBL was heavily pigmented and retained its ability to make pigment even following repeated passaging over several months. The 3 ovarian cancer cell lines (PEA1, PEO1, PEO14) were obtained locally.

Sequencing of the complete coding region of MC1R was performed using an automated sequencing kit following amplification of genomic DNA with primers that were located at either end of the single coding exon. Although PCR was effective for most cell lines, PCR persistently failed for DNA isolated from pigmented melanoma cell line HBL. It was found that repeated phenol/chloroform extraction was required in a larger volume in order to completely remove the pigment and obtain satisfactory amplification. MC1R polymorphisms were found in 3 out of 5 melanoma cell lines; Arg151Cys was found in A375, Val60Leu was found in C32 and Arg160Trp was found in WM115 (Figure 3.1 A-B and Table 3.1). In each case the cell line was heterozygous for the change with the exception of A375 where the Arg151Cys polymorphism was homozygous. No MC1R polymorphisms were present in G361 or HBL and no MC1R polymorphisms were found in any of the ovarian cancer cell line controls.

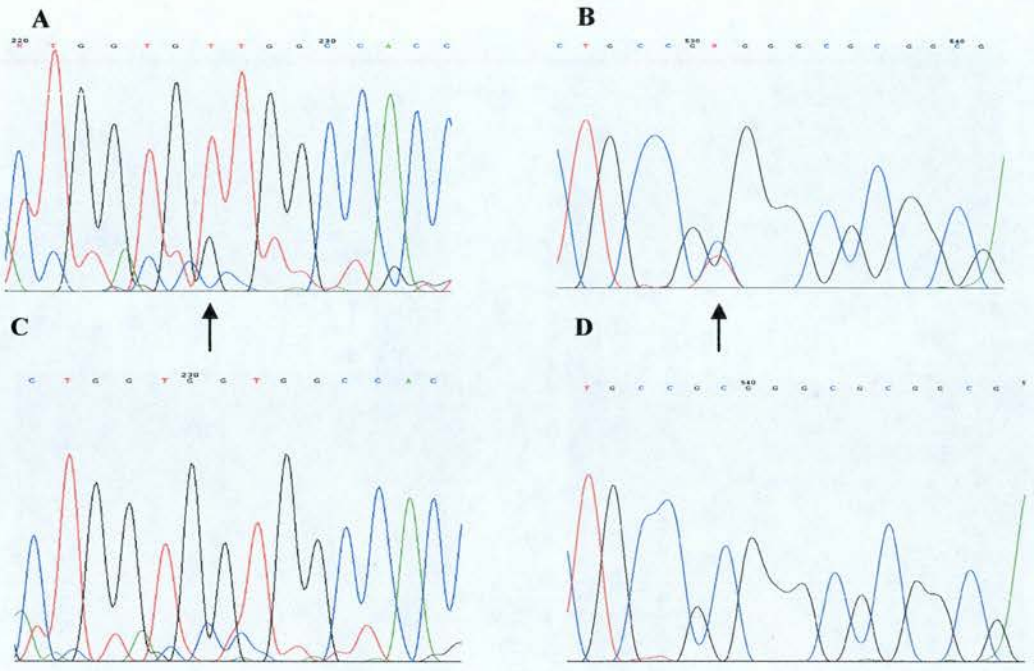

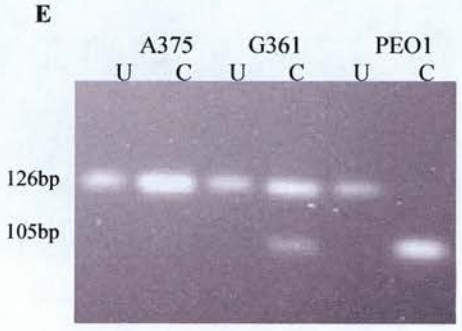

Cell line	MC1R status	BRAF V600E
A375	Arg151Cys	Homozygous mutant
C32	Val60Leu	Heterozygous mutant
G361	Wild type	Heterozygous mutant
HBL	Wild type	Wild type
WM115	Arg160Trp	Heterozygous mutant
PEA 1	Wild type	Wild type
PEO 1	Wild type	Wild type
PEO 14	Wild type	Wild type

Figure 3.1 Presence of MC1R polymorphisms and V600E BRAF mutations in melanoma cell lines. (A)-(D). Electropherograms showing sequencing results for selected melanoma cell lines. The arrows indicates the site of heterozygous missense mutations where 2 peaks are found rather than 1. **(A)** C32 : Val60Leu, **(B)** WM115: Arg160Trp, **(C)** and **(D):** G361: normal sequence. **(E)** BRAF RFLP result using Bts1 confirming A375 has a homozygous V600E mutation, G361 has a heterozygous mutation and PEO1 has no mutation. Absence of the lower band is consistent with presence of the mutation. U = uncut, C= cut.

Table 3.1 Summary of the MC1R sequencing results and the BRAF mutation analysis results for 5 melanoma cell lines (A375, C32, G361, HBL, WM115) and 3 ovarian cancer cell lines (PEA1, PEO1, PEO14).

3.2.2 Detection of BRAF mutations in melanoma cell lines

BRAF mutations have a central role in melanoma pathogenesis and recent evidence has suggested that activation of MC1R may have direct signalling effects on the BRAF/MAPK pathway (Dumaz et al, 2006). It was therefore felt to be important to determine whether any of the melanoma cell lines had activating mutations in the BRAF gene. Although several methods are available for determining the BRAF mutation status it was decided to use a PCR RFLP method to detect the most common activating BRAF mutation found in melanoma, V600E (Figure 3.1 E). The full description and application of this assay is discussed in Chapter 5. V600E BRAF mutations were found in 4 of the 5 melanoma cell lines (Table 3.1). Both mutant and normal DNA could be detected in C32, G361 and Wm115 suggesting that these cell lines were heterozygous for the activating mutation. No polymorphisms were found in HBL whereas in A375 only mutant DNA was detected suggesting that there had been loss of the normal allele. Once again HBL proved to be most difficult to obtain a PCR product from and required repeated phenol/chloroform extraction in order to produce a sample of DNA that was of suitable quality. No BRAF mutations were found in the ovarian cancer cell lines.

3.2.3 Expression of MC1R mRNA in melanoma cell lines

In order to characterise MC1R mRNA expression in the melanoma cell lines a northern blot was performed. Total RNA was extracted from pre-confluent cells, separated by electrophoresis, transferred onto a nylon membrane and the MC1R transcript was recognised by hybridisation to a MC1R cDNA probe which included the entire coding sequence of MC1R. In order to make the MC1R probe 20ng of MC1R PCR product, amplified from melanoma cell line DNA was cloned into a pGEMTeasy vector. DH5α cells were then transformed and colonies that incorporated the MC1R sequence were recognised by liberation of a 1.2kbp band following restriction digestion with EcoR1. Results were confirmed by sequencing.

MC1R mRNA was detected in all 5 melanoma cell lines whereas it was absent in the ovarian cancer cell line control (Figure 3.2A). The filter was stripped and re-probed with GAPDH to ensure that the amount of RNA loaded into the tracks was equivalent. The level of the 1.2kb MC1R transcript was highest in HBL where the signal was clearly seen and although not formally quantified, appeared considerably higher than in the other melanoma cell lines.

In an effort to obtain a more quantitative measure of MC1R mRNA expression, quantitative real-time RT-PCR was performed. B-actin was used as a housekeeping gene to normalise values and relative expression of MC1R mRNA was determined by the standard curve method. It was found that HBL had the highest expression of MC1R mRNA and this was approximately 100 times the expression seen in A375 (Figure 3.2B). MC1R transcript was also detectable in PEA1 although this was at a level that was lower than in any of the melanoma cell lines.

In order to investigate whether there was any evidence of MC1R gene amplification which would explain the higher MC1R mRNA levels seen in HBL compared with the other melanoma cell lines, a Southern blot was performed. DNA extracted from pre-confluent cells was subjected to overnight restriction digestion with Pst1 and then run out on a denaturing gel (Figure 3.2 C). DNA was transferred onto a filter and then hybridised with the MC1R probe described above. A signal was detected in all 7 cell lines that represented 2 bands of the predicted sizes of 1.1 and 1.2kbp respectively. The ethidium staining of the gel presented in figure 3.2 D suggested that the amount of DNA loaded in each track was equivalent. Results confirmed that differences in the DNA signal between melanoma cell lines were not as great as seen at RNA level. This made it unlikely that gene amplification was the explanation for the increased level of MC1R transcript seen in HBL. GAPDH reprobe would be required in order to distinguish any subtle differences in MC1R gene copy number between cell lines.

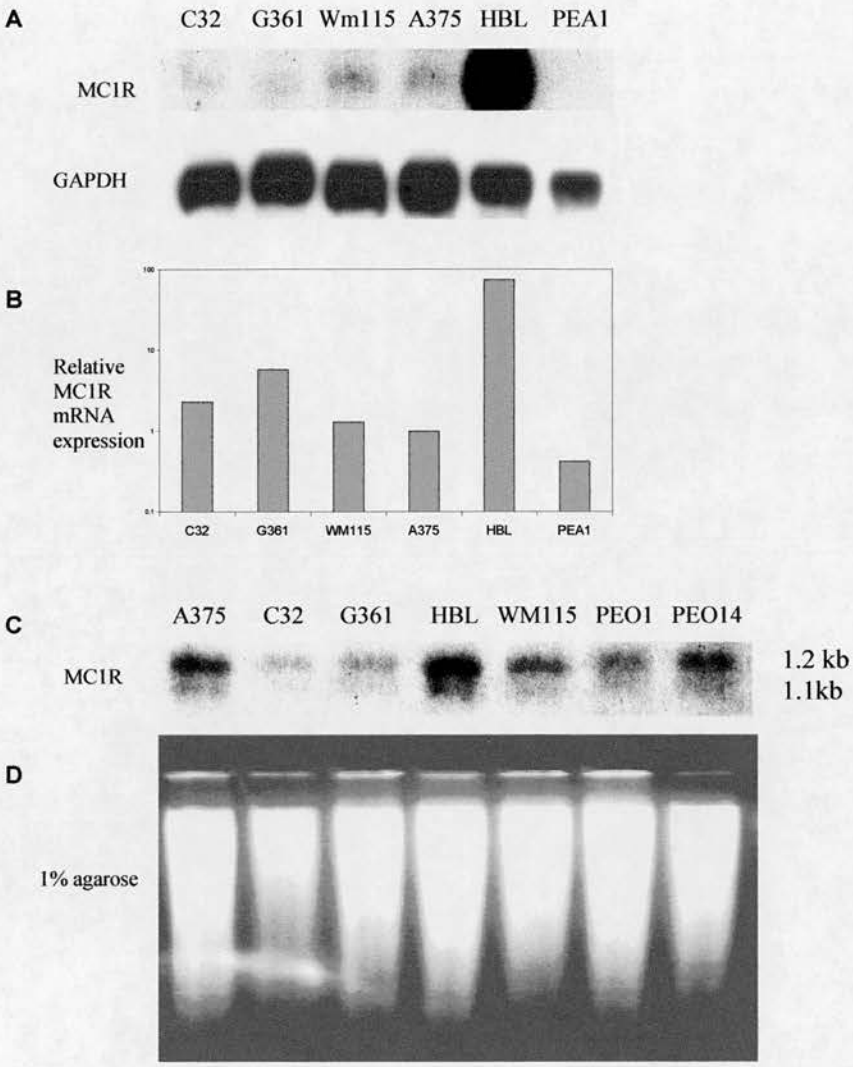

Figure 3.2 MC1R RNA expression in melanoma cell lines. (A) Northern Blot analysis using a MC1R probe incorporating the entire coding sequence. The filter was stripped and re-probed with GAPDH to check for equal loading. Results confirm the presence of the MC1R transcript in all melanoma cell lines (C32, G361, WM115, A375 and HBL) and the absence of the transcript in ovarian cancer cell line (PEA1). **(B)** Graph showing relative levels of MC1R mRNA in cell lines assessed by quantitative real-time RT-PCR using the standard curve method. **(C)** Southern blot analysis on genomic DNA following digestion with Pst1 using a MC1R probe incorporating the entire coding sequence. Bands of the predicted sizes of 1.1kbp and 1.2kbp were seen. **(D)** Agarose gel stained with ethidium bromide. Results confirm that differences in the signal between melanoma cell lines are not as great as seen at RNA level making gene amplification an unlikely explanation for the higher level of MC1R transcript seen in HBL.

3.2.4 Effect of DNA damage on cell survival in melanoma and ovarian cancer cell lines

In order to study the effect of DNA damage on cell survival, melanoma cell lines were treated with UVC or cisplatin. UVC is known to be a potent DNA damaging agent whereas cisplatin is a chemotherapeutic agent that causes DNA damage through various forms of crosslinking. Although UVB is a more relevant environmental source of radiation UVC was selected as it can be delivered in a more convenient manner (from a single lamp) and lower energies are required compared to UVB for similar types of DNA damage (Kowalczuk et al, 2006). Cells were plated out at a density that would allow exponential growth for 7 days and they were then treated with either UVC or cisplatin. When control dishes became confluent all cells were fixed in methanol, stained with crystal violet and the amount of stain taken up by the cells was quantified by spectrophotometry. Conventional colony forming assyas were not used due to the low plating efficiency of some of the melanoma cell lines.

UV impaired survival of all cell lines tested (Figure 3.3). There was a dose response effect up to the maximum dose delivered which was $100J/m^2$. Even at this dose there was some residual crystal violet staining of the dishes. Microscopy of the dishes revealed that this was partly due to non-specific staining of the plastic and partly due to surviving cells that were either shielded by the edge of the culture dish or resistant to the treatment. WM115 appeared to be the most resistant melanoma cell line. All 3 ovarian cancer cell lines had similar sensitivity to UV. Overall, there were no marked differences found in UV sensitivity between melanoma cell lines and ovarian cancer cell lines. The D50 values, which is the dose that caused a 50% reduction in cell survival, were 10 J/m^2 (A375), 14 J/m^2 (C32), 12 J/m^2 (G361), 14 J/m^2 (HBL) and $19J/m^2$ (WM115) for the melanoma cell lines and 19 J/m^2 (PEA1), 18 J/m^2 (PEO1) and 15 J/m^2 (PEO14) for the ovarian cancer cell lines.

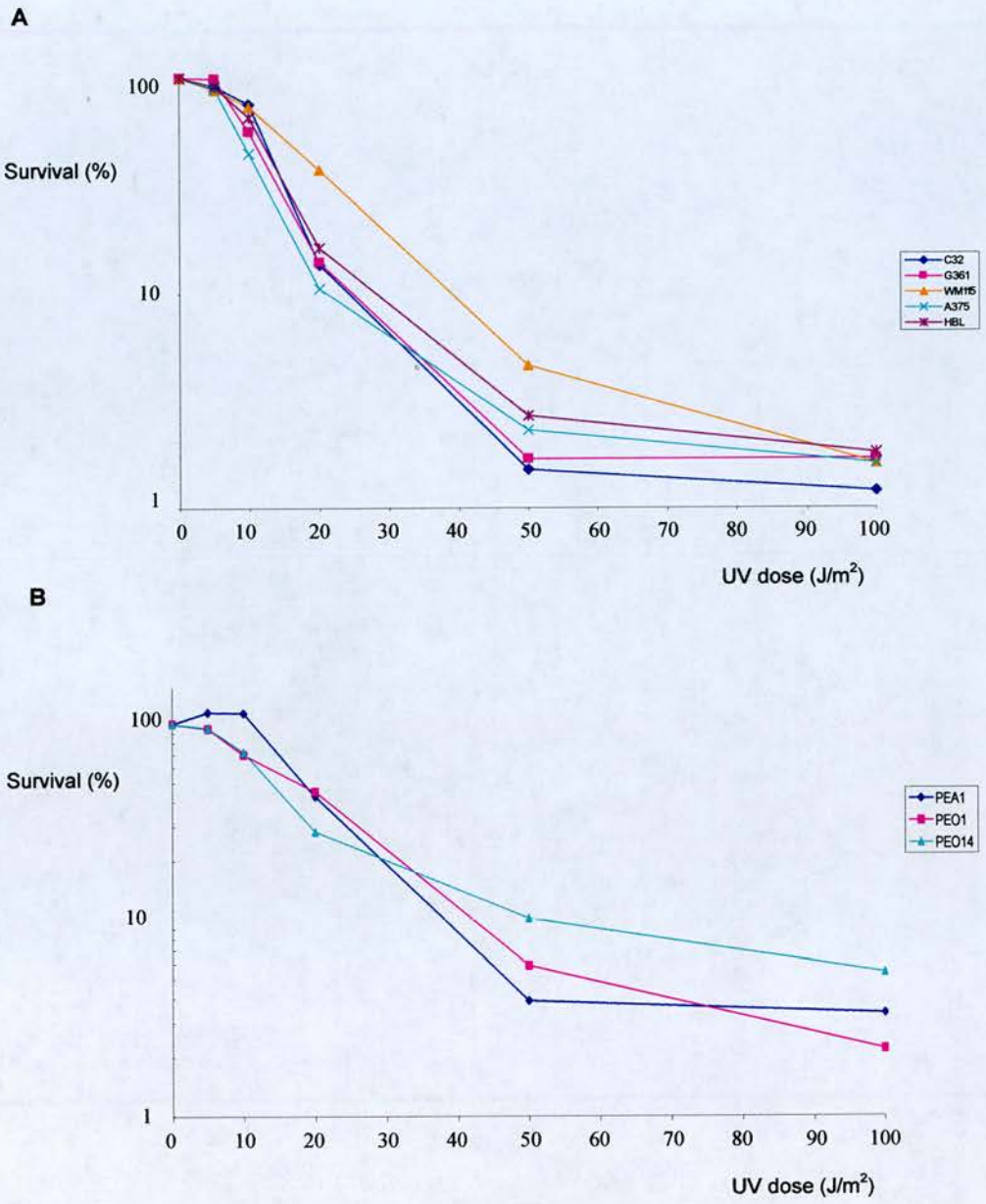

Figure 3.3. Survival of melanoma and ovarian cancer cell lines following UV irradiation. Survival of cells following UV irradiation was assessed when untreated control dishes reached confluency. The number of cells was measured by quantification of crystal violet staining. Each point represents the average of 2 dishes from one experiment. **(A)** Survival of melanoma cell lines A375, C32, G361, HBL and WM115, **(B)** survival of ovarian cancer cell lines PEA1, PEO1, PEO14.

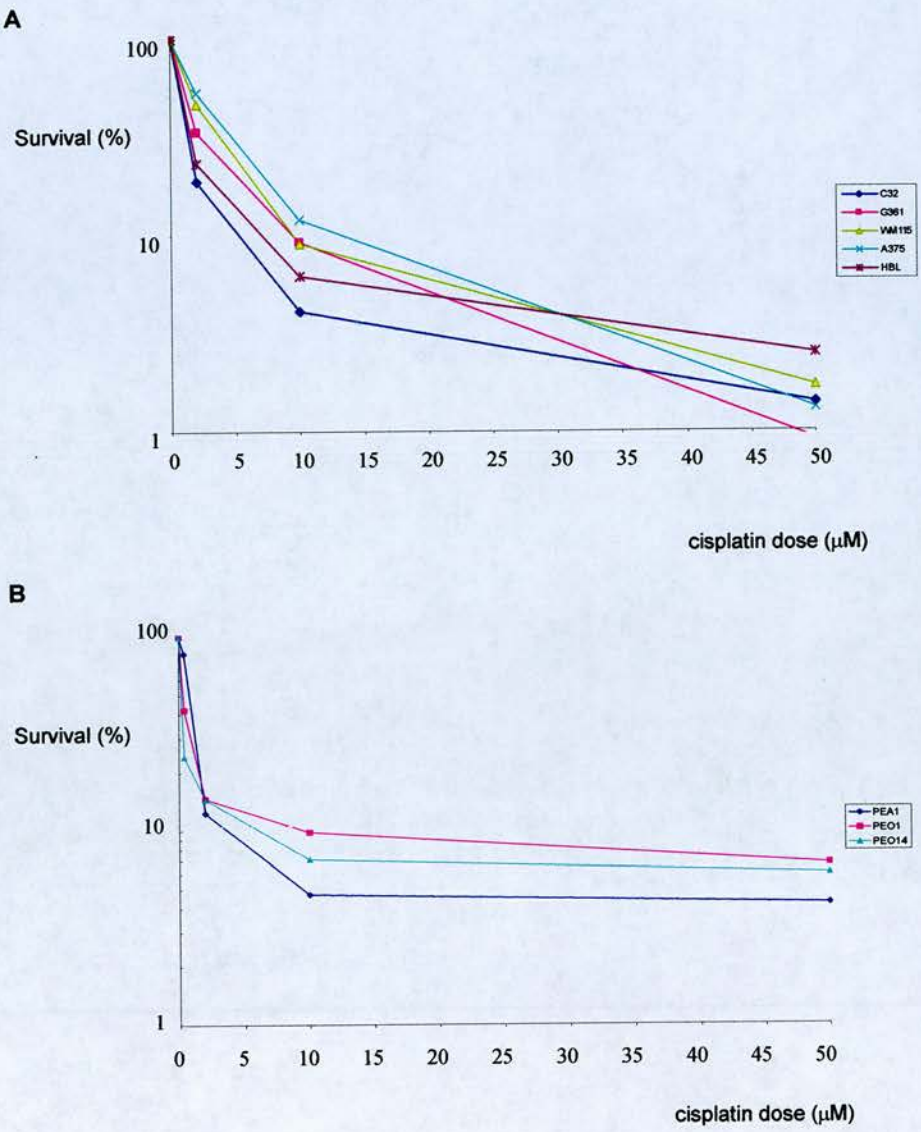

Figure 3.4. Survival of melanoma and ovarian cancer cell lines following treatment with cisplatin. Survival of cells following treatment with cisplatin was assessed when untreated control dishes reached confluency. The number of cells was measured by quantification of crystal violet staining. Each point represents the average of 2 dishes from one experiment. **(A)** Survival of melanoma cell lines A375, C32, G361, HBL and WM115, **(B)** survival of ovarian cancer cell lines PEA1, PEO1, PEO14.

Cisplatin impaired survival of all cell lines tested (Figure 3.4). The effect of cisplatin on survival of melanoma cells was similar in all 5 cell lines. All 3 ovarian cancer cell lines had a similar response to cisplatin at doses of 2 mM or greater but at a dose of 0.4mM there was no impairment in survival of PEA1 whereas there was a marked impairment in survival in both PEO1 and PEO14. This is reflected in the slightly higher D50 value for PEA1 as compared to the other 2 cell lines. This study would have to be repeated with more doses in the 0-2μM range to confirm whether this was a real difference. Overall, ovarian cancer cell lines were found to be more sensitive to cisplatin than melanoma cell lines. D50 values for the melanoma cell lines were approx 4, 2, 3, 3 and 2μM for A375, C32, G361, HBL and WM115 and 0.5, 0.5 and 1μM for PEO1, PEO14 and PEA1, respectively.

3.2.5 DNA damage-induced apoptosis in melanoma and ovarian cancer cell lines

Three melanoma cell lines C32, G361 and Wm115 and 3 ovarian cancer cell lines PEA1, PEO1 and PEO14 were used to study the effect of DNA damage on apoptosis. Levels of apoptosis were assessed using the annexin V assay and the DNA content assay. The DNA damage-inducing agents were UVC and cisplatin.

An increase in the frequency of early apoptotic, late apoptotic and dead cells were seen in response to increasing doses of UV in all cell lines using the annexin V assay (Figure 3.5 C-D). Although some apoptosis was evident 24 hours after $10J/m^2$ of UV, the level of apoptosis was much higher following $30J/m^2$. WM115 was most resistant to the effects of UV. Although a range of sensitivity was seen for both the melanoma and the ovarian cancer cell lines it was found that overall the ovarian cancer cell lines were more sensitive to DNA damage-induced apoptosis than melanoma cell lines. There was a lower level of early and late apoptotic cells seen in melanoma cell lines in response to UV ($10\ J/m^2$ and $30\ J/m^2$) although little

difference was seen between the frequency of dead cells. No relationship was found between MC1R genotype and sensitivity to DNA damage-induced apoptosis.

The other DNA damaging agent that was used in these studies was cisplatin. Although apoptosis was seen in both melanoma and ovarian cancer cell lines, levels of apoptosis were higher in the ovarian cancer cell lines (Figure 3.5 E-F). Additionally, it appeared that when melanoma cell lines were treated with higher doses of cisplatin (20μM) a considerable number of 'dead' cells resulted with only small numbers of apoptotic cells seen. This is in contrast to the profiles obtained following UV irradiation where very few 'dead' cells were seen.

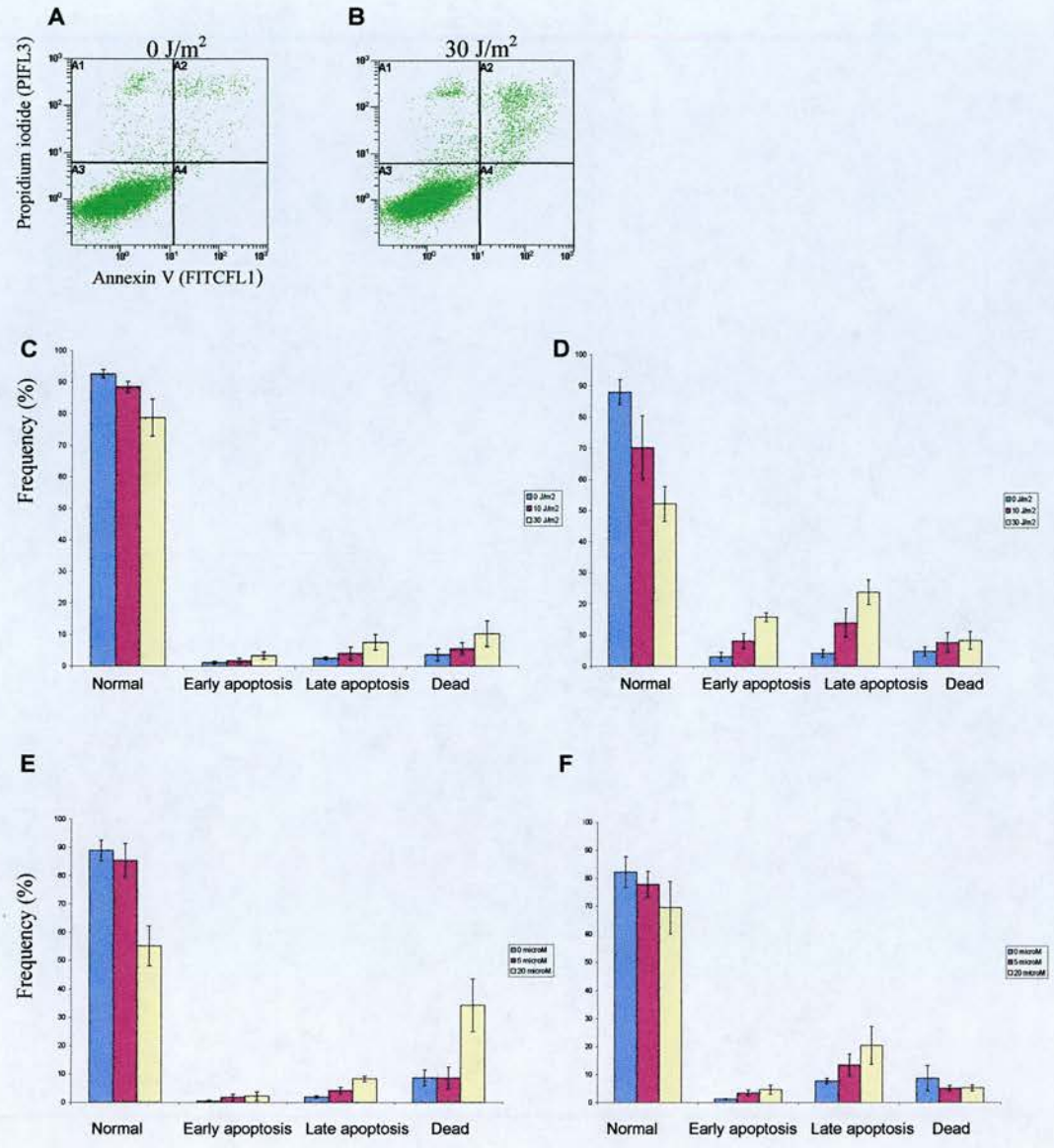

Figure 3.5. DNA damage-induced apoptosis in melanoma and ovarian cancer cell lines – the annexin V assay. (A) and **(B)** are examples of annexin V/propidium iodide assay results for G361 24 hours after 0 or 30J/m^2 UVC irradiation. The four quadrants A1-A4 represent dead cells, late apoptotic cells, normal cells and early apoptotic cells respectively. The increased number of cells in quadrant A2 of figure **(B)** indicates apoptosis in response to UV compared to untreated control cells **(A)**. **(C)-(D)** Average levels of apoptosis 24 hours after UV as measured by the annexin V/propidium iodide assay. **(C)** Melanoma cell lines (C32, G361, Wm115) following 0 (blue), 10 (red) and 30 J/m^2 (yellow) UVC respectively. **(D)** Ovarian cancer cell lines (PEA1, PEO1, PEO14). **(E)-(F)** Average levels of apoptosis 24 hours after cisplatin as measured by the annexin V/propidium iodide assay. **(E)** Melanoma cell lines (C32, G361, Wm115) following 0 (blue), 5 (red) and 20uM (yellow) cisplatin respectively. **(F)** Ovarian cancer cell lines (PEA1, PEO1, PEO14). Each bar represents the mean percentage of cells +/- standard error of the means.

3.2.6 Effect of α-MSH, NDP-α-MSH or MC1R antibody on proliferation and DNA damage-induced apoptosis in melanoma cell lines

The effect of the presence of ligand or antibody against the extracellular domain of MC1R on proliferation or response to DNA damage-induced apoptosis was investigated. G361 was selected for these studies because firstly, it did not contain any MC1R polymorphisms, secondly, it was isolated from a pigmented melanoma that was likely to have a functional MC1R pathway and thirdly, it had moderate sensitivity to DNA damage-induced apoptosis that would allow alterations in the threshold for apoptosis to be assessed in the apoptosis assay.

Melanoma cell line G361 was cultured in the absence or presence of α-MSH or NDP-α-MSH, a super-potent α-MSH analogue, in order to assess the effect on proliferation. The doses of α-MSH (1pM – 1μM) were comparable with doses that have been shown to have an effect on the MC1R pathway in previous studies in melanocytes (Kadekaro et al, 2005). α-MSH or NDP-α-MSH was replenished every 48 hours. Cells were fixed and stained when control dishes were confluent and cell number was quantified by measurement of crystal violet staining by spectrophotometry. Addition of α-MSH (Figure 3.6 A) or NDP-α-MSH (data not shown) to culture medium had no effect on cell proliferation compared to controls at the doses tested.

Given that there was likely to be α-MSH in the serum used to supplement the culture medium it was speculated that the MC1R may have already been saturated by ligand and no additional effect of exogenous ligand could therefore be seen. Unfortunately attempts to grow G361 cells in serum-free media by gradually titrating in increasing amounts of serum-free media versus normal media were unsuccessful.

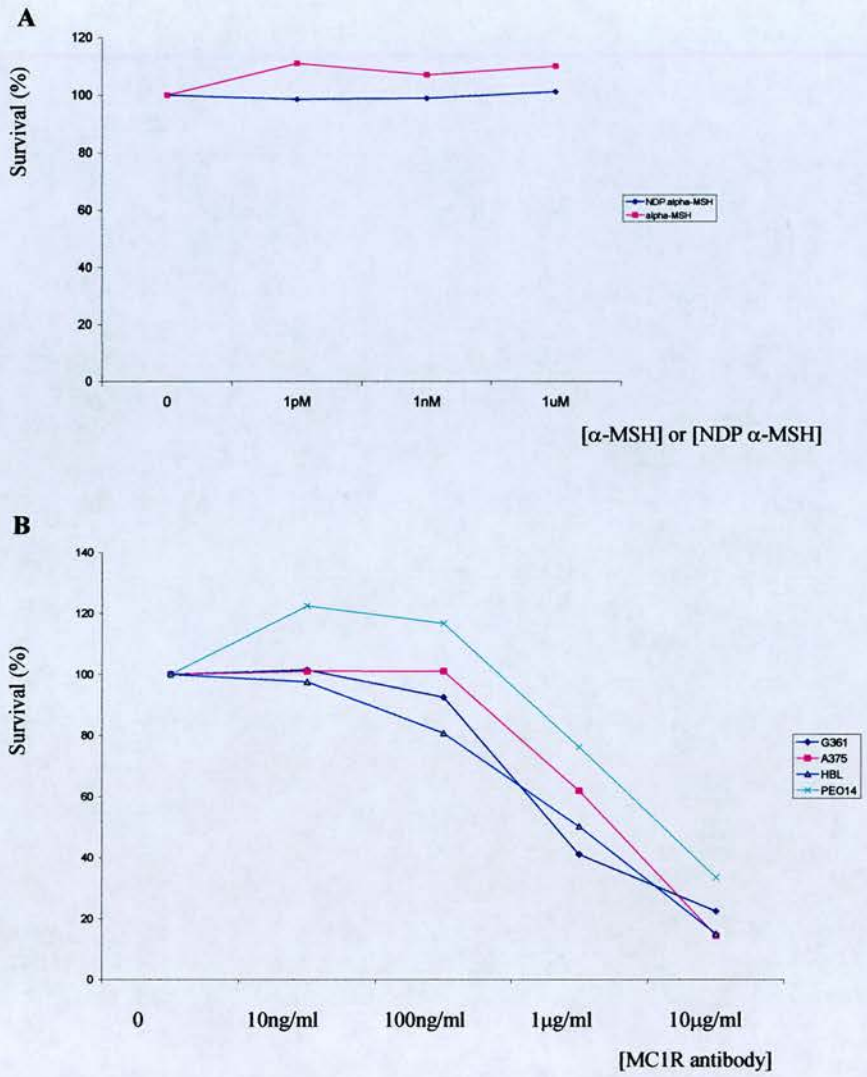

Figure 3.6. Effect of α-MSH or MC1R antibody on proliferation. (A) shows survival of G361 melanoma cells following treatment with α-MSH or NDP α-MSH relative to untreated controls. **(B)** shows survival of G361, A375 and HBL melanoma cells and PEO14 ovarian cancer cells following treatment with MC1R antibody relative to untreated controls. Each point represents the mean of two dishes from one experiment.

A

[α-MSH]	Dose of UVC (J/m2)	Normal cells (%)	Apoptotic/Dead cells
0	0	87	13
0	30	71	29
0	50	58	43
1nM	0	87	13
1nM	30	80	20
1nM	50	55	45
1μM	0	87	13
1μM	30	82	18
1μM	50	60	40

B

[MC1R ab]	Dose of UVC (J/m2)	Normal cells (%)	Apoptotic/Dead cells
0	0	89	11
0	20	54	46
10ng/ml	0	91	9
10ng/ml	20	53	47
100ng/ml	0	91	9
100ng/ml	20	49	51

C

Agent	Proliferation	Apoptosis
α-MSH	No effect	No effect
NDP α-MSH	No effect	No effect
MC1R antibody	Inhibitory at high dose	No effect

Table 3.2. Effect of α-MSH and MC1R antibody on DNA damage-induced apoptosis in melanoma cell line G361. **(A)** The effect of α-MSH on apoptosis following treatment with 0, 30 or 50 J/m^2 UVC. **(B)** The effect of MC1R antibody on apoptosis following treatment with 0 or 20 J/m^2 UVC. **(C)** Summary of results.

Sensitivity to UV mediated apoptosis in melanoma cell lines was assessed using the annexin V assay following irradiation with UVC. G361 cells were cultured in the presence of α-MSH for 48 hours prior to UV irradiation at the same doses as used in the proliferation assay. The degree of DNA damage-induced apoptosis was unaffected by the presence of α-MSH (Table 3.2A).

The next strategy that was investigated was to assess the potential impact of blocking binding of ligand to MC1R on DNA damage-induced apoptosis. Melanoma cell line G361 was cultured in the presence or absence of MC1R antibody at concentrations of 10ng/ml-10μg/ml. The antibody recognised the N-terminal extracellular domain and although it was anticipated that it may block binding of ligand to the receptor there was no data available on whether the antibody was inhibitory or activating. At high doses, inhibition of proliferation of melanoma cell line G361 was seen (Figure 3.6B). This effect was also seen however in the ovarian cancer cell line PEO14 which does not express MC1R which suggested that it was a non-specific effect of the antibody rather than an effect that was due to binding to the receptor. When melanoma cells were cultured in the presence of the antibody prior to and after UVC irradiation, there was no difference in UVC mediated apoptosis in melanoma cell lines compared to controls grown in the absence of the antibody (Table 3.2B).

3.2.7 Optimisation of siRNA in melanoma cell line G361

As there was no proof that MC1R was blocked by the antibody in the above experiment siRNA was used to knock-down expression of MC1R and investigate the effect on sensitivity to apoptosis. Small interfering RNA (siRNA), sometimes known as short interfering RNA or silencing RNA, is a class of 20-25 nucleotide-long double-stranded RNA molecules that play a variety of roles in biology. Most notably, siRNA is involved in the RNA interference (RNAi) pathway where the siRNA interferes with the expression of a specific gene (Hamilton et al, 1999). siRNAs can

be exogenously introduced into cells by various transfection methods to bring about the specific knockdown of a gene of interest. Essentially any gene of which the sequence is known can thus be targeted based on sequence complementarity with an appropriately tailored siRNA. This has made siRNAs an important tool for investigating gene function.

The Nucleofector technology is a novel transfection method that offers advantages over other established methods of transfection, particularly in difficult-to-transfect cell lines. It is a non-viral method based on a unique combination of electrical parameters and cell-type specific solutions. Nucleofector technology offers highly efficient and robust transfection of DNA, siRNA or mRNA with high cell viability.

Melanoma cell line G361 was selected for these studies as firstly, it had no MC1R polymorphisms, secondly, it grew well in culture and thirdly, it showed some sensitivity to DNA damage-induced apoptosis which would be further investigated in these studies. Optimal conditions for nucleofection of G361 were established with a pmaxGFP vector. A number of different nucleofector solutions and nucleofection programmes were investigated in order to find the conditions that gave highest viability and transfection. Cell viability and transfection efficiency were assessed after 24 hours by FACS analysis following labelling with propidium iodide. The highest transfection efficiency achieved was 66% with a viability of 83% when solution L was used in conjunction with nucleofector programme X005 (Table 3.3). High levels of transfection and good cell viability were then confirmed at both 24 and 48 hour time points (Figure 3.7 A).

The nucleofection conditions that were established using pmaxGFP were then adopted for studies to assess knockdown of cyclophilin B using siRNA (SMARTpool, Dharmacon). Cyclophilin B knockdown was assessed at the protein level by Western blot. G361 cells were nucleofected with 100nM cyclophilin B siRNA and protein was extracted at 24, 48 and 72 hours. Knockdown of cyclophilin B compared to mock nucleofected cells of approximately 80% was confirmed at 48 hours and 72 hours by Western Blot (Figure 3.7 B).

	Solution L		Solution V	
Programme	TE	V	TE	V
A020	48	86	41	87
T020	56	67	62	75
T030	28	30	33	46
X001	49	90	47	88
X005	66	83	55	87
L029	57	66	65	87
D023	49	69	62	84
No Prog	0	88	0	83
No GFP	0	78	0	71

Table 3.3. Nucleofection optimisation using pmaxGFP. Transfection efficiency (TE) and viability (V) are shown for melanoma cell line G361 24 hours after transfection of pmaxGFP using different nucleofection solutions (L and V) and programmes.

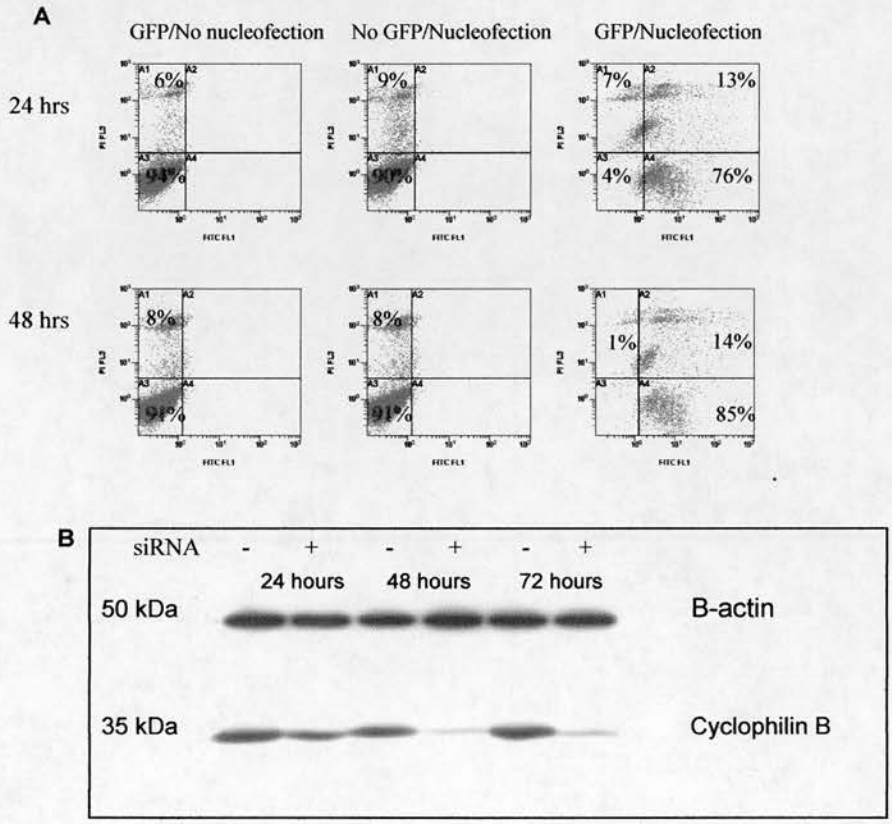

Figure 3.7. Optimisation of siRNA conditions. (A) Nucleofection transfection efficiency in melanoma cell line G361 using GFP vector and nucleofection programme X-005 and solution L analysed by FACS with propidium iodide staining. Transfection efficiency = A4/All = 76% at 24 hours and 85% at 48 hours. Viability = (A3 + A4)/All = 80% at 24 hours and 85% at 48 hours. **(B)** Cyclophilin B siRNA mediated knockdown. Knockdown of cyclophilin B at 48 and 72 hours confirmed by Western Blot 48 and 72 hours after nucleofection with cyclophilin B siRNA (100nM).

The effect of MC1R siRNA (ON TARGET plus SMARTpool, Dharmacon) on MC1R expression was then investigated. SMARTpool is a mixture of 4 siRNAs that target the same gene. Two MC1R antibodies were tested but despite several attempts it was evident that no clear band of the appropriate size could be visualised in Western blots of melanoma cells. It was therefore decided to assess MC1R knockdown at the mRNA level by performing real time RT-PCR (Figure 3.8). Relative concentrations of MC1R mRNA were measured using the standard curve method. B-actin was used as the housekeeping gene in order to normalise the expression level of MC1R. A standard curve was run for each pair of gene-specific primers on cDNA extracted from G361 melanoma cells in order to determine PCR efficiency (Figure 3.8C). Melt curves were used to confirm specificity of the PCR products. A no reverse transcriptase control was included on each run in order to rule out the possibility of contamination.

Total RNA was extracted from G361 melanoma cells either 24 hours or 48 hours after nucleofection with 100nM MC1R siRNA. RNA was also extracted from no nucleofection and mock nucleofection controls. For each experiment DNA was removed from the RNA preps prior to reverse transcription using a DNA-free kit to avoid obtaining a signal generated from contaminating DNA. Reverse transcription was performed using random primers. Quantitative RT-PCR results revealed that knockdown of MC1R mRNA was variable. The maximum knockdown achieved was 70% (Figure 3.8D) although in some experiments knock-down was as low as 35%. A dual nucleofection approach in which cells were nucleofected 24 hours apart generally gave higher levels of knockdown than single nucleofection. Maximal knockdown was evident 48hours after nucleofection irrespective of whether the nucleofection was single or dual. The dual nucleofection approach was selected for further studies of the effect of MC1R siRNA on sensitivity to DNA damage-induced apoptosis.

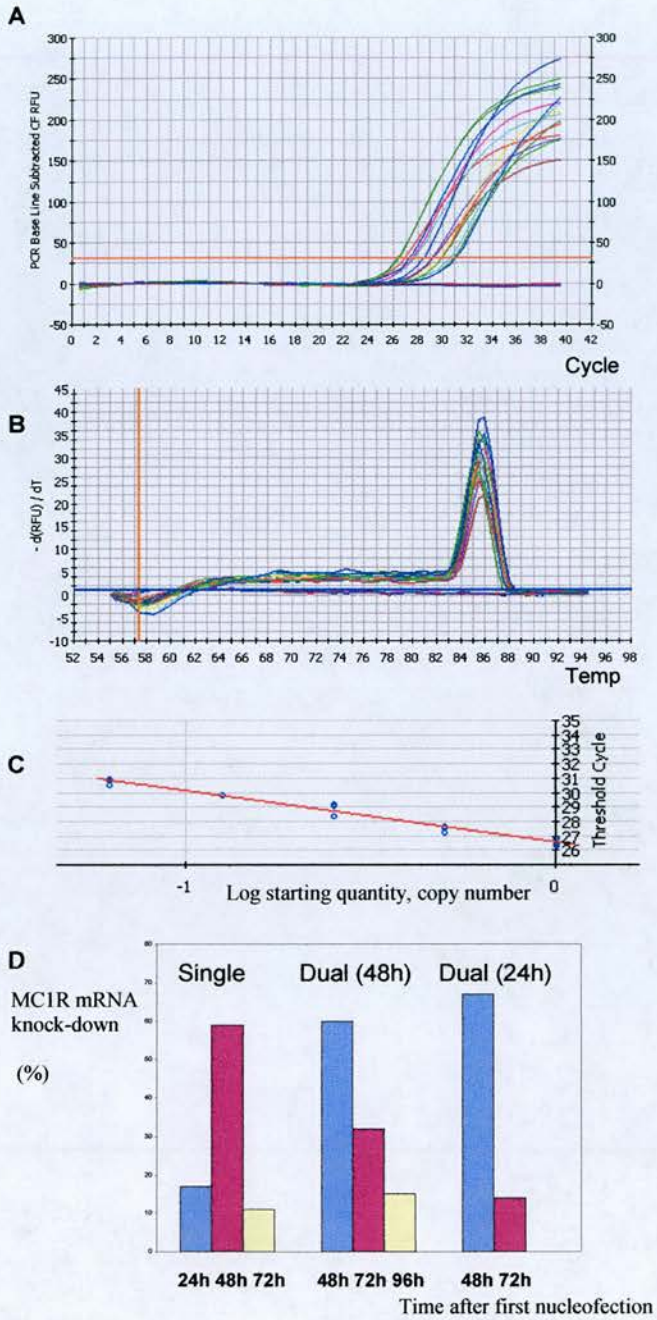

Figure 3.8. MC1R Real time RT PCR optimisation. (A) Amplification curve for MC1R. Each curve represents an individual sample. **(B)** Melt curve showing strong specific peaks for each PCR product suggesting that primers anneal specifically, **(C)** Example of standard curve used for measuring relative expression of MC1R transcript showing a good correlation between the standards (correlation coefficient >0.99, PCR efficiency 95%). **(D)** Levels of knockdown of MC1R transcript 24, 48 or 72 hours after either single or dual nucleofection with MC1R siRNA. Dual (48h) indicates siRNA nucleofection 48 hours apart whereas Dual (24h) indicates siRNA nucleofection 24 hours apart. Maximal knockdown was evident 48hours after nucleofection irrespective of whether it was single or dual.

3.2.8 Effect of MC1R siRNA treatment on UV-induced apoptosis in melanoma cell line G361

In order to investigate the effect of reduced expression of MC1R on UV-induced apoptosis in melanoma cell line G361, the annexin V apoptosis assay was performed following UVC irradiation of siRNA treated cells.

G361 cells were nucleofected with MC1R siRNA on 2 separate occasions 24 hours apart. 18 hours after the second nucleofection, cells were treated with UVC and following a further 24 hours cells were harvested and assessed for levels of apoptosis. This time point was chosen for UV irradiation as it was thought that it would give sufficient time for levels of protein to fall following an earlier reduction in MC1R mRNA levels. Levels of MC1R mRNA knockdown were assessed using quantitative real-time RT-PCR using the standard curve method as described previously. Levels of MC1R transcript were found to be 62% lower in siRNA treated cells versus controls at the time of UV irradiation. These studies were performed in duplicate.

Following treatment with siRNA (100nM) there were no obvious changes in the appearance of the cells or in gross rate of proliferation relative to cells that were put through the nucleofection procedure without any siRNA. The annexin V assay confirmed that there was no difference in levels of apoptosis between siRNA treated cells and controls (Figure 3.9). The levels of UV-induced apoptosis found using the annexin V assay were found to be generally higher during these experiments than had been found on studies earlier in the chapter. It is not clear whether this is because the nuclefection procedure made cells more sensitive to the subsequent effects of UV or somehow the cells had become more sensitive to DNA damage as a result of an unidentified change in these cultures or culture conditions.

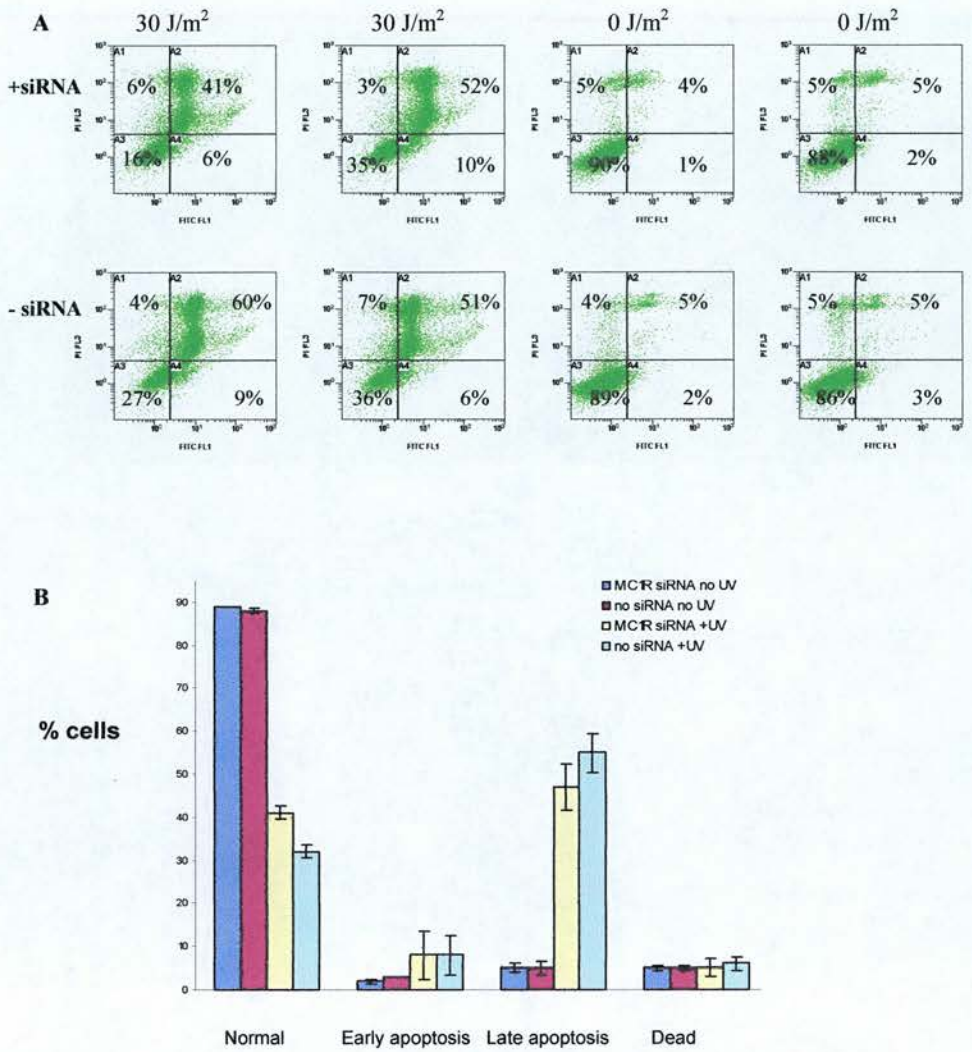

Figure 3.9. Effect of MC1R siRNA treatment on UVC-induced apoptosis. Level of apoptosis in G361 melanoma cells was assessed by the annexin V/propidium iodide assay 24 hours after UV irradiation. Dual MC1R siRNA (100nM) nucleofection (24 hours apart) was performed and cells were then irradiated with UVC 18 hours after the 2nd nucleofection. MC1R knock-down at RNA level of 62% relative to controls was confirmed at the time of UV irradiation by quantitative RT-PCR. Controls were cells that had been treated in the same way as siRNA nuclefected cells with the exception that normal buffer was used rather than buffer containing siRNA. **(A)** Annexin V/ propidium iodide apoptosis profiles in full (in duplicate) for G361 cells 24 hours after UVC irradiaton. **(B)** Graphical illustration of results according to frequency of cells in each quadrant of the annexin V assay. Each bar represents the average of 2 dishes +/- standard deviation. siRNA had no effect on the levels of apoptosis following UV treatment.

3.3 Discussion

In contrast to keratinocytes which are quite prone to apoptosis melanocytes have been widely reported to be resistant to UV radiation-induced apoptosis (Jhappan et al, 2003). The mechanism for resistance to apoptosis is not fully understood although may include elevated expression of anti-apoptotic proteins such as Bcl-2 (Plattenberg 1995). Recent studies have suggested that α-MSH can reduce UV radiation-induced apoptosis in human melanocytes (Bohm et al, 2004, Kadekaro et al, 2005) and MC1R therefore appears to not only be a central mediator in the pigmentation pathway but may also be important in the control of growth of melanocytes and the response to UV radiation-induced DNA damage. The studies presented in this chapter set out to further investigate the MC1R pathway in cutaneous melanoma cell lines.

Sequencing of the complete coding region of MC1R after PCR amplification of genomic DNA with suitable primers showed that 3 of the 5 melanoma cell lines harboured MC1R variants. The variants found were Val60Leu in melanoma cell line C32, Arg160Trp in WM115 and Arg151Cys in A375. Red hair colour (RHC) variants have been classified by strength of association with red hair into strong and weak RHC alleles. Arg151Cys and Arg160Trp variants are known as strong RHC alleles whereas Val60Leu is considered as a partial RHC causing allele. Functional studies of the Val60Leu, Arg151Cys and Arg160Trp variants have demonstrated a decreased ability to stimulate cAMP compared to wild-type (Reviewed in Healy 2004 and Sturm 2002). Both C32 and WM115 cell lines were heterozygous for the respective MC1R variants and one can therefore postulate that although response to α-MSH may be impaired these cell lines will retain some MC1R function. A375 was homozygous for the Arg151Cys variant and was likely to have the most significant impairment of signalling through the MC1R pathway.

BRAF mutations were found in 4 out of 5 cell lines. No details were available from the melanoma cell line with normal BRAF, HBL, as to whether this originated from

a primary site with a lower rate of mutation such as acral sites or sites of chronic sun exposure (see Chapter 4 for further discussion).

MC1R expression at the RNA level was confirmed in all melanoma cell lines tested. The highest expression was found in HBL which is the cell line which has the highest level of pigmentation. It is recognised that melanoma cell lines tend to lose their ability to produce melanin pigment following several passages in culture and it is possible that a general downregulation of the pigmentation pathway in cell culture could involve loss of MC1R expression. A relationship between MC1R expression and presence of pigment would require further investigation. The finding of high MC1R expression in HBL compared to other melanoma cell lines is consistent with a previous study which showed that HBL was the cell line with the highest number of MC1R binding sites per cell (Eves et al, 2003).

In order to investigate the importance of MC1R in the response of melanoma cells to DNA damage-induced apoptosis, conditions were established for delivering DNA damaging agents at a dose that led to some degree of apoptosis. The DNA damaging agents chosen were UVC and cisplatin. UVC is a potent DNA damaging agent that causes cyclobutane pyrimidine dimers (CPD) and 6-4 photoproducts (6-4 PP) whereas cisplatin is a chemotherapeutic agent that causes different types of DNA damage by various forms of cross-linking.

Broadly speaking only small differences in sensitivity to UV between melanoma lines and ovarian cancer lines across a wide range of doses of UV were seen. In contrast to the response of melanoma and ovarian cancer cell lines to UV irradiation, ovarian cancer cell lines were more sensitive to treatment with cisplatin than melanoma. This result is consistent with the presence of different mechanisms being used by the cell to respond to UVC mediated DNA damage versus cisplatin mediated DNA damage (Damsma et al, 2007). Alternative approaches to assess sensitivity to DNA damage such as colony forming assays would perhaps offer a more sensitive approach to revealing differences between cell lines.

Higher levels of apoptosis in response to cisplatin were also seen in ovarian cancer cell lines compared to melanoma cell lines. This is consistent with the clinical observation that melanoma is relatively resistant to cisplatin whereas ovarian cancer tends to have a good response to cisplatin based chemotherapy. It was interesting that high doses of cisplatin caused a marked increase in apoptosis in ovarian cancer cell lines but in contrast appeared to cause an increase in the number of dead cells with little evidence of apoptosis in melanoma lines. This suggests that the resistance of melanoma cells to apoptosis may not be simply overcome by increasing doses of DNA damaging agents as this appears to cause cell death by an alternative mechanism (i.e. necrosis). This result implies that although in the treatment of patients with metastatic melanoma with chemotherapy it may be important to overcome blocks to apoptosis, cell death and tumour responses may be achieved through non-apoptotic mechanisms.

The precise role that α-MSH plays in the development and progression of melanoma is unclear. A number of *in vitro* studies have investigated the influence of α-MSH on melanoma cell behaviour including proliferation, migration and invasion (Robinson et al, 2002, Eves et al, 2002). Whereas the effect of α-MSH on melanocytes is predominantly growth-promoting one recent study revealed that stimulation of melanoma cell lines with α-MSH resulted in reduced proliferation of melanoma cells (Robinson and Healy 2002). Activation of the MAPK pathway may be important in mediating the anti-proliferative affect (Smalley and Eisen 2000). A further study revealed that α-MSH had an inhibitory effect on cell migration although this effect was not seen in C8161 melanoma cells that lack a functional MC1R receptor (Zhu et al, 2004). The results in this chapter showed that α-MSH or NDP-α-MSH had no effect on proliferation of melanoma cell lines or of sensitivity to UV mediated apoptosis at the doses tested. It wasn't possible to conclude whether signalling through the MC1R pathway has no role in the control of proliferation or DNA damage-induced apoptosis in melanoma cell lines or whether alternatively the MC1R signalling pathway was already saturated by α-MSH in the culture medium (as a constituent of fetal calf serum). Attempts to culture melanoma cells in serum-free media were unfortunately unsuccessful. The reason for the inconsistency between the

results discussed above and previous studies which showed an effect of α-MSH on proliferation of melanoma cells is not clear although it should be noted that previous studies were performed predominantly on murine melanoma cells and some studies used α-MSH from different suppliers. The role of α-MSH in human melanoma cell behaviour therefore remains unclear.

Investigation of the use of an antibody to the N-terminal extracellular domain of MC1R revealed an inhibitory effect on proliferation at high doses. In the interpretation of these studies it was not possible to conclude whether the antibody bound to the MC1R in culture and if so, whether this binding was specific or had any effect on downstream signalling. There was no previous data available on whether the antibody used was inhibitory or activating. As inhibition of proliferation of ovarian cancer cell line controls was also seen it was likely that the inhibition of growth at high doses was a non-specific toxic effect of the antibody in culture rather than a result of binding to MC1R. A systematic attempt to reduce expression of MC1R was therefore made using siRNA.

The siRNA studies showed that it was possible to achieve approximately 70% knockdown of MC1R mRNA in melanoma cell line G361 following nucleofection with pooled siRNA oligonucleotides. Optimal conditions for knockdown were found to be dual nucleofection, 24 hours apart. Although no formal assessment of proliferation was made it was evident that treatment with MC1R siRNA had no gross effect on proliferation of G361 cells. The principal phenotype that was investigated was the response of siRNA treated cells to UVC mediated DNA damage. It was found that there was no difference in levels of apoptosis between cells that had been treated with MC1R siRNA and untreated cells. The principal weaknesses of this study were firstly, the degree of knockdown achieved and secondly, the absence of confirmation of an effect of MC1R siRNA on expression of MC1R protein. Knockdown of MC1R was found to be 62% in siRNA treated cells in the apoptosis experiment but due to the absence of a reliable MC1R antibody it was not clear whether any knockdown of MC1R protein was achieved at the timepoint that UV irradiation was delivered. It was felt that delivering UV at 42 hours after the first

nucleofection would provide a reasonable time period for MC1R protein levels to be reduced given that RNA levels had fallen by 24 hours. Clearly these studies would have been improved by either developing a MC1R antibody that could reliably quantify levels of MC1R protein or using an antibody to a tagged version of the protein.

Although the pilot experiments presented above do not give a definitive answer as to the importance that MC1R has in cutaneous melanoma a number of conclusions can be made. Firstly, MC1R polymorphisms are found commonly in melanoma cell lines. Secondly, there is no clear relationship between presence of a polymorphism and sensitivity to DNA damage induced apoptosis in a limited panel of melanoma cell lines. Thirdly, MC1R transcript is expressed in all melanoma cell lines tested. Fourthly, the presence of α-MSH, NDP-α-MSH or MC1R antibody has no effect on sensitivity to DNA damage-induced apoptosis in melanoma cells. Finally, knockdown of MC1R mRNA by 62% has no effect on DNA damage-induced apoptosis in melanoma cell line G361. Further studies would be required to confirm the results of these pilot experiments and to investigate whether these results are repeated in other melanoma cell lines and using other agents that interrupt MC1R signalling. Whether MC1R has a key role in the control of proliferation and apoptosis in response to α-MSH in melanoma cells as it does in melanocytes, or whether other key signalling pathways such as the MAPK and PI3K pathways which are often constitutively activated have a more dominant influence on these key aspects of melanoma behaviour remains unclear.

Chapter 4

Establishment and characterisation of Edmel 3 – a new melanoma cell line

4.1 Introduction

Primary cell culture is the process by which cells are liberated from fresh tissue and plated in a suitable environment where they can attach, divide and grow. Cells are usually dissociated from a tissue fragment using proteolytic enzymes and subsequently grown in medium supplemented with serum and antibiotics in a plastic culture dish. Some cell lines will stop dividing in culture after several passages whereas others will continue to divide indefinitely. Single cells can be isolated from established cultures in order to grow large numbers of genetically identical daughter cells (a clone). Although not all tumours will give rise to cell lines that can be maintained indefinitely, many melanoma cell lines have been successfully established and stored (Murata et al, 2007).

Studies on cultured melanoma cells have made important contributions to melanoma research over many years. They have allowed detailed investigation into the genetic changes underlying melanoma and have provided the means of testing novel anti-cancer compounds both *in vitro* and when cell lines are implanted as xenografts in SCID mice. Amongst the most widely studied melanoma cell lines are those included in the NCI-60 panel which have been extensively genotyped and used for testing thousands of compounds that may have potential as anti-cancer agents (Covell et al, 2007). Established melanoma cell lines continue to be widely used in research into melanoma pathogenesis and in the development of new therapies.

Following surgery for primary melanoma, tumours are usually fixed in their entirety for diagnosis and as a result no surplus fresh material is available for research purposes. An alternative source of fresh tissue that can be used for isolating melanoma cells is from patients undergoing surgical resection of metastatic disease. Surgery is carried out for patients with metastatic melanoma either as a staging procedure, to improve survival, or to provide symptomatic benefit. In this setting,

tumour volume tends to be larger than that seen in primary melanoma and the whole specimen is often not required for histological assessment.

Although many melanoma cell lines are widely available through cell and tissue banks such as the American Type Culture Collection (ATCC), the isolation of novel human melanoma cell lines for use in cell culture studies would offer significant advantages over established cell lines such as those used in Chapter 3. Firstly, the cells would be free from genetic changes that tend to accumulate in cell lines following long term culture. Secondly, a full clinical history for the patients from whom they were isolated would be available allowing correlation of *in vitro* findings with the clinical picture. Thirdly, corresponding clinical samples would be available from the pathology archive for comparative studies.

The aim of the work in this chapter was to establish and characterise novel melanoma cell lines from fresh human melanoma tissue fragments removed during surgery. The characterisation included basic morphology and growth characteristics, immunohistochemistry, response to DNA damage and ability to form xenografts in SCID mice. An attempt was also made to correlate the findings with the clinical samples from which the cells were derived.

4.2 Results

4.2.1 Establishment of a melanoma cell line

The surgical specimens used to isolate melanoma cells were from 6 patients undergoing surgery for resection of symptomatic subcutaneous or lymph node metastases. The tissue fragments were selected by the surgeon in theatre as being macroscopically consistent with melanoma. In all cases tissue was received within an hour of the procedure. All tissue taken was surplus to clinical requirements and was taken in compliance with approved ethical procedures. The source and history of the melanoma samples which were used in this chapter are summarized in table 4.1.

On receipt of the tissue specimens in the lab, it was evident that the identification of melanoma tissue as opposed to normal tissue in the tissue fragments was problematic. This was particularly true in the cases in which no or very little pigment was present. For those fragments in which the division between melanoma and non-melanoma tissue was unclear the whole sample was used for culture whereas in those where the melanoma tissue was more obvious an attempt was made to dissect out this tissue alone.

Following dissection, chopping up and trypsinisation of the tissue fragments, cells from 5 out of the 6 melanoma samples became established. No cells became established from sample Edmel 4 but in all other cases it was evident that cells had attached onto the surface of the culture dish within 24 hours of processing. It was clear that some of the cultures consisted of mixed populations of cells with the most prominent cell type having a morphological appearance consistent with fibroblasts. These were elongated cells that were dendritic in nature and tended to form swirls in denser cultures. Although it was anticipated that the melanoma cells would outgrow

the fibroblasts it was found that even after several passages fibroblasts often remained the dominant cell type.

Sample	Patient	Type of lesion	Outcome
Edmel 1	66 year old Male	Lymph node metastasis	Fibroblasts only
Edmel 2	25 year old Female	Lymph node metastasis	Fibroblasts only
Edmel 3	44 year old Male	Lymph node metastasis	Melanoma cell line established
Edmel 4	61 year old Female	Subcutaneous metastasis	No growth
Edmel 5	57 year old Female	Lymph node metastasis	Fibroblasts only
Edmel 6	44 year old Female	Lymph node metastasis	Fibroblasts only

Table 4.1. Origin of melanoma samples and outcome of primary culture.

4.2.2 Overcoming the presence of fibroblasts

A number of methods were employed to try and promote growth of melanoma cells over fibroblasts. Partial trypsinisation took advantage of a possible difference in how tightly cells adhered to the plastic culture dish – melanoma cells were likely to adhere less tightly than fibroblasts and therefore it was thought that they may detach from the dish more readily during trypsinisation. In practice, it was found that when the cells that became detached early during trypsinisation were grown in subsequent cultures, fibroblasts once again predominated. No advantage of partial trypsinisation was therefore found.

Another method that was employed to try and eliminate fibroblasts from culture was the use of UV irradiation. Melanoma cells are characterised by resistance to DNA damage-induced apoptosis and it was anticipated that a dose of UV could be established that would effectively kill off fibroblasts but to which melanoma cells

would survive. In practice, no differential effect was found and no dose could be established that only effected the fibroblast population.

It is recognised that primary melanocytes do not survive in culture without certain growth factors and supplements. These are most commonly provided by using media that has been used for growing keratinocytes – so called 'conditioned media'. The other factor that is often added to melanocyte culture to stimulate growth is the phorbol ester 12-O-tetradecanoylphorbol acetate (TPA). The addition of either conditioned media or TPA to culture media did not increase the yield of melanoma cells compared with fibroblasts.

Although the methods employed to try and preferentially select for growth of melanoma cells were largely unsuccessful, in the majority of cases cells continued to grow and divide for several weeks. In all but one case however (Edmel 3) the growth slowed and eventually the cells stopped growing around passage 3-5. It was felt likely that the majority of these cultures were fibroblasts.

4.2.3 Morphological characteristics of Edmel 3

Edmel 3 consisted of a mixed population of epithelioid and spindle-shaped cells (Figure 4.1). This is in contrast to other established melanoma cell lines described in Chapter 3 such as G361, and WM115 where cells had a much more uniform morphology. The epithelioid cells varied in shape from triangular to cuboid and spherical. The spindle cells were much more elongated and dendritic in nature. No melanin pigments were evident in either of the cell types.

Edmel 3 was derived from a fragment of tissue that was dissected from a subcutaneous lymph node that had been replaced by metastatic melanoma. The diagnosis of primary melanoma had been made in 1997 following surgical

removal of a nodule from the back. The primary melanoma from which the metastasis developed was a pleomorphic, mixed population of spindle and epithelioid cell with a mild inflammatory infiltrate (Figure 4.1). It was of nodular type and had a mitotic rate of 6 per 10 high-powered fields (x250). The Breslow thickness was 5.5mm with a Clark level of IV. The lymph node metastases had appeared in 2007, after a disease-free interval of 10 years. At the time of surgery the lymph node had been reported to be slow-growing and staging investigations confirmed that no other metastatic disease was apparent. Histological examination revealed that there were a number of lymph nodes in the subcutaneous fat which were involved by melanoma. One lymph node was almost entirely replaced by melanoma whereas the others showed melanoma predominantly in the subcapsular sinus. The morphology of the metastases was similar to that of the primary lesion in that both spindle cell and epithelioid cells were present.

The morphological characteristics of Edmel 3 were consistent with the melanoma tissue from which it was derived. The appearance in culture remained relatively unchanged over several months of passaging although in addition to epithelioid and spindle cells large round cells became more obvious.

4.2.4 Edmel 3 immunohistochemistry

Immunohistochemistry (IHC) is performed on clinical melanoma specimens if there is any doubt over the diagnosis, particularly in patients presenting with metastatic disease. Although IHC was not necessary during the routine clinical management of this case, S100 and melan-A immunohistochemistry were performed on Edmel 3 in order to firstly, provide further evidence that this was indeed a melanoma cell line and secondly, to allow a comparison with the immunohistochemical profile of the clinical samples from which Edmel 3 was derived. The principal antibodies that are used for confirming a diagnosis of

melanoma include S100 and melan-A. S100 is a multigene family of low molecular weight Ca^{2+} binding proteins. S100B is most abundant in glial cells and melanocytes and is expressed in the majority of melanomas (Orchard 2000). Melan-A was isolated as a melanoma-specific antigen and is a transmembrane protein of unknown function. It is expressed in approximately 76% of melanomas (Chen et al, 1996).

Edmel 3 cells were plated out on cover slips and then stained with S100 or melan-A using standard DAB immunochemistry. S100 gave strong cytoplasmic staining in all cells (Figure 4.2). In contrast, Edmel 3 cells were negative for melan-A (Figure 4.3). Melanoma cell line G361 which was used as a positive control had strong staining with both antibodies. In all immunochemistry experiments no staining was seen in the negative (no primary antibody) controls nor in non-melanoma cell lines.

Immunohistochemistry was also perfomed on formalin fixed, paraffin emebedded clinical samples from which Edmel 3 was derived. Fresh sections were cut from both the primary and metastatic melanoma samples and stained with S100 and melan-A using standard DAB immunohistochemistry. The primary lesion was strongly positive for both S100 and melan-A whereas the metastatic deposit stained strongly for S100 but weakly for melan-A (Figures 4.2 and 4.3). It therefore appeared that the expression of melan-A was reduced during the transition from primary to metastatic melanoma and lost during the transition from metastatic melanoma to primary culture.

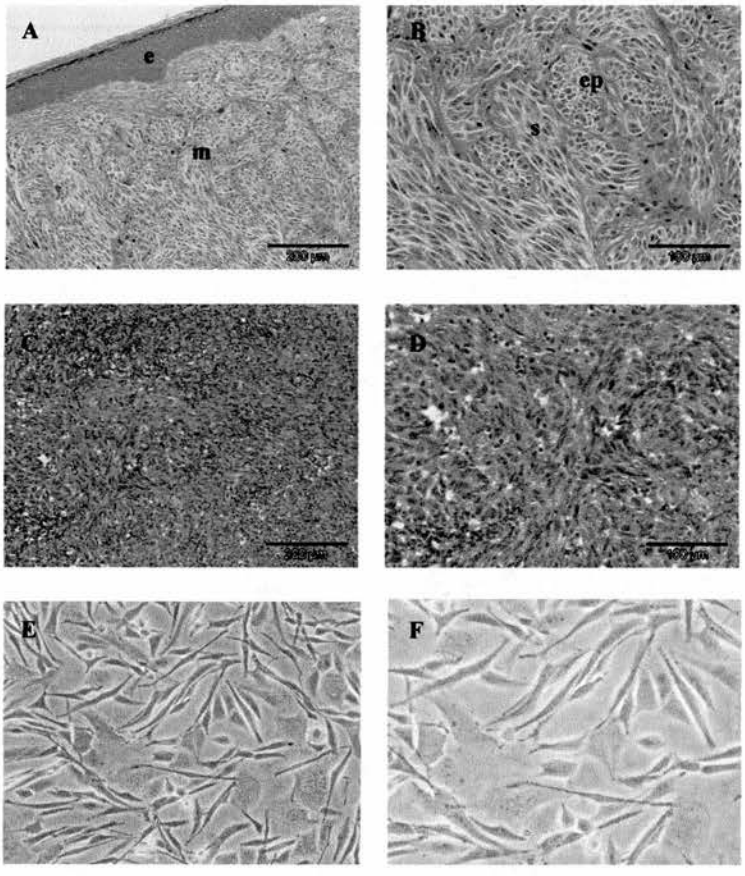

Figure 4.1. Morphological appearance of Edmel 3. (A) Primary melanoma x200. **e** indicates the epidermis and **m** is melanoma. **(B)** Primary melanoma x400. **s** indicates area with spindle cell morphology, **ep** indicates epithelioid morphology. **(C)** Metastatic deposit in lymph node x200. **(D)** Metastatic deposit in lymph node x400. **(E)** Edmel 3 x200. **(F)** Edmel 3 x320. (A)-(D) are tissue sections stained with H and E; (E)-(F) are phase contrast digital photomicrographs.

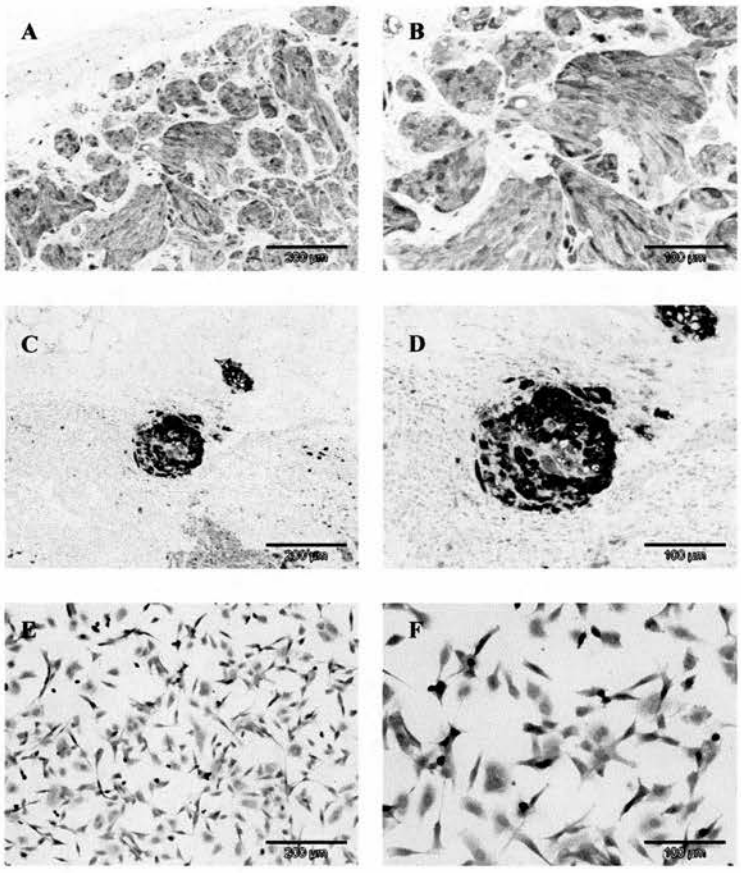

Figure 4.2. S100 immunohistochemistry. **(A)** Primary melanoma x200, **(B)** Primary melanoma x400, **(C)** Metastatic deposit in sub-capsular region of lymph node x200, **(D)** Metastatic deposit in lymph node x400, **(E)** Edmel 3 x200, **(F)** Edmel 3 x320.

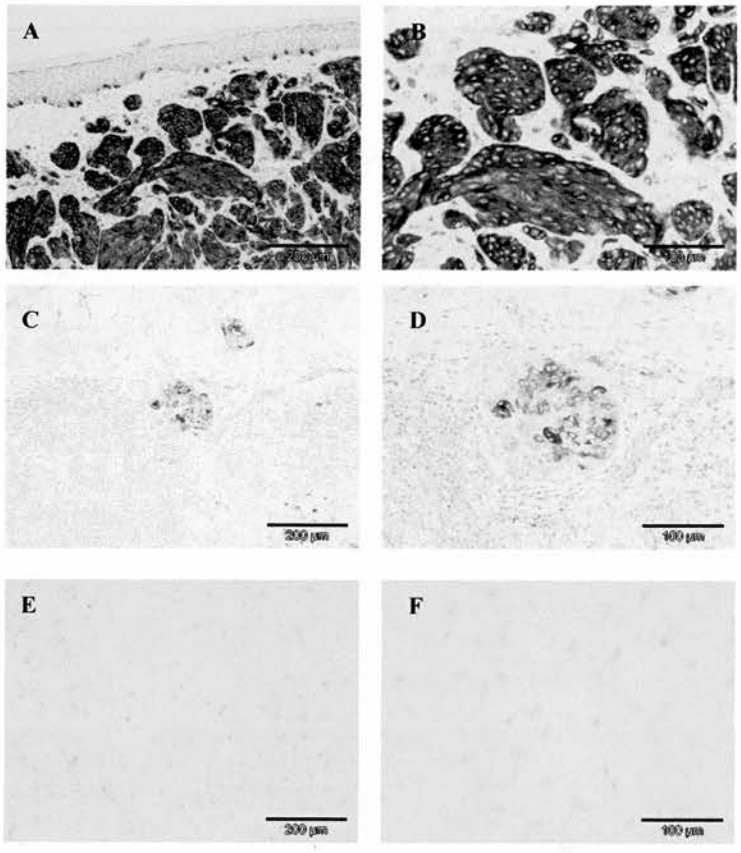

Figure 4.3. Melan A immunohistochemistry. **(A)** Primary melanoma x200, **(B)** Primary melanoma x400, **(C)** Metastatic deposit in lymph node x200, **(D)** Metastatic deposit in lymph node x400, **(E)** Edmel 3 x200, **(F)** Edmel 3 x320.

4.2.5 Subcloning of Edmel 3

Although melanomas consisting of both epithelioid and spindle cell types have previously been described the clinical significance of each of the cell types is unclear. Furthermore, it is uncertain whether each of the cell types could arise from the same cell or whether they represent two separate populations of different origin, perhaps with different metastatic potential. An attempt was therefore made to clone each of the cell populations.

Edmel 3 was plated at low density in order to allow clones to develop from single cells. When clones of approximately one thousand cells in size were established they were isolated using a cloning ring, trypsinised and then plated in separate culture dishes. From 8 clones that were picked 4 clones successfully became established (Figure 4.4).

The newly isolated clones (clones 1, 2, 4 and 5) varied in appearance with some growing in dense circular aggregates and others growing in a much more spread-out manner. It was evident that the morphology of these clones differed from one another; clone 1 consisted of a mixture of epithelioid and spindle shaped cells whereas clone 4 grew in a much more uniform manner with most of the cells being epithelioid (Figure 4.4). In clone 5 it was apparent that although both spindle cells and epithelioid cells grew within the same culture, some areas seemed to favour one cell type more than the other. Given that both epithelioid and spindle cell cells grew from the same clone it appeared that these cell types could develop from the same progenitor cell and it did not therefore seem possible to sub-clone each of these histological variants.

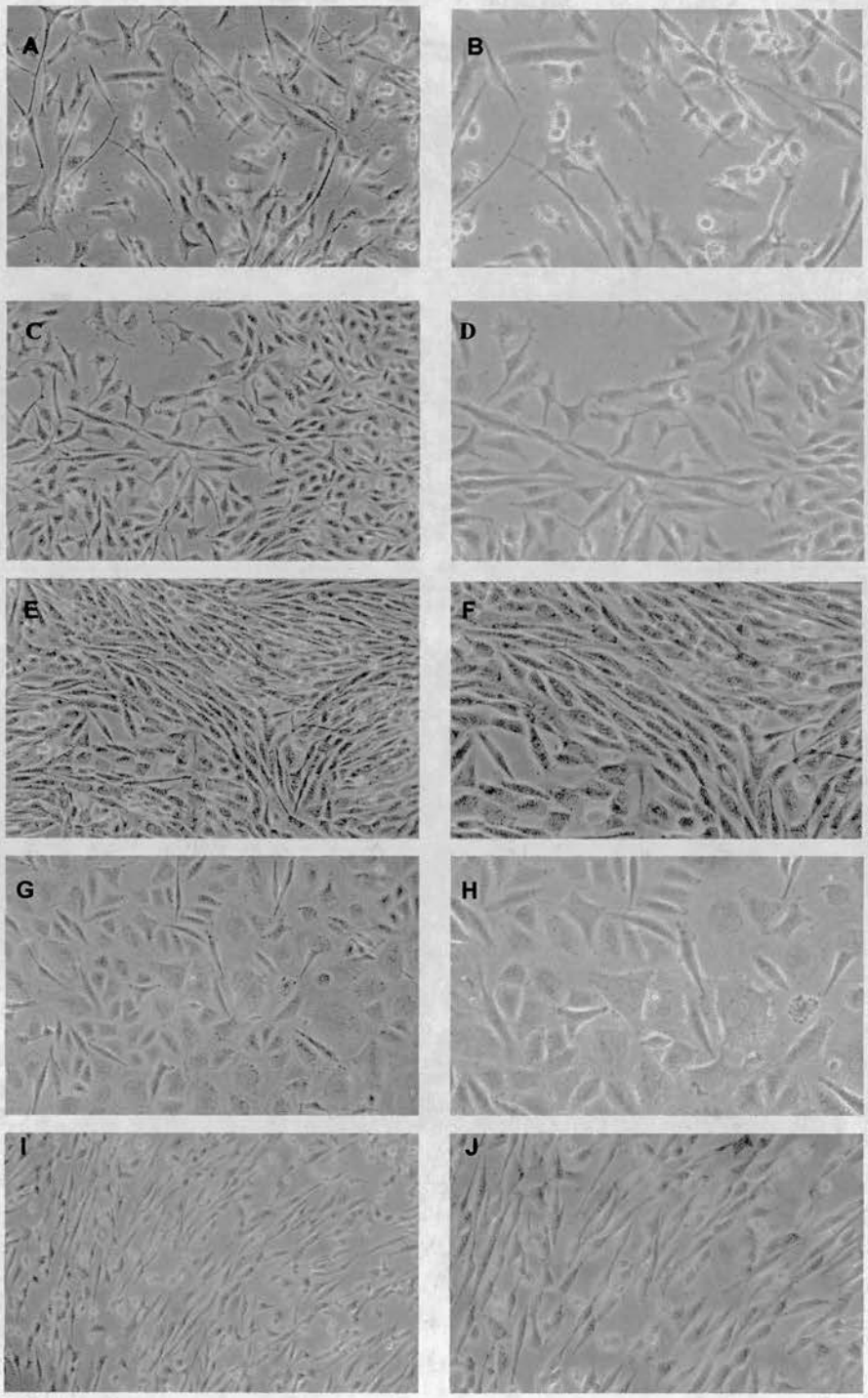

Figure 4.4. Phase contrast photomicrographs of Edmel 3 subclones. (A) Edmel 3 subclone 1 x200, **(B)** subclone 1 x320, **(C)** subclone 2 x200, **(D)** subclone 2 x320, **(E)** subclone 4 x200, **(F)** subclone 4 x320, **(G)** subclone 5 x200, **(H)** subclone 5 x320, **(I)** subclone 5 x200, **(J)** subclone 5 x320. (G) and (H) represent an area of the subclone 5 culture where both epithelioid and spindle cells can be seen whereas (I) and (J) represent an area of culture where spindle cells predominate.

4.2.6 Growth characteristics of Edmel 3

Edmel 3 was the only cell culture in which it was clear that melanoma cells outgrew any competing cells in culture. The growth of Edmel 3 was slower than most of the established melanoma cell lines that we had experience of in the lab and the use of alternative growth media such as RPMI rather than DMEM and the use of extra supplements such as 20% FCS rather than 10% made little or no difference. The growth rate was constant for the first few passages but interestingly, after 4 passages, the growth of Edmel 3 slowed up markedly. Morphologically, the cells remained healthy during this time although there was little evidence of growth for approximately 8 weeks. Subsequently cells began to grow spontaneously at a rate that was similar to earlier passages. The cause of the rate slowing was not clear.

A formal assessment of proliferation of Edmel 3 was made in comparison to melanoma cell lines G361 and ovarian cancer cell line PEO1. The proliferation assay was performed in Edmel 3 cells that had been passaged 12 times. Cells were plated at a density that allowed growth for an 8 day period without cells reaching confluency. Cells were trypsinised and counted at 48 hour intervals in duplicate (Figure 4.5). An estimate of the doubling time according to the following formula was used: $Td=(t_2-t_1)*\log(2)/\log(q_2/q_1)$ where t_1 and t_2 are 2 time points and q_1 and q_2 are the cell numbers at time points t_1 and t_2. Doubling times were as follows: G361; 37 hours, PEO1; 64 hours, Edmel 3; 104 hours. These results confirmed that Edmel 3 grew considerably slower than G361, the cell line that was used for most of the studies in Chapter 3.

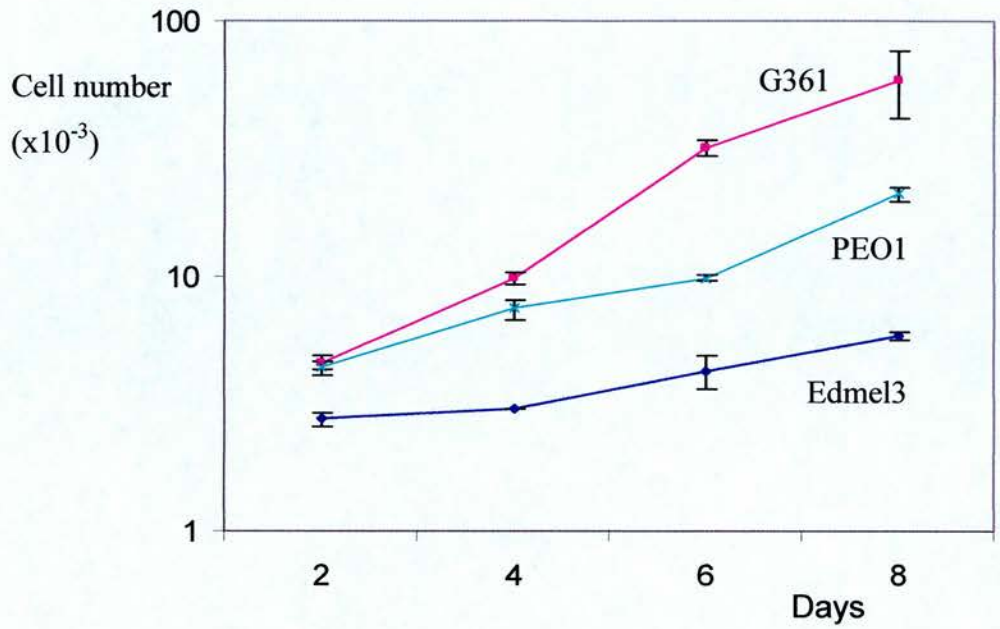

Figure 4.5. Growth of Edmel 3 *in vitro* compared to controls. Edmel 3 (p12), G361 and PEO1 were plated at low density and cell counts were performed every 2 days. Results represent the average of cell counts on 2 dishes +/- standard deviation.

4.2.7 BRAF mutation assessment

BRAF mutations have a central role in melanoma pathogenesis and are frequently found in both primary and metastatic melanomas as well as in melanoma cell lines. BRAF PCR-RFLP was performed in order to determine whether Edmel 3 had an activating mutation in BRAF. A full description of the method is given in Chapter 5. The assay revealed that the BRAF PCR product liberated a 105 kb fragment following digestion with Xba 1 which suggested that Edmel 3 was heterozygous for the activating V600E BRAF mutation.

4.2.8 MC1R Sequencing

Sequencing of the complete coding region of MC1R was performed using an automated sequencing kit following amplification of genomic DNA with suitable primers (as described in Chapter 3). No MC1R polymorphisms were found.

4.2.9 *In vivo* tumourigenicity

In order to assess tumourigenicity, Edmel 3 cells were injected subcutaneously into SCID mice. A375 was used as a control as it is known to readily form xenografts in mice. In brief, cells were grown in standard culture dishes and then trypsinised and counted. Cells were resuspended in either standard DMEM media or in matrigel and then were injected subcutaneously into the flanks of SCID mice. Growth was monitored over a 16 week period (Figure 4.6).

A375 cells quickly became established as xenografts and grew rapidly over the first 3 weeks prior to animals being sacrificed when tumours reached the pre-determined

size. Growth was enhanced by the presence of matrigel. Although small lumps became established using Edmel 3, the rate of growth was initially very slow. After approximately 10 weeks of a low rate of growth there was a marked increase in growth although even at this time the rate of growth was slower than for A375. Growth was slightly more rapid in the presence of matrigel.

Pathological examination of H&E stained sections of several xenografts (Figure 4.7) revealed that A375 tumours were amelanotic melanomas with a mixed morphological pattern. Apoptotic cells were numerous throughout as were large areas of necrosis. Edmel 3 was predominantly a spindle cell melanoma although areas of epithelioid morphology were also seen. The morphology was therefore similar to that seen in the original clinical tissue samples. The mitotic rate was higher in Edmel 3 compared with A375 although this probably reflected a higher cell density in Edmel 3 compared with A375. The pathology was reported by Dr David Brownstein.

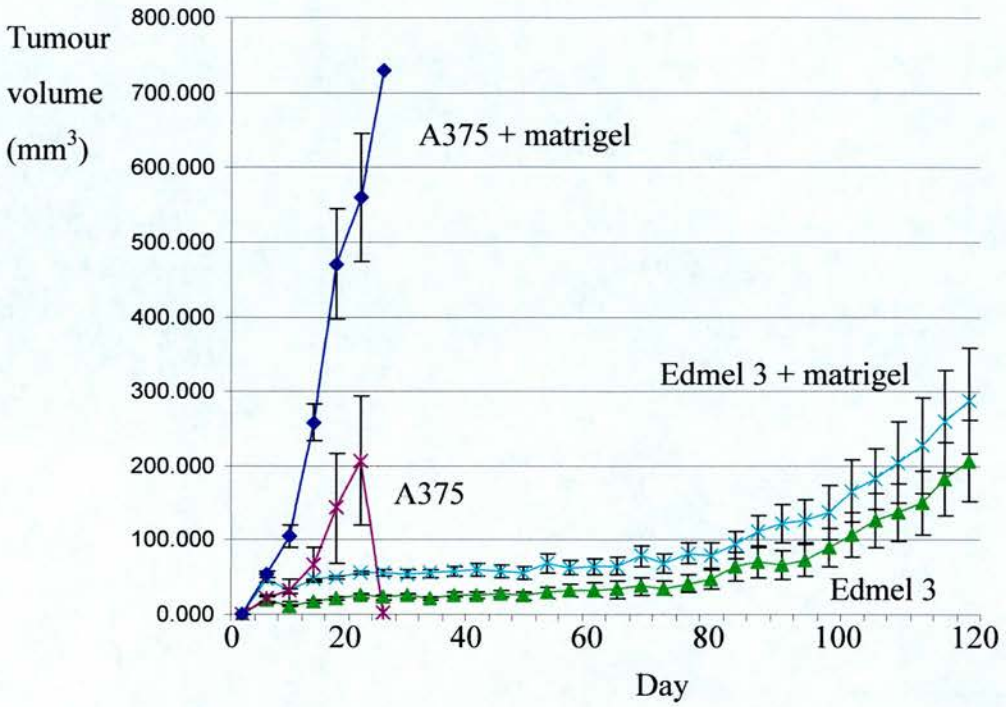

Figure 4.6. Growth of Edmel 3 *in vivo*. Growth of Edmel 3 following subcutaneous implantation in SCID mice was measured in comparison with melanoma cell line A375. Each line represents the average of 5 mice with 2 xenografts per mouse. Results are shown for growth in the absence or presence of matrigel +/- standard deviation. The reason for the apparent drop off in growth in A375 was that 4 mice were culled after tumours reached pre-determined size limits and the remaining mouse had no growth of tumour.

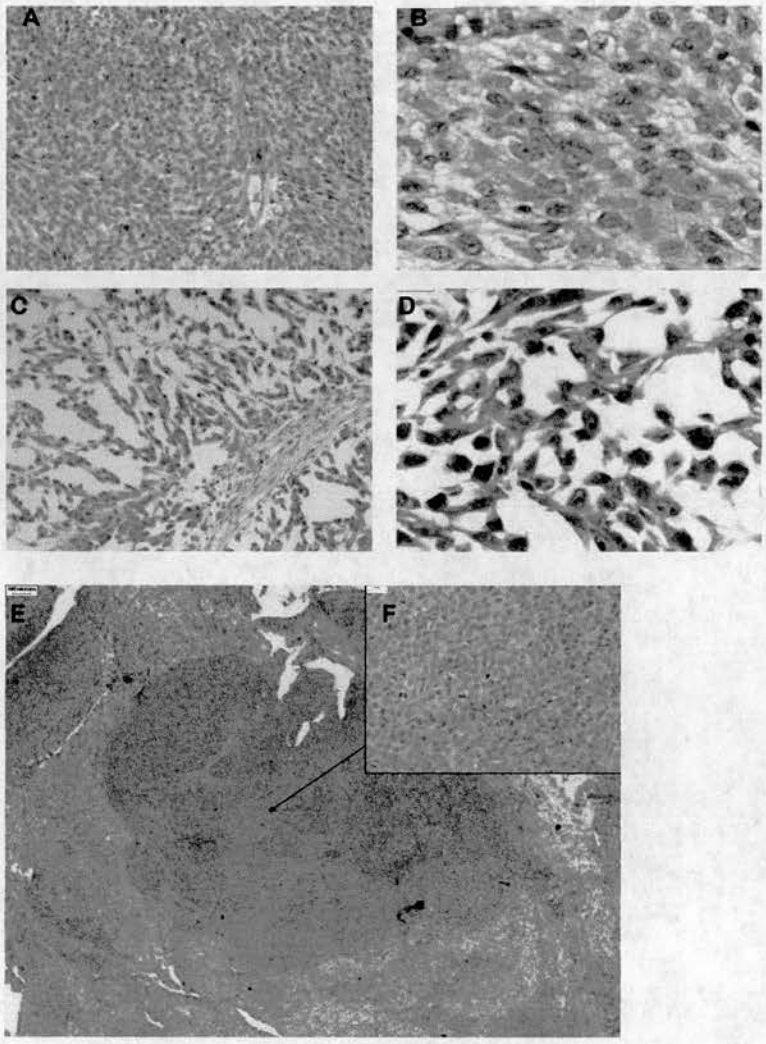

Figure 4.7. Pathology of Edmel 3 and A375 xenografts. **(A)** and **(B)** Edmel 3 xenograft, showing predominantly spindle cell morphology, **(C)** and **(D)** A375 xenografts showing mixed anaplastic pattern, **(E)** Edmel 3 xenograft with spindle cell pattern with focal area of epithelioid morphology **(F)**. Magnification is x200 for **(A)**, **(C)** and **(F)**, x400 for **(B)** and **(D)** and x100 for **(E)**.

4.2.10 Sensitivity to DNA damage

A DNA content assay was performed in order to assess the sensitivity of Edmel 3 to DNA damage-induced apoptosis following irradiation with UVC in comparison with G361 (Figure 4.8 and Table 4.2). In untreated controls the number of cells in the 'S-phase' area of the DNA content profile was much less in Edmel 3 compared with G361 control cells. This suggested that fewer replicating cells were present which is consistent with the growth experiments. Twenty-four hours after UVC irradiation there were very few cells in the sub-G1 area of the DNA content profile with Edmel 3 which suggested that very little apoptosis had occurred. This was in contrast to G361 cells where a large number of cells in the sub-G1 area were seen. Even at a dose of 50 J/m^2 only 17% of cells were in the sub-G1 area compared to 47% of G361 cells. In contrast, there was an increase in the number of cells in the 'S-phase' area in Edmel 3 cells following UV suggesting that cells were arrested in S-phase due to non-repaired DNA damage and weren't proceeding to mitosis or engaging apoptosis at this time-point.

In order to further assess the response to DNA damage an annexin V assay was performed including time points at both 24 and 48 hours (Figure 4.9). This assay confirmed that the levels of apoptosis in Edmel 3 were much less than G361 at the 24 hour point which is consistent with the DNA content assay. 15% of Edmel 3 cells were apoptotic at this time point which is similar to the 13% of cells seen in the DNA content assay. At 48 hours however, levels of apoptosis in Edmel 3 had increased. The percentage of cells in apoptosis after 48 hours was 53% for Edmel 3 versus 68% for G361. These results suggested that the apparent resistance of Edmel 3 to DNA damage-induced apoptosis in the DNA content assay was due to a difference in the timing rather than the absolute level of the apoptotic response. The delay in apoptosis in Edmel 3 is likely to in part be due to a slower growth rate compared to G361 (confirmed in Figure 4.5). The results also suggested that a different mechanism for DNA damage-induced apoptosis may exist in these different cell lines: Prior to

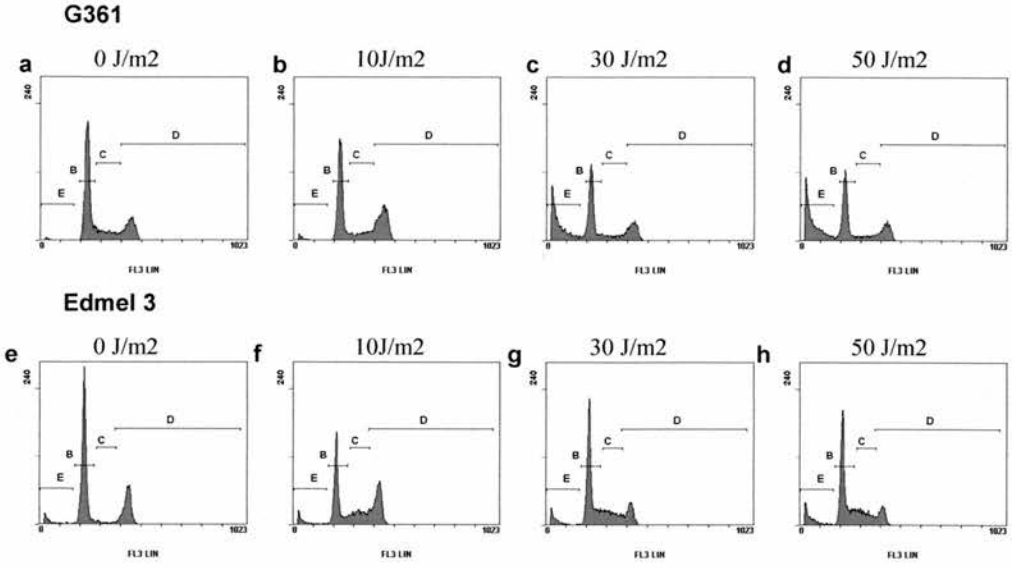

	sample	Apoptosis	G1	S-phase	G2
G361	**a**	4%	58%	26%	12%
	b	6%	50%	26%	19%
	c	35%	35%	20%	10%
	d	47%	30%	15%	8%
Edmel 3	**e**	5%	70%	10%	15%
	f	8%	31%	49%	12%
	g	11%	37%	47%	5%
	h	17%	34%	43%	5%

Figure 4.8 and Table 4.2. DNA damage-induced apoptosis in Edmel 3. (a) to (h) represent DNA content assay profiles 24 hours after UVC irradiation. The table shows the results of a cell cycle analysis programme that quantifies the frequency of cells at each of the 4 regions of the graph: Region E = apoptotic cells, B = cells in G1, C = cells in S-phase, D = cells in G2. The increased number of apoptotic cells in G361 compared to Edmel 3 following UV is clearly seen.

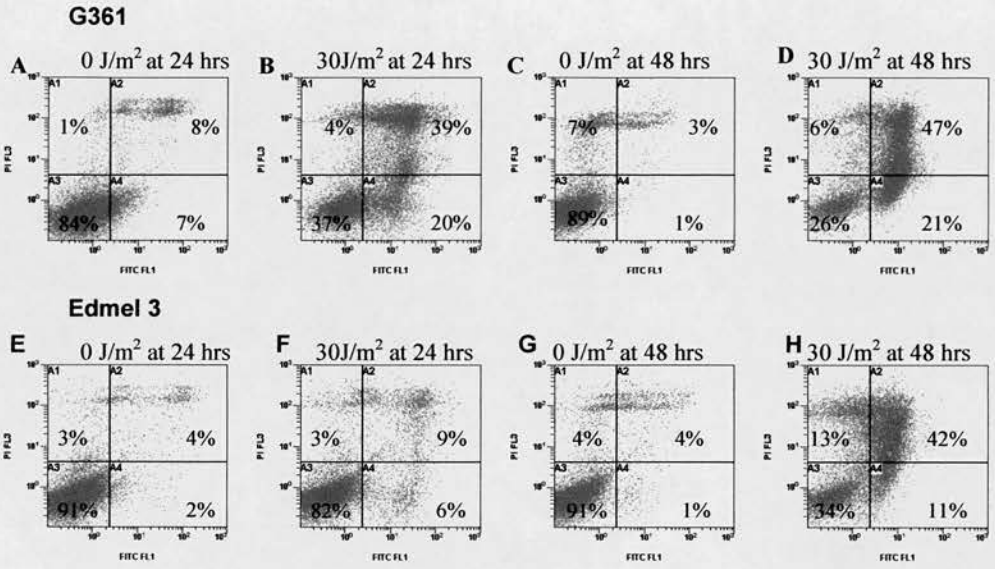

Figure 4.9. DNA damage-induced apoptosis in Edmel 3. (A) to (H) represent profiles from the annexin V apoptosis assay 24 or 48 hours after UVC irradiation. Percentages of cells in each quadrant are marked. Apoptosis was evident in G361 cells 24 and 48 hours after irradiation whereas it was only evident in Edmel 3 cells after 48 hours. Y-axis represents propidium iodide (PIFL3) and x-axis represents annexin V (FITCFL1).

apoptosis there was a build up in cells in S phase in Edmel 3 cells whereas in G361 there appeared to be an increase in cells in G2 rather than S-phase.

4.3 Discussion

A number of problems had to be overcome in order to successfully establish a novel melanoma cell line. Firstly, it was not always possible to be able to recognise macroscopically which part of the surgical specimen contained the melanoma tissue. This was often made more challenging by the absence of significant pigment in some of our samples. As a consequence of this it was likely that a significant proportion of the tissue that was being broken up for culture was normal tissue which would lead to a higher chance of non-tumour cells surviving in culture. Secondly, it became clear that fibroblasts were growing quite readily from some of the isolates in competition with melanoma cells. Despite use of various stategies to overcome the problem of fibroblasts in the culture (including selective trypsinisation, use of UV and alterations of culture conditions), it proved quite difficult to culture a pure population of melanoma cells. In most instances cells that were morphologically consistent with fibroblasts predominated and few cells that were morphologically consistent with melanoma cells became established. The fibroblasts tended to survive in culture for approximately 5 passages which is consistent with previous findings (Ben-Porath and Weinberg 2004). At this stage they stopped growing and although they did not die straight away none of the cells started to grow again and it was likely that they had entered a senescent state. It was apparent that the success of establishing Edmel 3 was largely due to the nature of the tumour from which it was derived rather than the particular strategy used. This was a tumour that appeared to break up quite easily and had a high proportion of tumour to non-tumour cells present.

A number of improvements to the procedure for isolating melanoma cells could be considered. Firstly, the involvement of a pathologist would be of great benefit. The

availability of a pathologist to review the histology of the surgical specimen immediately following surgery would help ensure that it was only melanoma-rich tissue that was being supplied for attempts at culture. The disadvantage of this may be that it would slow down the transport of tissue from theatre to the lab which may compromise the ability of the cells to survive. Secondly, a protocol whereby cells from primary melanomas could be received without compromising their clinical management would be of great benefit. This would arguably be a more valuable resource given the wide availability of cell lines from metastatic melanoma samples. Finally, for future attempts at isolation of melanoma cells it may be advantageous to try other strategies during the processing of tissue such as use of enzymes to digest extra-cellular matrix prior to plating and use of FACS to sort melanoma cells from competing cells in culture.

It can often be difficult to distinguish tumour cells from other cell types that may successfully grow in culture. This may be particularly true in the case of melanoma which in tissue sections can be histologically very similar to other cell types (Banerjee and Harris 2000), particularly when amelanotic. In clinical specimens a panel of antibodies is often required to confirm a diagnosis of melanoma. S100 is positive in the majority of melanomas whereas melan A is positive in a lower proportion of metastatic melanomas and is often negative in spindle type melanomas (Banerjee and Harris 2000). Although in clinical practice if there is still doubt about the diagnosis further immunohistochemistry is often used, this was not performed for Edmel 3. It was felt that as the mixed morphology in culture was consistent with the original tumour there was little doubt that Edmel 3 was a pure melanoma culture.

Spindling of cells in melanoma is a common and well known occurrence which clinically may lead to the misdiagnosis of a melanoma as a sarcoma or sarcomatoid carcinoma (Levene 1980). In order to further investigate the significance of having a mixed population of epithelioid and spindle-shaped cells in the same tumour an attempt was made to isolate the 2 individual cell populations. Although sub-populations of Edmel 3 cells were successfully cloned it was not possible to isolate

clones containing only one cell type. It was therefore likely that both spindle and epithelioid cell types could be derived from the same progenitor cell. Interestingly, each of the clones had a slightly different appearance in culture, some growing in tight colonies, others growing in a more diffuse manner. The significance of these differences is uncertain and it may be that in subsequent passages the differences become less obvious.

The growth of Edmel 3 was generally slower than most of the other cell lines studied in the lab. The cause of the dramatic slowing of growth around passage 4 however was unclear. Cells that are grown in culture can respond to stress either by entry to senescence, by undergoing apoptosis or by undergoing a transient growth arrest (Ben-Porath and Weinberg 2004). As senescence is an irreversible process it is likely that Edmel 3 cells underwent a process of growth arrest precipitated by stress associated with the change in environment during the transition from *in vivo* to *in vitro*. During this process it is thought that cells need to learn to respond to different cues although the underlying mechanism is poorly understood (Ben-Porath and Weinberg 2004). When Edmel 3 culture started to grow once again, all areas of the culture dish appeared to increase their growth rate around the same time. This makes it unlikely that it was due to overgrowth of a variant subpopulation.

Tumourigenicity studies confirmed that although Edmel 3 appeared to establish itself as xenografts in SCID mice their growth was very slow. Whilst A375 xenografts became established very quickly and grew exponentially for 3 weeks there was little growth of Edmel 3 xenografts for the first 10 weeks. Pathology studies confirmed that A375 xenografts were more anaplastic than Edmel 3 and there was more apoptosis and necrosis evident which probably reflected the increased growth rate of these tumours in comparison to Edmel 3. It was interesting that the increased growth rate of A375 was not supported by a higher number of mitoses present per high-powered field but this was largely thought to reflect a much lower cell density in A375 in comparison to Edmel 3. The morphology of Edmel 3 xenografts was a

mixture of spindle cells and epithelioid cells and therefore it retained the appearance of the melanoma tissue from which the cell line was derived.

Unlike some of the cell lines that were characterised in chapter 4 no MC1R polymorphisms were found in Edmel 3. This is unsurprising given that these cells were isolated from a male with dark hair. MC1R polymorphisms would be more expected in individuals with fair skin, red hair, freckling or blue eyes. Edmel 3 was found to be heterozygous for the V600E BRAF mutation. In clinical samples, the rates of BRAF mutation are highest in those primary tumours from a site of intermittent sun exposure; 78% of melanomas from intermittent sun-exposed sites have BRAF mutations compared with 10% in sites of chronic sun exposure (Curtin et al, 2005). Characterisation of a large panel of melanoma cell lines has suggested a BRAF mutation rate of approximately 75% (Haluska et al, 2006). It is not clear whether this high rate reflects the fact that more melanomas from intermittent sites of sun exposure are nodular and more likely to metastasise (the source for most melanoma cell lines) or alternatively, that those melanoma cells that have a BRAF mutation have some sort of growth advantage and are therefore more likely to grow in culture. The primary lesion from which the mestastasis developed from which Edmel 3 was subsequently derived was on the back, a site of intermittent sun exposure.

Edmel 3, in common with other melanoma cell lines tested, was found to be resistant to DNA damage-induced apoptosis. The delayed response to DNA damage in Edmel 3 compared to other melanoma cell lines was probably in part due to the slower growth rate of this cell line. This is consistent with the clinical history which reports that firstly, the interval between diagnosis of the primary lesion and development of the metastasis was approximately 10 years and secondly, the growth of the metastases was slow. Although this was a particularly long disease free interval it is not uncommon for melanoma to metastasise at 10 years and beyond. Whilst the patient from which Edmel 3 was derived did not receive chemotherapy it could be postulated that the clinical response to standard DNA damaging agents such as

dacarbazine would be low, given the low percentage of cycling cells seen in the DNA content profiles and the relative resistance to DNA damage-induced apoptosis of Edmel 3.

In conclusion I have successfully established and characterised a new melanoma cell line, Edmel 3. This cell line maintains the morphological features of both the metastatic melanoma from which it was derived and the original primary melanoma from 10 years ago. The melanoma cell line is from a site of intermittent sun exposure, carries an activating BRAF mutation, is characterised by relatively slow growth in culture and resistance to DNA damage-induced apoptosis and forms xenografts when injected subcutaneously into SCID mice. This cell line will be a valuable tool for further *in vitro* melanoma studies as well as allowing a 'pure' melanoma sample to act as a control for ongoing gene expression studies.

Chapter 5 Development of a tissue microarray for investigation of melanoma progression and prognosis

5.1 Introduction

Tissue microarrays (TMAs) consist of paraffin blocks in which up to 1000 separate tissue cores are assembled in array fashion to allow simultaneous histological analysis (Kononen et al, 1998). The current technique, developed in the late 1990s, uses a hollow needle to remove tissue cores as small as 0.6mm in diameter from regions of interest in paraffin embedded tissues such as clinical biopsies or tumour samples. These tissue cores are then inserted into a recipient paraffin block in a precisely spaced array pattern. Sections from this block can be cut with a microtome, mounted on a microscope slide and then analysed by various standard histological methods. Each microarray block can be cut into 100-500 sections which can be subjected to independent tests. Tests commonly employed in tissue microarray include immunohistochemistry (IHC) and fluorescent in situ hybridisation. Tissue microarrays provide a highly efficient method of evaluating the expression and activity status of relevant molecules in a large number of tissue samples and are particularly useful in analysis of cancer samples. In this chapter TMAs are used to study both the changes in protein expression at different stages of melanoma progression and to investigate potential prognostic markers.

The pathogenesis of melanoma is widely accepted as being a multistep process that may include the phases benign naevi, dysplastic naevi, in-situ melanoma, radial and vertical growth phase melanoma and metastatic melanoma (Clark et al, 1984). The mechanisms that mediate the transition between each step of the pathway remain largely unknown although a number of key proteins involved in proliferation, control of apoptosis and invasion have been implicated (Hsu et al, 2002). It is hoped that further investigation into changes in protein expression during melanoma progression (assessed by immunohistochemistry) will provide an insight into the molecular mechanisms underlying progression of melanocytes into melanoma.

Prognostic markers are markers that have a recognised association with clinical outcome such as survival (McShane et al, 2005). The best current prognostic marker in melanoma, lesion thickness, is unreliable and in some cases is not an accurate indicator of biological behaviour; a significant minority of patients with very thin (<1mm) melanomas go on to develop metastatic disease (Balch et al, 2000). The identification of new molecular prognostic markers in primary melanoma would be an important advance as not only may they help in deciding which patients require more aggressive treatment they may also offer further clues into melanoma pathogenesis and the identification of novel therapeutic targets.

The most comprehensive TMA study published to date included 220 primary and metastatic melanomas from patients in Vancouver, Canada (Dai et al, 2005). It also contained 16 benign naevi and 66 dysplastic naevi. Correlation of protein expression by immunohistochemistry with clinical outcome revealed that p-Akt (Dai et al, 2005) and PUMA (Karst et al, 2005) had prognostic value in this group of patients. Furthermore p-Akt was found to be an independent prognostic factor in patients with thin melanomas. Another large TMA has been built from primary melanomas from 343 patients in San Francisco, US. Osteopontin (Rangel et al, 2008) and nuclear receptor coactivator-3 (Rangel et al, 2006) were found to be independent prognostic markers in this group of patients. Two smaller TMAs have been constructed at the MD Anderson Cancer Centre, US and Yale University, US. They contain 22 and 214 primary melanomas respectively as well as a small number of other melanocytic lesions. These TMAs have confirmed that altered expression of activator protein 2-alpha is associated with melanoma progression and prognosis (Berger 2005). The largest published melanoma TMA in the UK consisted of 120 patients with melanoma from Middlesex. CD44v3 (Pacifico et al, 2006) and nm23 (Pacifico et al, 2005) were found to be novel prognostic markers in primary melanoma.

The proteins that have been chosen for investigation in this chapter are B-catenin, bcl-2 and galectin-3. B-catenin is a multi-functional protein that controls a number of cell activities in both the membrane and the nucleus (Peifer and Polakis, 2000). It

binds to the cytoplasmic tail of E-cadherin and therefore has an important role in cell adhesion. The Wnt/B-catenin signalling pathway affects a number of cellular activities including proliferation, migration and differentiation (Peifer and Polakis, 2000). Loss of B-catenin membrane expression has been associated with increased cell invasiveness although the differential expression of B-catenin during melanoma progression is controversial. Some studies report that B-catenin expression is not significantly changed whereas others reveal down-regulation of membranous expression during melanocytic progression (Reviewed in Bachman et al, 2005). The prognostic role of B-catenin in melanoma is unclear.

Bcl-2 oncoprotein is an inhibitor of apoptotic death that is involved in the control of the intrinsic apoptotic pathway. It is thought to function principally by binding and sequestering activators of apoptosis (Letai 2007). Experimental transfection of cells with bcl-2 confers a multidrug resistant phenotype in both haematologic and solid tumour cells (Schmitt et al, 2000). Conversely, pharmacologic reduction or targeted inactivation of bcl-2 amplifies apoptotic responses to chemotherapy in multiple *in vivo* models (Jansen et al, 1998). Oblimersen, an anti-sense oligonucleotide has been shown to sensitise melanoma cells to chemotherapy in preclinical studies (Jansen et al, 2004) and in Phase III testing of oblimersen plus dacarbazine versus dacarbazine alone has shown a positive impact on progression free survival (Millward et al, 2004). Bcl-2 is highly expressed in melanocytes and melanomas although its contribution to chemoresistance and prognosis is controversial (Lomuto et al, 2004).

Galectin-3 is a member of the family of lectins which selectively binds b-galactosidase residues (Krzeslak and Lipinska, 2004). It is a chimeric molecule consisting of both carbohydrate recognition and collagen-like domains. It is predominantly localised in the cytoplasm although may translocate to the nucleus or be secreted from the cell by ectocytosis. Galectin-3 plays an important role in adhesion, proliferation, differentiation and angiogenesis and metastasis in multiple tumours (Nakahar et al, 2005). Both pro- and anti- apoptotic activity of galectin-3 have been found depending on the type of tumour studied. A recent study has

suggested that galectin-3 expression may be associated with melanoma progression and may have some potential as a prognostic marker (Prieto et al, 2006).

The aims of the work in this chapter were to firstly, develop a tissue microarray that includes all stages of melanoma development, secondly, investigate changes in the expression of key proteins during melanoma progression and thirdly, identify novel prognostic markers in primary melanomas. A schema detailing the various stages in this study is shown in Figure 5.1. The design and construction of the TMAs is discussed in the first part of the chapter whilst the rest of the chapter contains the results including some ongoing work on assessment of BRAF mutations in melanoma samples.

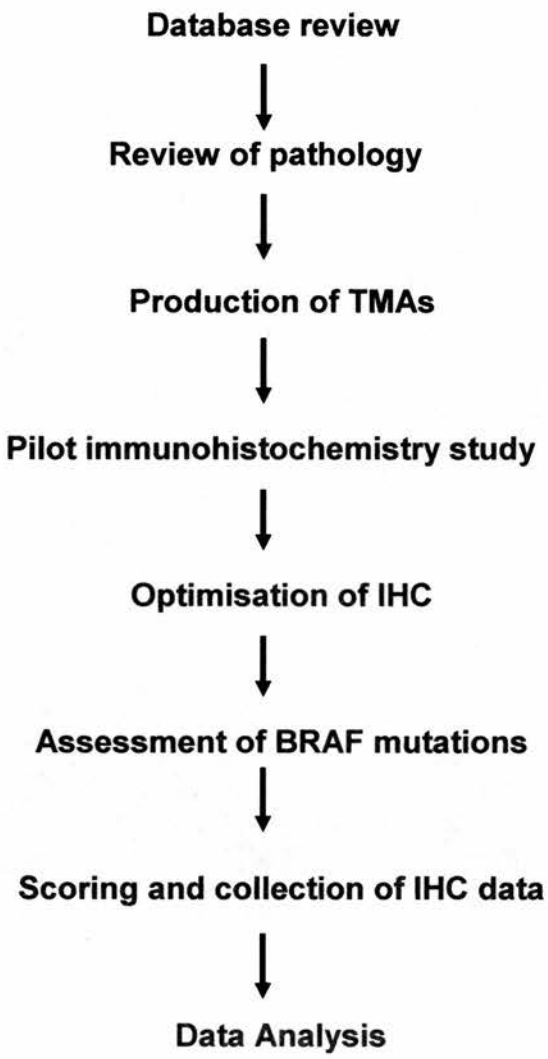

Figure 5.1. Schema of steps in the design, construction and analysis of the tissue microarrays. The parts of the diagram in blue represent the design and construction of the TMAs and the parts of the diagram highlighted in red represent the results.

5.2 TMA design and construction

The TMAs were designed to include all stages of melanoma progression including benign naevi, dysplastic naevi, in-situ melanoma, radial and vertical growth phase melanoma and metastatic melanoma. Collection of detailed clinicopathologic data was however restricted to primary melanomas. The local ethics committee granted ethical approval for this study (REC reference number: 06/S1103/9).

5.2.1 Database review

The numbers of samples to be included on the TMAs were 400 primary melanomas and 50 of each other category (naevi, dysplastic naevi, in-situ melanomas and metastatic melanomas). In order to ensure adequate follow up for calculation of survival, patients diagnosed with cutaneous melanoma from 1993-1997 were selected. Power calculations were performed in order to ensure sufficient numbers of patients were included in the study to detect differences in protein expression between groups. Patients with non-cutaneous sites of primary (inc genital, mucosal, uveal) and those patients who had their surgical specimens stored at other centres were excluded.

Clinicopathologic data were collected on all patients with primary cutaneous melanoma diagnosed in Edinburgh from 1993-1997 using the Scottish Melanoma Group (SMG) database. The SMG was set up in 1979 with the aim of gathering detailed clinico-pathological, treatment and follow up details for all patients with invasive primary melanoma of the skin diagnosed in Scotland. The SMG covers a relatively stable population of approximately 5 million and is one of very few population-based registries in the world. All pathologists complete a detailed form at diagnosis and this information is entered in to the SMG database. Detailed follow-up is gathered at 2, 5, 10 and 20 years after the diagnosis. The data collected in this

study included patient age and sex, tumour thickness, type, site, stage, and presence of ulceration, date and site of recurrence and disease-specific and overall survival. Basic data were also collected on all patients with metastatic melanoma diagnosed during 1993-1997 as well as approximately 50 patients with naevi, dysplastic naevi and in-situ melanoma respectively.

5.2.2 Review of pathology

Formalin-fixed paraffin-embedded tissue samples were retrieved from the pathology department. Corresponding haematoxylin and eosin (H&E) slides were reviewed by a pathologist (Dr Tamasin Doig) in order to firstly, confirm the diagnosis and secondly, to mark off the areas in the sample that were most representative of the lesion as a whole for subsequent coring. Areas of melanomas that had a marked stromal component were avoided where possible. Those samples in which there was insufficient material for coring or where the initial diagnosis had not been confirmed were excluded from the study. Conventional H&E stained melanoma sections were also assessed from each primary melanoma sample for the degree of solar elastosis.

5.2.3 Construction of TMAs

The TMAs were constructed according to standard procedures. In brief, from each 'donor' block, 0.6mm tissue cores were sampled using a Beecher Instruments manual arrayer and mounted into 'recipient' paraffin blocks. The construction was performed by Dr Tamasin Doig and myself. In samples where sufficient material was present duplicate cores were taken. Where possible, cores were taken from both the invasive and non-invasive components of the tumour. In total, 20 separate TMAs were constructed. This was in order to make it possible to perform IHC on specific types of lesion (e.g. in-situ melanoma) and also to make the scoring as manageable as possible by avoiding very large numbers of cores on a single array.

5.3 Results

5.3.1 Pilot immunohistochemistry study

A pilot study of B-catenin and bcl-2 immunohistochemistry (IHC) was performed on whole melanoma sections in order to confirm that differences in staining could be detected for these antibodies in melanoma specimens of suitable age. E-cadherin IHC was also performed although galectin-3 was used for the main TMA study in preference to E-cadherin due to the emergence of data that suggested that galectin-3 may have a role in melanoma progression and prognosis. There were well characterised antibodies available for all three proteins that were expected to provide a good range of types and intensities of staining. Twelve formalin fixed paraffin-embedded melanoma specimens were selected from the tumour archive at the Royal Infirmary of Edinburgh Department of Pathology. They were 6 melanomas from patients who developed recurrence within 5 years and 6 from those that did not. The 2 groups were matched for melanoma thickness. Sections of each melanoma were stained for B-catenin, bcl-2 and E-cadherin by standard peroxidase/diaminobenzidine (DAB) immunohistochemistry.

A number of systems are in use for scoring IHC TMA studies. One widely used method assigns a score for staining intensity and frequency each according to a 4 point scale (0-3) with a total score representing the sum of these two values (0-6). An alternative method which was adopted for these studies is the histoscore which assesses the percentage of cells at each of 4 intensity levels (0-3), multiplied by the intensity, giving a total score up to 300. Where more than one part of the cell is stained (e.g. nucleus and cytoplasm) each cellular compartment is scored separately. A range of scores were found for each of the antibodies (Figure 5.2). All cases showed membranous expression of B-catenin with 9 of the 12 showing high intensity staining in all cells. 3 cases showed nuclear staining. Eleven of twelve cases showed

B-catenin

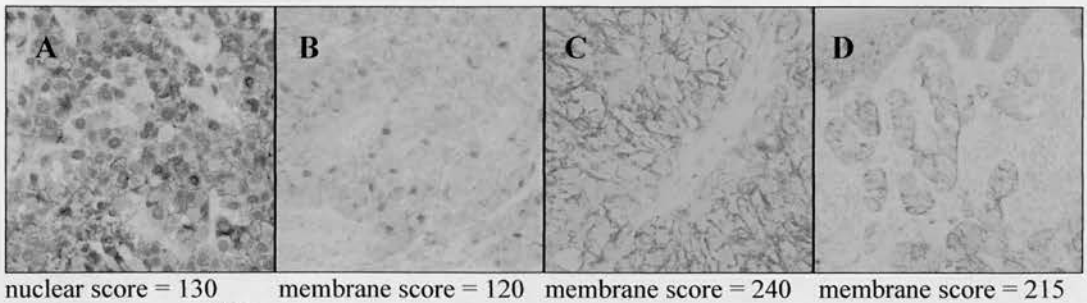

nuclear score = 130 membrane score = 120 membrane score = 240 membrane score = 215
membrane score = 170

Bcl-2

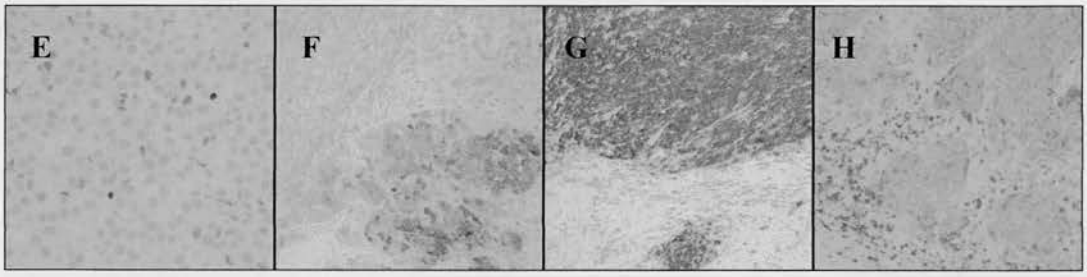

cytoplasmic score = 0 cytoplasmic score = 180 cytoplasmic score = 290 cytoplasmic score = 200

E-cadherin

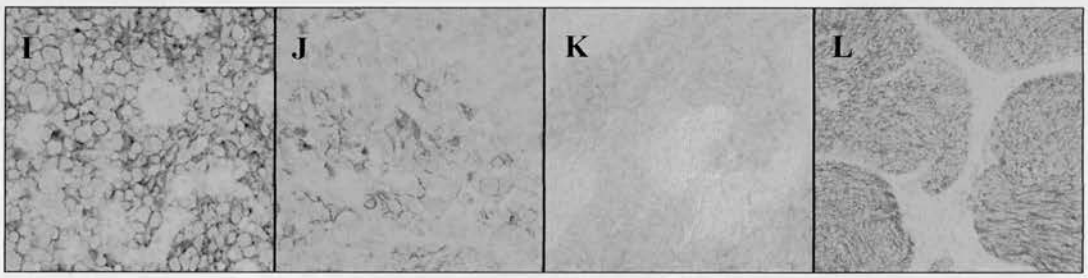

membrane score = 275 membrane score = 180 membrane score = 210 membrane score = 280

Figure 5.2. B-catenin, Bcl-2 and E-cadherin immunohistochemistry in primary melanomas. B-catenin: (A) Case 1, x400. Nuclear and membranous staining. **(B)** Case 4, x400. Membranous staining with occasional nuclear positivity. **(C)** Case 8, x400. Strong membranous staining. No nuclear staining. **(D)** Case 12, x200. Membranous staining. **Bcl-2: (E)** Case 1, x400. Negative staining. **(F)** Case 2, x200. Variation in staining intensity between dermal nests. **(G)** Case 6, x100. Uniform strong positive staining. Note lymphoid cells at deep aspect acting as internal control. **(H)** Case 8, x200. Positive staining in dermal nests, but note difference in staining intensity compared to lymphocytes. **E-cadherin: (I)** Case 1, x400. Strong membranous staining. **(J)** Case 2, x400. Membranous staining of variable intensity. **(K)** Case 6, x200 Variable staining pattern with positive and negative nests. **(L)** Case 7, x200. Strong membranous staining. Scores represent the product of frequency (0-100%) and intensity of staining (0-3) which give a total up to 300 (e.g. score for (L) = (80 x 3) + (20 x 2) = 280).

cytoplasmic expression of bcl-2. The staining pattern and intensity were variable. All twelve tumours showed membranous E-cadherin expression, with some variation of staining intensity within individual tumours. There were no notable differences in staining between the 6 cases which developed recurrence versus those that did not. The scores assigned to selected cases are shown in Figure 5.2.

From the 3 antibodies tested B-catenin and bcl-2 were selected for investigation in the main TMA study. E-cadherin was not selected due to the lack of differences in expression seen between melanoma samples. It was felt that the uniformity of expression seen in this pilot study would make it less likely that the comparison of E-cadherin expression with clinicpathologic variables in the main TMA study would provide any meaningful data. Galectin-3 was selected as the third protein to study due to emergence of promising data which suggested its potential as a marker of progression and prognosis in cutaneous melanoma (Prieto et al, 2006).

5.3.2 Optimisation of immunohistochemistry conditions using a practice TMA

Although melanomas arise from the main pigment producing cells of the body it is not uncommon for them to be amelanotic (Thompson et al, 2005). Conversely, however, some melanomas have such large amounts of pigment in their cytoplasm that it can present problems for interpretation of standard DAB-based immunohistochemistry. In order to investigate optimum staining and to assess the impact of the presence of pigment on interpretation of scoring a small 'practice' TMA was constructed containing a total of 20 cores from thick primary and metastatic melanomas. These were samples from 1993-1997 for which there was surplus tissue available. A number of cores were selected from heavily pigmented areas of tumour. The practice TMA was used to investigate optimum conditions for IHC including use of alternative counterstains, alternative detection systems and different thickness of section.

5.3.2.1 Investigation of azure blue as an alternative counterstain

Azure blue has the effect of turning melanin pigments blue/green and can therefore be helpful in the interpretation of DAB immunohistochemistry in heavily pigmented lesions (Kligora et al, 1999). It was compared to haematoxylin as a counterstain using sections cut from the practice TMA. S100 was selected as the antibody as it is known to be positive in the majority of melanomas (Sundram et al, 2003).

S100 gave strong cytoplasmic staining in all melanoma cells in the majority of cores on the 'practice' TMA. It was found that when haematoxylin was used as a counterstain it was difficult to accurately assign the contribution of pigment versus DAB to the overall appearance (Figure 5.3 A and B). With the use of azure blue all melanin pigment turned blue/green (Figure 5.3 E-H). This enabled more accurate determination of the contribution of DAB to overall staining in heavily pigmented cores. It was found however that azure blue had some disadvantages in comparison to haematoxylin. Firsly, it was inferior to haematoxylin for detailed assessment of tissue as the cellular architecture was not as well defined (see Figure 5.3 E to H). This may be a particular problem when trying to determine which parts of a tumour core are melanoma cells and which are non-tumour/stroma. Secondly, the blue/green colour that resulted from the uses of azure blue faded quite quickly with time. This would make it necessary to score the IHC results rapidly which in practice could be problematic. It was therefore concluded that although azure blue may have a useful role in routine pathology of pigmented lesions it would not be taken forward as a standard counterstain for the main TMA study.

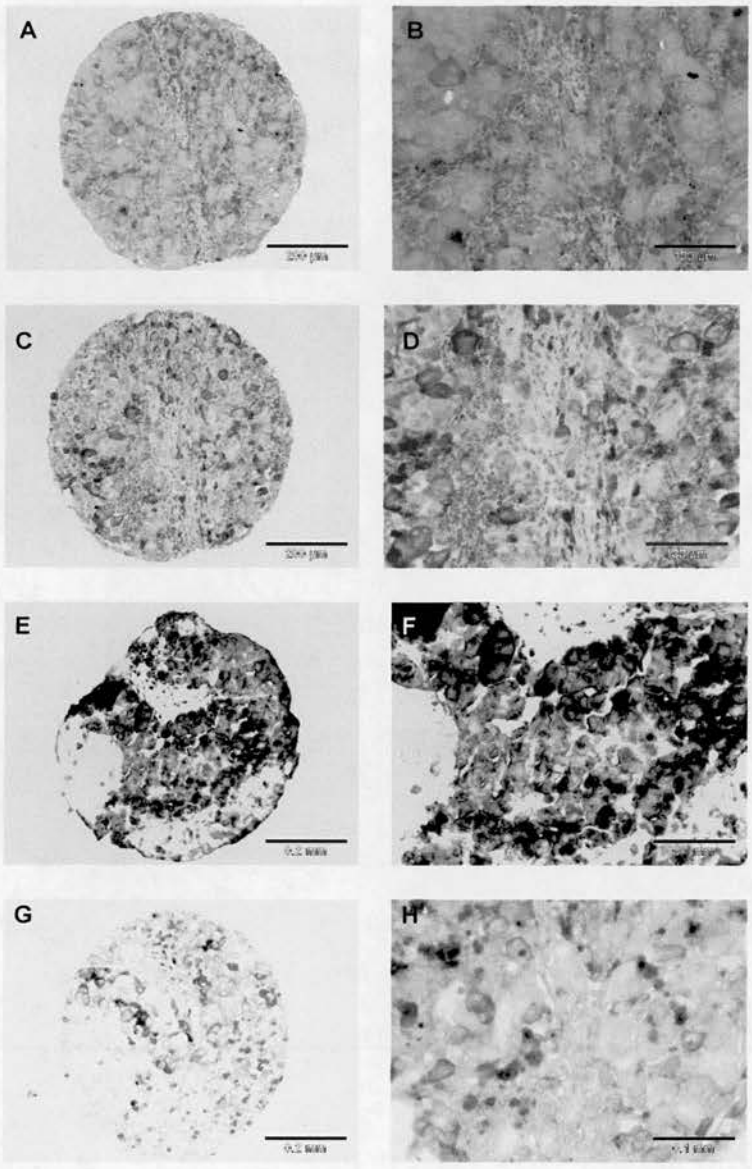

Figure 5.3. Comparison of S100 immunohistochemistry using azure blue versus haematoxylin counterstaining. (A) and **(B)** S100 IHC with haematoxylin counterstaining. **(C)** and **(D)** Negative (no primary antibody) control with haematoxylin counterstaining, **(E)** and **(F)** S100 IHC with azure blue counterstaining, **(G)** and **(H)** Negative (no primary antibody control) with azure blue counterstaining. **(A)**, **(C)**, **(E)** and **(G)** are x200 and **(B)**, **(D)**, **(F)** and **(H)** are x400. Note the difficulty in estimating the contribution of DAB or pigment to the staining pattern in **(A)** and **(B)**.

5.3.2.2 Investigation of Permanent red as an alternative detection system

An alternative strategy that was employed to overcome the problem that pigment can pose in the interpretation of DAB immunohistochemistry was the use of an alternative detection system. Permanent Red (DAKO^{TM}) is based on alkaline phosphatase chemistry rather than HRP and its final product is red rather than brown. It was investigated as an alternative to DAB in the practice TMA.

The Permanent Red detection system was compared to DAB using the S100 antibody. With the use of Permanent Red it was possible to distinguish the presence of melanin pigment from the red colour produced by the detection system (Figure 5.4 A). It was apparent however that there was a lower quality of staining with Permanent Red which included some background staining being seen even on the glass slide in between cores. Permanent Red was also assessed using a Ki67 antibody which was expected to give staining that was positive in a lower percentage of cells compared with S100. In tonsil tissue which was used as a control it gave clear red nuclear staining which was of similar intensity to DAB (not shown). There was a tendency once again however for there to be some background staining on the slide in between the cores. In melanoma cores where Ki67 expression was low it was found that DAB gave a clearer signal than Permanent Red suggesting that firstly, the red staining was more difficult to distinguish from the haematoxylin counterstain and perhaps secondly, the Permanent red system was not as sensitive as DAB (Figure 5.4 G-J).

On the basis of the above results it was decided to employ DAB/haematoxylin immunohistochemistry as the standard approach for the main TMA study. It was accepted that there would be a small number of cores that contained large amounts of pigment for which interpretation of results may be more difficult. It was anticipated that this problem could be minimised by having an H&E slide available for comparison during the scoring of the TMAs.

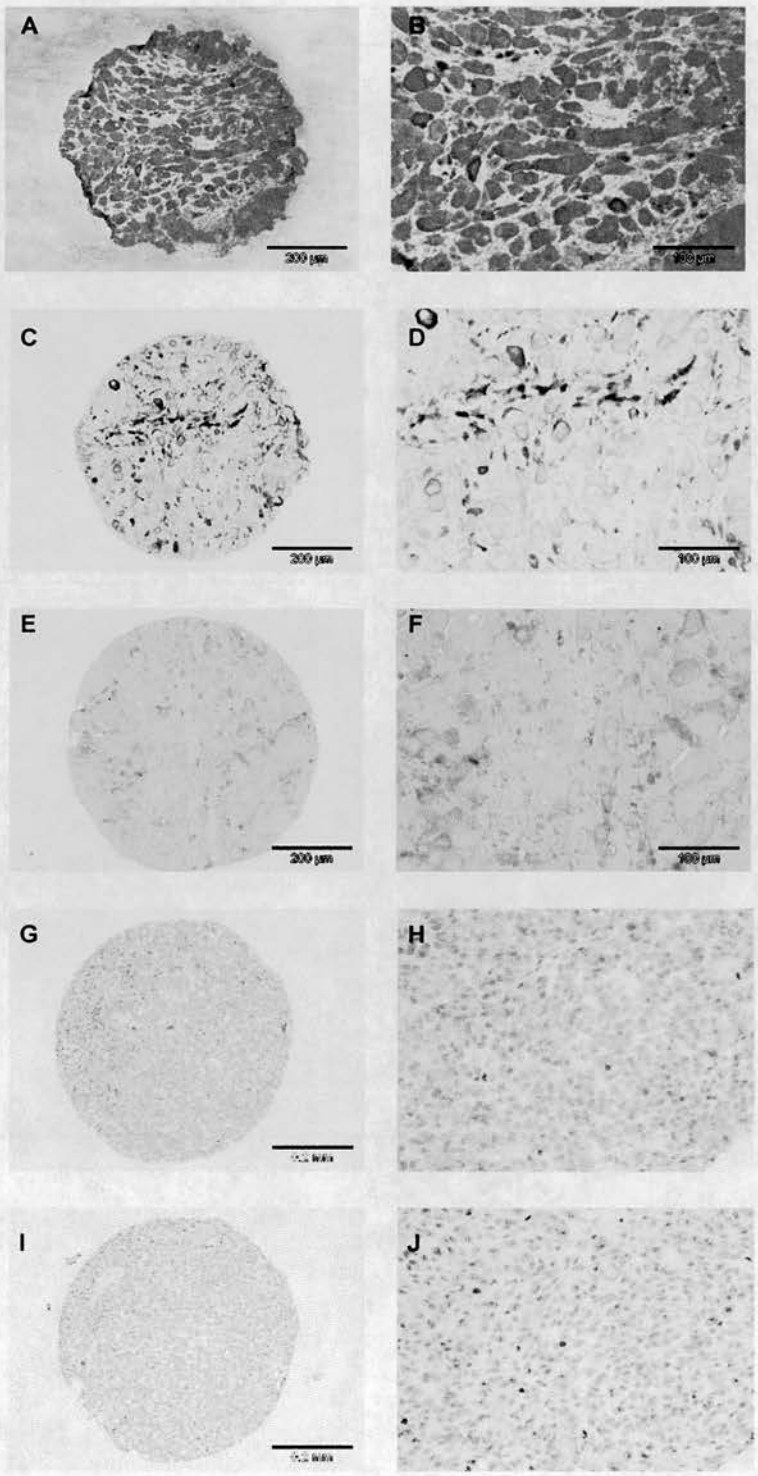

Figure 5.4. Comparison of S100 immunohistochemistry using Permanent red versus DAB. (A) and **(B)** S100 IHC with Permanent Red detection system, **(C)** and **(D)** Negative (no primary antibody) control, **(E)** and **(F)** S100 IHC with DAB detection system, **(G)** and **(H)** Ki67 IHC with Permanent Red detection system, **(I)** and **(J)** Ki67 IHC with DAB detection system. **(A), (C), (E), (G)** and **(I)** are x200 and **(B), (D), (F), (H)** and **(J)** are x400.

5.3.2.3 Investigation of the use of 'thin' TMA sections

The majority of TMA studies use 3-4μm sections for IHC staining (Dai et al, 2005). Given that the tumours we are working with are generally smaller than those used in other TMA studies (e.g. breast cancer TMAs) and the amount of tumour available in thin melanomas may be quite small, it was decided to investigate whether thinner sections could be used for immunohistochemistry in order to have more TMA sections available to work with. S100 was used as the antibody as it was expected to yield positive results in the majority of cores. A comparison was made between 1μm, 2μm and 3μm sections.

It was found that the intensity and quality of staining was very similar in all sections (Figure 5.5 and Table 5.1). It was also confirmed that there appeared to be no increase in lost or inadequate cores with the use of thinner sections. There were concerns however that cutting 1μm sections could technically be more challenging and may lead to a greater number of lost cores and it was therefore decided to use 2μm sections rather than the standard 3μm for further antibody optimisation and for the main TMA study.

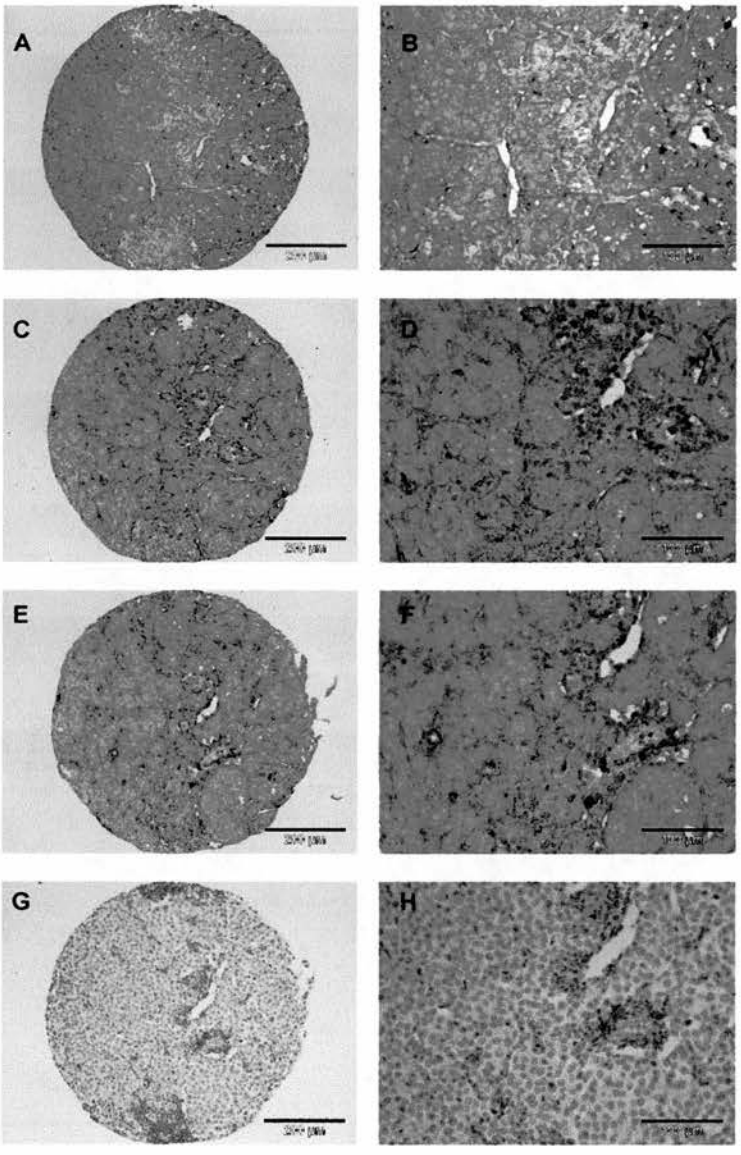

Figure 5.5. Comparison of S100 immunohistochemistry in sections of 1μm, 2μm and 3μm thickness. **(A)** and **(B)** S100 IHC using 1μm section, **(C)** and **(D)** S100 IHC using 2μm section, **(E)** and **(F)** S100 IHC using 3μm section, **(G)** and **(H)** Negative (no primary antibody) control x400. **(A)**, **(C)**, **(E)**, and **(G)** are x200 and **(B)**, **(D)**, **(F)**, and **(H)** are x400.

Sample	1 μm section	2 μm section	3 μm section
1	280	280	270
2	280	280	250
3	110	110	50
4	200	200	200
5	80	70	Lost core
6	230	180	250
7	130	100	130
8	180	200	200
9	290	220	230
10	170	140	110
11	230	230	200
12	210	200	210
13	210	230	200
14	210	200	200
15	220	250	Lost core
16	200	200	215
17	200	200	200
18	200	200	200

Table 5.1. Comparison of S100 Histoscores for sections of 1μm, 2μm and 3μm thickness.

Samples 1-18 represent the cores on the practice TMA that had staining with S100. Scores represent the product of frequency (0-100%) and intensity of staining (0-3) which give a total up to 300.

5.3.3 Assessment of BRAF mutations

Activating mutations in the BRAF oncogene are common in both naevi and melanomas and play a crucial role in melanomagenesis (Rodolfo et al, 2004). 80% of these mutations correspond to the hotspot transversion mutation T1799A that causes the amino acid substitution V600E (Panker et al, 2006). The rate of BRAF mutation varies according to the site of the melanoma and is highest on sites of intermittent sun exposure (Curtin et al, 2005). In order to further investigate the relationship between presence of BRAF mutation, history of UV exposure and the expression of various signalling proteins, an assay was developed for detection of V600E BRAF mutations in melanoma samples. The assay was adapted from a method previously used for the determination of BRAF mutations in thyroid cytology specimens (Chung et al, 2006).

Genetic analysis by restriction fragment length polymorphism (RFLP) allows the examination of nucleic acids for the presence of known sequence variants. A segment that is to be searched for a mutation is amplified from genomic DNA, digested by the appropriate restriction enzyme, and then separated by agarose gel electrophoroesis. Although RFLP analysis is highly sensitive and relatively easy to apply, many polymorphisms are the result of single-base substitutions that fail to create or remove a restriction site and therefore cannot be readily typed by simple PCR and RFLP analysis. To overcome this, a mismatch PCR primer can be used to artificially create a restriction site in the amplified product and allow the detection of the presence of a base substitution by RFLP.

5.3.3.1 Method 1: Bts1 RFLP

a) Melanoma cell lines

Genomic DNA isolated from 5 melanoma and 3 ovarian cancer cell lines was amplified using primers that yielded a 126bp PCR product incorporating the V600E hotspot. Several primer combinations were tested and PCR conditions were optimised in order to obtain a consistent result. Figure 5.6 is a schematic representation of the relevant part of the BRAF gene including the position of these and other primers. Results for the melanoma cell lines and ovarian cancer cell lines tested are shown in Figure 5.7. Overnight digestion of the PCR product with Bts1 resulted in a product of 105bp when wild-type BRAF was present. The absence of digestion was therefore suggestive of the presence of a V600E mutation. No PCR product was seen in the negative (no DNA) controls. The presence of a V600E BRAF mutation in the melanoma cell lines and the absence of mutation in ovarian cancer cell lines was consistent with published results (see Chapter 3).

b) Melanoma tissue samples

DNA was isolated from 0.6mm cores of formalin-fixed paraffin embedded melanoma tissue. Although the cores were taken from areas that were rich in tumour cells it was likely that the cores also contained variable amounts of non-tumour material. Several methods were used to isolate DNA from the melanoma tissue cores. Firstly, digestion in tail buffer and proteinase K with PCR direct from the lysate. Secondly, digestion in tail buffer and proteinase K with subsequent phenol/chloroform extraction and precipitation in isopropanol. Thirdly, digestion and extraction in sodium hydroxide followed by TrisHCl buffer. Fourthly, a column based method using a QIA quick micro column kit. It was found that the method that gave the most consistent results and the strongest PCR products was the QIA quick micro column method. This method was therefore used to isolate DNA from further cores taken from metastatic or primary melanoma specimens.

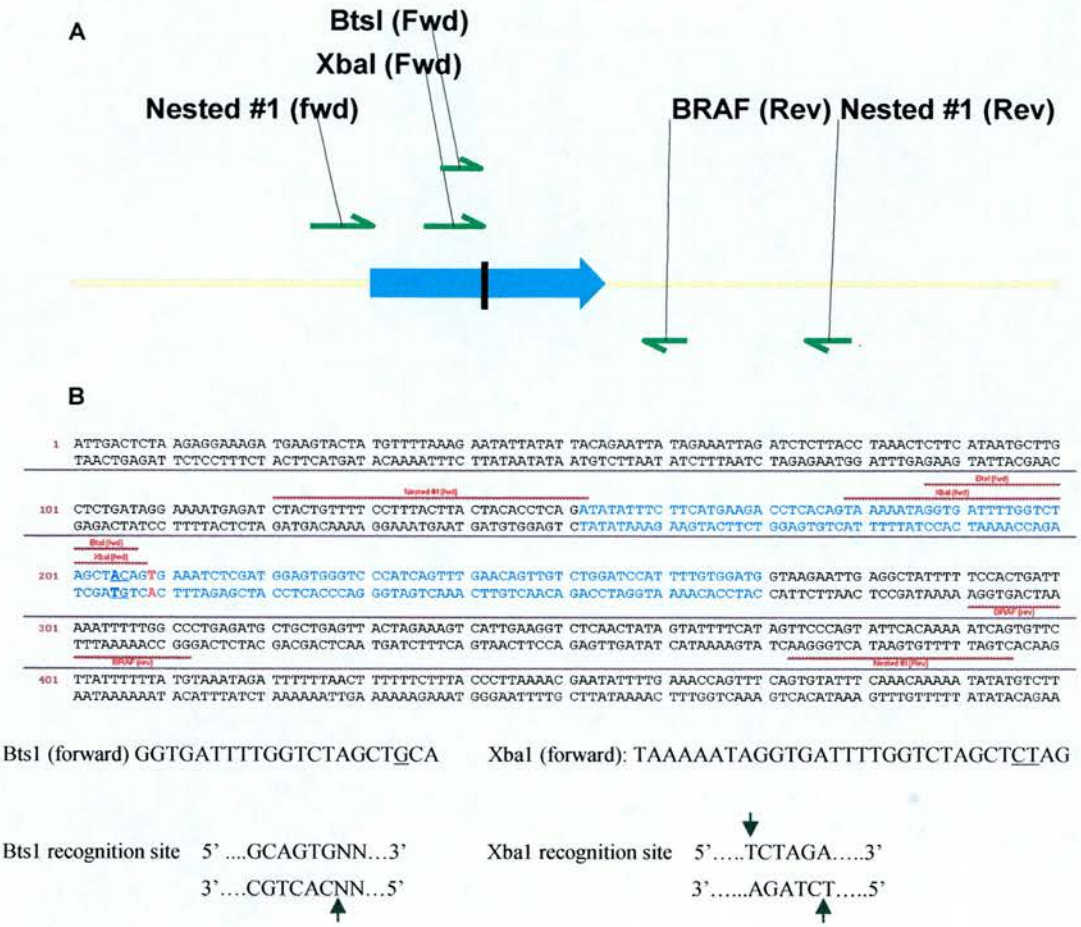

Figure 5.6. BRAF PCR RFLP analysis. (A) Schematic diagram showing position of primers used for BRAF PCR. The site of the transversion mutation T1799A is marked with a black bar. **(B)** Sequence of genomic DNA (exon 15) containing coding sequence in blue and primers in red. Mismatched primer nucleotides are in bold for Bts1 and underlined for Xba 1. The primer sequences and recognition sites for Bts1 (forward) and Xba1 (forward) are shown at the bottom of the diagram with the mismatched nucleotides underlined (1 mismatch for Bts1 and 2 mismatches for Xba1). The site of the T1799A mutation is in red. Primers used for BRAF method 1 were Bts1 (F) and BRAF (R), for method 2 were Xba1 (F) and BRAF (R) and for the nested approach were Nested # 1 (F) and Nested #1 (R).

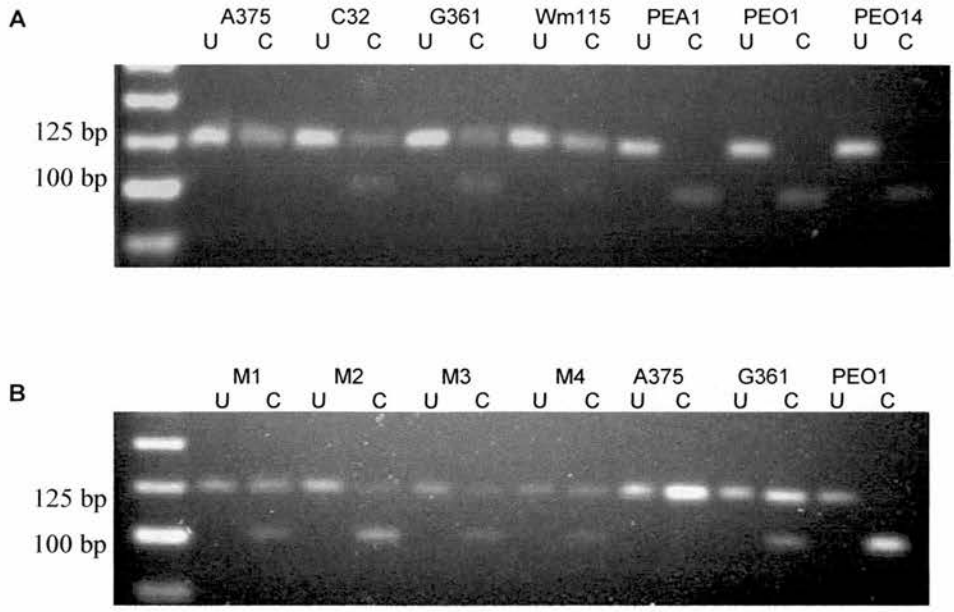

Figure 5.7. BRAF PCR RFLP (Bts1) mutation analysis. (A) Results of Bts1 digestion of PCR products amplified from DNA from cell lines A375, C32, G361 and Wm115 (melanoma) and PEA1, PEO1 and PEO14 (ovarian cancer cell lines). **(B)** Results of Bts1 digestion of PCR products amplified from DNA from melanoma samples (M1 to 4) and control cell lines (A375, G361 and PEO1). The Bts1 restriction enzyme cuts in the presence of the wild-type BRAF sequence. The presence of two bands of similar intensity (126bp and 105bp) is suggestive of 1 mutant BRAF and 1 normal BRAF (as in G361, M1, M3, and M4). The absence of a 105bp band (as in A375) suggests either a homozygous BRAF mutation or a single BRAF mutation with loss of the normal copy. The absence of a 126bp band is suggestive of normal BRAF (as in M2 and PEO1). U = uncut, C= cut.

A number of issues arose during PCR and RFLP analysis on DNA isolated from melanoma samples. Firstly, the PCR products were often low in abundance which made interpretation of the results of RFLP difficult due to the faintness of the lower band. Secondly, the interpretation of the results of those samples in which two bands were seen was problematic. An example of this is sample M2 in Figure 5.7. The faint upper band in M2 could either be due to the presence of a mutation in a core from mixed tumour (with BRAF mutation) and normal tissue or due to incomplete digestion of entirely wild-type BRAF DNA by the enzyme. It was felt therefore that it would be necessary to improve the assay in order to make results more readily interpretable.

5.3.3.2 Method 2: Xba1 RFLP

a) Melanoma cell lines

The Xba1 assay had a similar design to the Bts1 assay in that a restriction site was created during amplification of the BRAF sequence. The most notable differences in the design of this assay were that firstly, the primer contained 2 mis-matched nucleotides and secondly, the Xba1 restriction site was only created by the presence of a BRAF V600E mutation. The advantage of this assay was that the presence of a mutation led to digestion and therefore failure to cut couldn't lead to false positive results.

Genomic DNA isolated from several melanoma and ovarian cancer cell lines was amplified using primers that yielded a 134bp PCR product incorporating the V600E hotspot. Several primer pairs were compared and PCR conditions were optimised in order to give the most consistent PCR product. Following overnight digestion of the PCR product with Xba1 a product of 105bp was produced when the mutant BRAF sequence was present. Results for the melanoma cell lines and ovarian cancer cell

lines tested were consistent with findings from the Bts1 assay (2 cell lines are shown in Figure 5.8 B).

In order to establish the sensitivity of the RFLP (Xba1) assay serial dilutions of mutant and non-mutant DNA were made up and subjected to PCR and digestion as described above. Accurate concentrations of DNA were quantified by spectrophotometry following RNAse treatment. The abundance of the PCR products was similar for each PCR reaction and no PCR product was seen in the negative (no DNA) control. Following Xba1 digestion a 105bp band was seen in samples containing 25% or more mutant DNA (Figure 5.8A). This result suggested that this assay could only detect mutant BRAF if it was present in at least 25% of cells isolated.

b) Melanoma tissue samples

Although the use of Xba1 led to clear results when applied to melanoma cell lines the abundance of the PCR product from DNA isolated from melanoma samples remained relatively low making the RFLP results difficult to interpret. Increasing the PCR reaction to 40 cycles resulted in a more abundant PCR product but this was at the expense of an increased frequency of false positive results i.e. either PCR products appearing in the no-DNA controls or BRAF mutations being detected in non tumour DNA controls. Although both these problems could be minimised by more stringent PCR technique it was felt that given the relatively small amounts of DNA available from the melanoma samples it would be advantageous to investigate further improvements in the assay in order to ensure consistent results.

It is recognised that DNA extracted from formalin-fixed paraffin-embedded specimens is often fragmented and PCR can be difficult when amplifying products greater than 100bp in length. In order to try and increase the efficiency of the PCR on DNA isolated from fixed melanoma tissues a number of different primer combinations were tested. These included a primer combination that gave a smaller PCR product, a longer reverse primer to try to increase binding and nested primers.

The use of nested primers (see Figure 5.6) gave the most abundant PCR products. A panel of 10 melanoma samples were therefore tested using the nested primer approach (Figure 5.8 B). Mutant BRAF was detected in all 4 metastatic melanomas samples but in none of the primaries. PCR was unsuccessful in one of the primaries (P4). Six of the PCR products were selected in order to confirm results using direct sequencing. The sequencing results in all cases agreed with the results seen with RFLP. It was interesting to note that in sample M6 no normal allele was detected by sequencing. This implies that all tumour DNA was mutant and there was very little non-tumour DNA in the sample and therefore the undigested PCR product seen in Figure 5.8 B was due to incomplete digestion by the enzyme rather than the presence of non-mutant DNA. The nested primer PCR (Figure 5.8 B) was carried out by Dr Jim Selfridge.

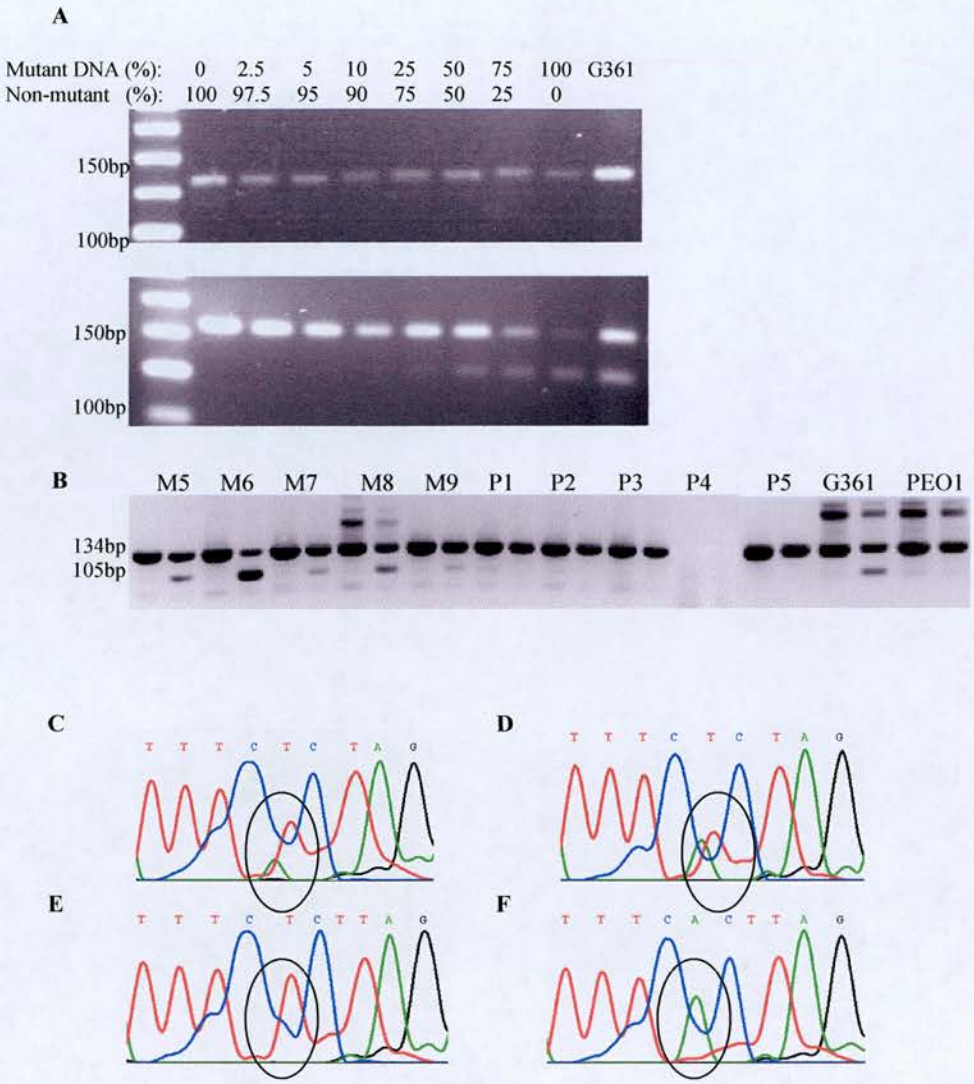

Figure 5.8. BRAF PCR RFLP (Xba1) mutation analysis. **(A)** Results of Xba1 digestion of PCR products amplified from mutant (from A375 cells) and non-mutant (from PEO1 cells) DNA. Ratios of mutant to non-mutant DNA are shown. The upper gel shows relatively equal abundance of PCR products and the lower gel shows results of Xba1 digestion. The lowest concentration of mutant DNA where a band was observed was in lane 5 where 25% of the DNA was mutant. **(B)** Results of Xba1 digestion of PCR products amplified from DNA isolated from metastatic melanoma samples (M5-M9), primary melanomas (P1-P5) and control cell lines (G361 and PEO1). For each sample the 2 lanes represent the PCR product without or with Xba1 digestion. The presence of a band of 105bp is suggestive of the presence of mutant DNA as in samples M5-M9. **(C)-(F)** DNA sequencing results for samples G361, M7, M6 and P1 respectively. Two peaks in the region marked indicates heterozygosity for the transversion mutation T1799A. A single green peak indicates only the wild-type allele is detected (TTTC**A**CTTAG). A single red peak indicates only the mutant allele is detected (TTTC**T**CTTAG).

5.3.4 TMA data analysis

5.3.4.1 Clinicopathologic features of TMAs

Clinicopathologic data on 474 patients with cutaneous melanoma diagnosed between 1993 and 1997 were retrieved from the SMG database. 53 cases of normal naevi, 31 cases of dysplastic naevi, 59 in-situ melanomas, 312 cases of primary melanoma and 69 metastatic melanomas were represented on the TMAs and were evaluable for immunohistochemical staining. The TMA blocks are shown in Figure 5.9 along with representative cores from each type of lesion.

Characteristics for all patients with primary melanoma that were included in the final analysis were compared to those excluded from the final analysis (Table 5.2). The reasons for exclusion included lack of availability of tissue (either missing tumour blocks or insufficient material present), loss of cores during the construction process, insufficient amount of tumour being present on the final TMA slides or the presence of abundant pigment that made results uninterpretable.

The mean age of the cases included in the final analysis ('included') was 53.3 and was 54.4 for those 'excluded' from the final analysis (Welch two sample t-test, t=-0.59, df=319, p=0.5552). The median duration of follow up was 5.4 years for 'included' cases versus 5.8 years for 'excluded' cases (Welch two sample t-test, t=-1.5, df=276, p=0.13). Generally the 'included' and 'excluded' groups were very similar although there were significant differences for Breslow thickness and histological type. For Breslow thickness there were a higher number of very thin (≤1mm) and thick (>4mm) melanomas in the excluded group. For thin lesions it was likely that the difference could be explained by there being some lesions that were too small to core and still have sufficient tissue for clinical purposes. For thick lesions some samples were unavailable for inclusion due to a previous study that

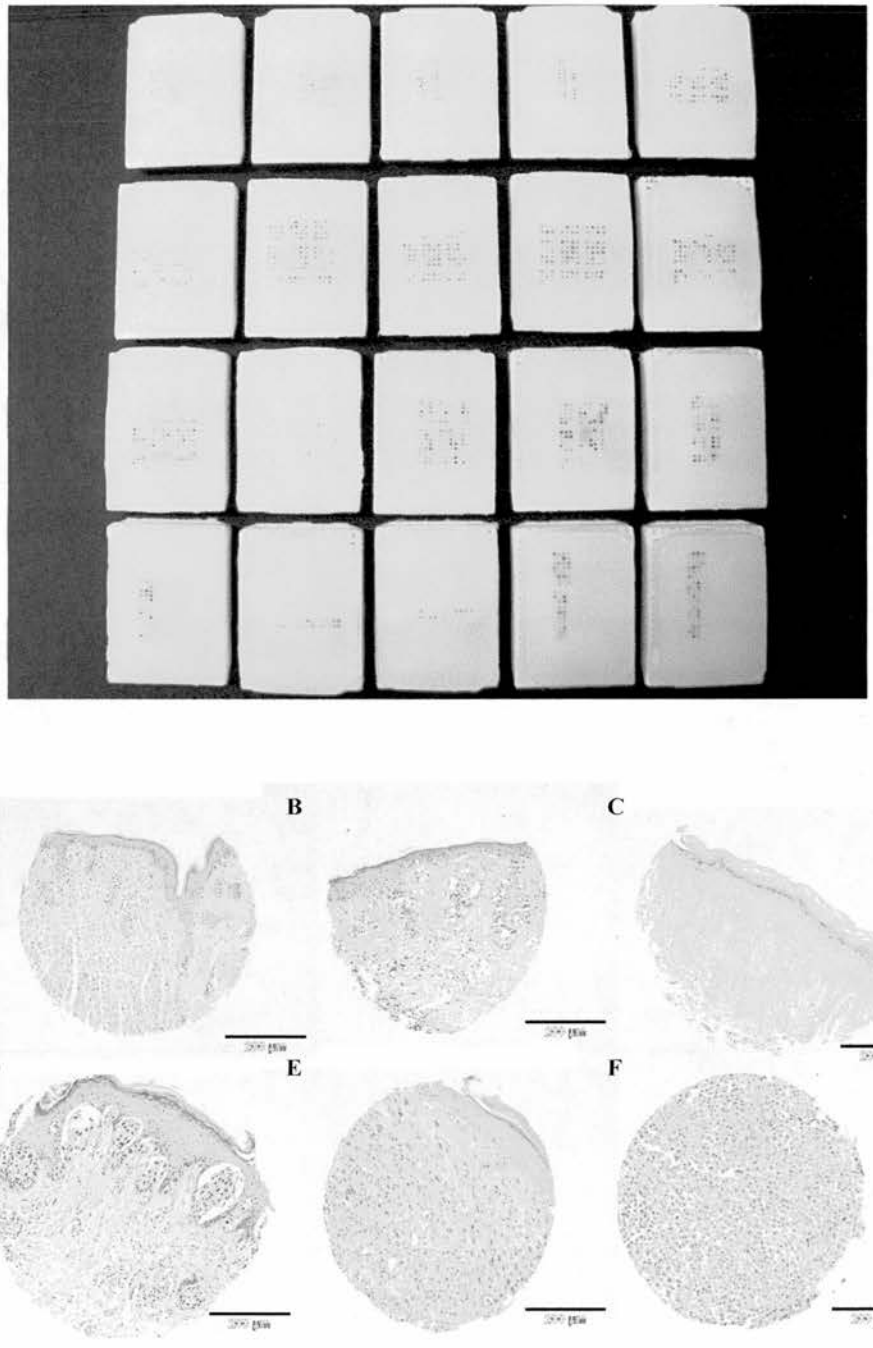

Figure 5.9. TMA blocks and representative H&E cores. Upper panel is a photograph of the 20 TMA blocks. Lower panels are representative H&E sections of cores from several TMAs (x200). **(A)** Naevus, **(B)** Dysplastic naevus, **(C)** In-situ melanoma, **(D)** Thin (radial growth phase) melanoma, **(E)** Thick (vertical growth phase) melanoma. **(F)** Metastasis.

Variable	Included patients No./(%)	Excluded patients No./(%)	Pearson's Chi-squared Test
Sex			
M	118 (38)	60 (37)	
F	194 (62)	101 (63)	p=0.91
Breslow			
≤1.0mm	178 (57)	102 (63)	
1.01-2.0mm	66 (21)	17 (11)	
2.01-4.0mm	40 (13)	15 (9)	
>4.0mm	28 (9)	27 (17)	p=0.003
Site			
Sun exposed	45 (15)	35 (22)	
Sun protected	258 (83)	123 (76)	
Acral	8 (3)	3 (2)	p=0.13
Ulceration			
Present	63 (20)	31 (19)	
Absent	197 (63)	114 (71)	
Incipient	41 (13)	14 (9)	
Unknown	12 (4)	2 (1)	p=0.15
Type			
SSM	240 (77)	100 (62)	
Nodular	36 (12)	19 (15)	
LMM	26 (8)	25 (12)	
Acral	8 (3)	12 (8)	
Other	2 (1)	5 (3)	p=0.002
Status			
Alive	244	121	
Dead (melanoma)	44	22	
Dead (other)	24	18	p=0.45

Table 5.2. Clinicopathologic characteristics of primary melanoma cases. Included patients (n=312) are those with immunohistochemistry scores that were included in the final analysis. Excluded (n=162) are cases that were excluded from the final analysis due to lack of or unsuitable tissue for scoring. The final column shows the p-value for a statistical comparison of 'included' and 'excluded' cases for each variable using Pearson's chi-squared test. SSM=superficial spreading melanoma, LMM= lentigo-maligna melanoma.

used up most of the available tissue. The very small p-value attached to the comparison of the 'included' and 'excluded' groups for histological type was likely to largely reflect the differences seen in the groups with small sample numbers such as 'acral' and 'unknown'.

5.3.4.2 Solar elastosis

Solar elastosis is a histologic indicator of chronic sun damage. The degree of solar elastosis in the dermis of each primary melanoma sample was scored according to a recently described method (Landi et al, 2006). The aim was to provide a quantitative assessment of sun damage in the skin in which the melanomas arose. The scores (0-11) took account of both the amount and distribution of the elastosis seen (see Methods).

A range of solar elastosis scores was seen (n = 284, mean = 4.5). Representative slides are shown in Figure 5.10. Solar elastosis scores were higher in samples arising from sun-exposed sites (mean = 8, n = 47) and were low in sun-protected sites (mean = 4, n = 251). Table 5.3 shows a comparison of solar elastosis score and site of melanoma. As expected high solar elastosis scores were associated with history of sun-exposure. Acral melanomas (pathological diagnosis) were associated with an average solar elastosis score of 1.8 (n = 6). The Solar Elastosis scoring was performed on H&E stained sections by Dr Tamasin Doig.

5.3.4.3 Immunohistochemistry scoring

2μm slides were cut from each of the TMA blocks and stained with B-catenin, bcl-2 or galectin-3 antibodies using standard DAB immunohistochemistry. Monoclonal antibodies were used for all 3 proteins that had been shown in previous studies to be specific and had been validated for clinical use. For each staining run a no primary

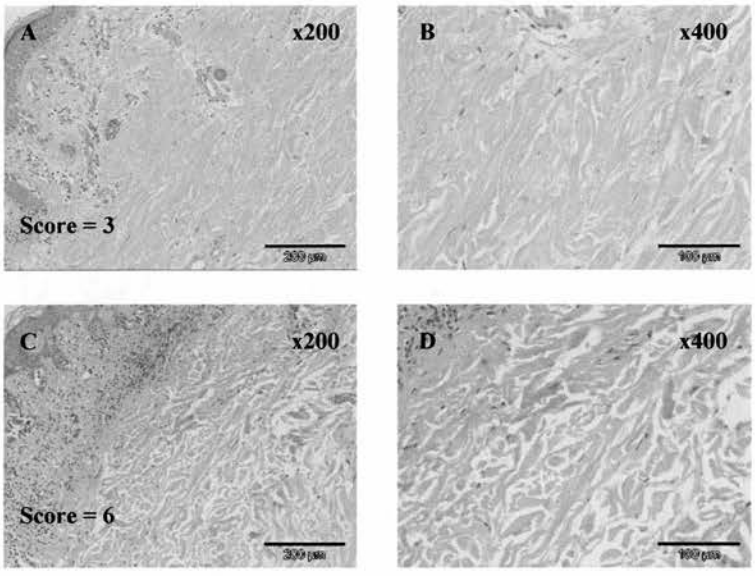

Figure 5.10. Solar elastosis scoring. Solar elastosis was assessed in the normal skin surrounding the melanomas on H&E stained sections. **(A)** and **(B)** show scattered elastotic fibres between collagen bundles. **(C)** and **(D)** show densely scattered elastotic fibres distributed predominantly as bushels. Although it is difficult to pick out the basophilic elastotic fibres in these slides the resultant disruption of the architecture of the collagen bundles in **(C)** and **(D)** can clearly be seen. **(A)** and **(C)** are x200 and **(B)** and **(D)** are x400.

	Sun-exposed site	**Sun-protected site**
Solar elastosis >6	**21**	**10**
Solar elastosis ≤6	**15**	**247**

Table 5.3. Comparison of solar elastosis scores and location of melanoma. Solar elastosis scores were divided into low (0-6) or high (7-11). Fisher's exact test $p=2 \times 10^{-16}$. Sun-exposed sites represent those on the head and neck whereas sun-protected are all other sites.

antibody control was included. Staining was assessed by 2 observers independently (Dr Tamasin Doig and myself). An H&E slide from each TMA block was available during scoring to help interpretation of staining in the presence of pigment. The histoscore method of scoring was used which takes into account location, intensity and frequency of staining as described earlier in this chapter.

B-catenin staining was predominantly membranous although some metastatic melanoma samples showed nuclear staining. Moderate staining was also seen in keratinocytes. The pattern of expression of bcl-2 staining was cytoplasmic. Lymphocytes which were present in some melanoma samples stained strongly for bcl-2 and therefore acted as an internal control. Galectin-3 staining was both cytoplasmic and nuclear. Galectin-3 also gave some positive staining in keratinocytes and macrophages. For B-catenin and galectin-3, each cellular compartment was scored separately. Representative images are shown in Figures 5.11-5.13.

Comparison of scoring between 2 observers was possible for membranous B-catenin, cytoplasmic bcl-2, and cytoplasmic galectin-3. In addition to a cytoplasmic score being given for galectin-3, observer 2 (pathologist) gave a separate score for nuclear galectin-3 scoring. Figure 5.14 shows the comparison of IHC histoscores between observer 1 and observer 2 for each of the 3 antibodies. Although there was generally good correlation between observers it was evident that at higher histoscores there was a tendency for observer 2 to score higher than observer 1 for both bcl-2 and b-catenin. Interclass correlation co-efficients were calculated to be 0.56, 0.49 and 0.67 for bcl-2, b-catenin and galectin-3 (cytoplasmic) respectively. For cores where there was a discrepancy between observer histoscores of 100 or more, these cores were reviewed and a consensus score was reached.

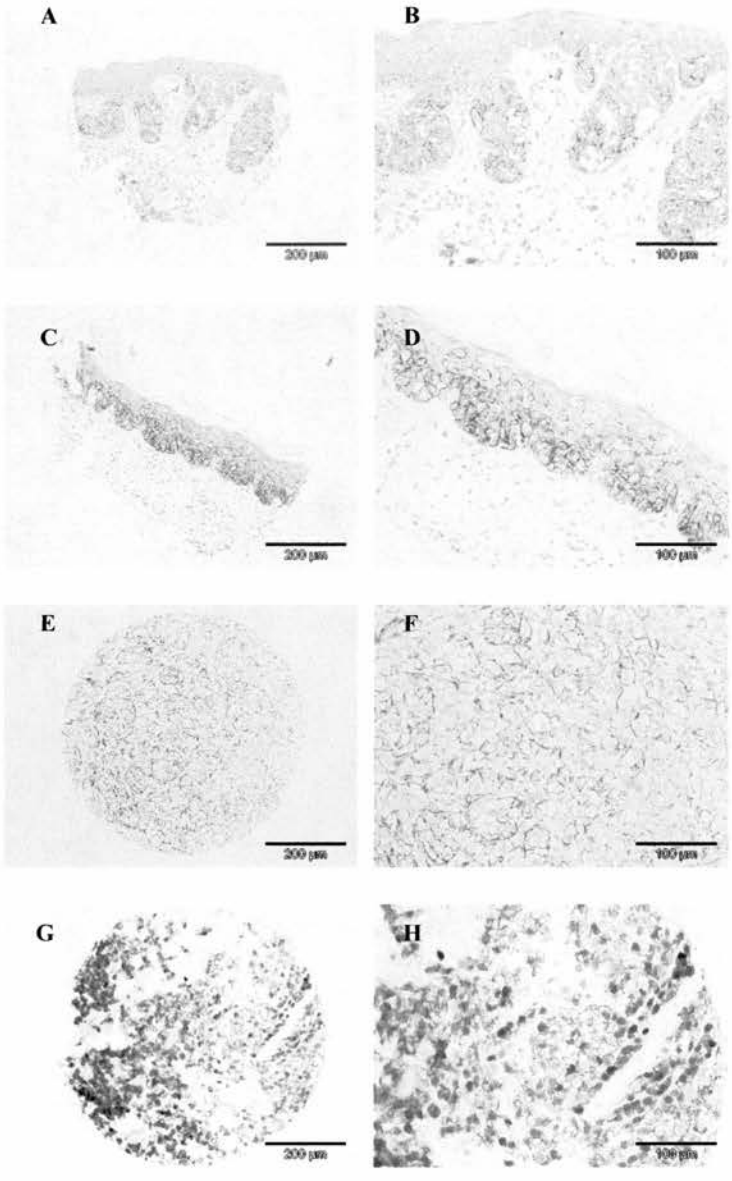

Figure 5.11. B-catenin immunohistochemistry. Representative images of B-catenin immnunohistochemical staining in human melanocytic lesions. **(A)** and **(B)** Dysplastic naevus showing moderate membranous staining, **(C)** and **(D)** In-situ melanoma showing moderate membranous staining, **(E)** and **(F)** Primary melanoma showing weak to moderate membranous staining, **(G)** and **(H)** Metastatic melanoma showing strong nuclear staining and moderate cytoplasmic staining. Magnification is x200 for **(A), (C), (E)** and **(G)** and x400 for **(B), (D), (F)** and **(H).**

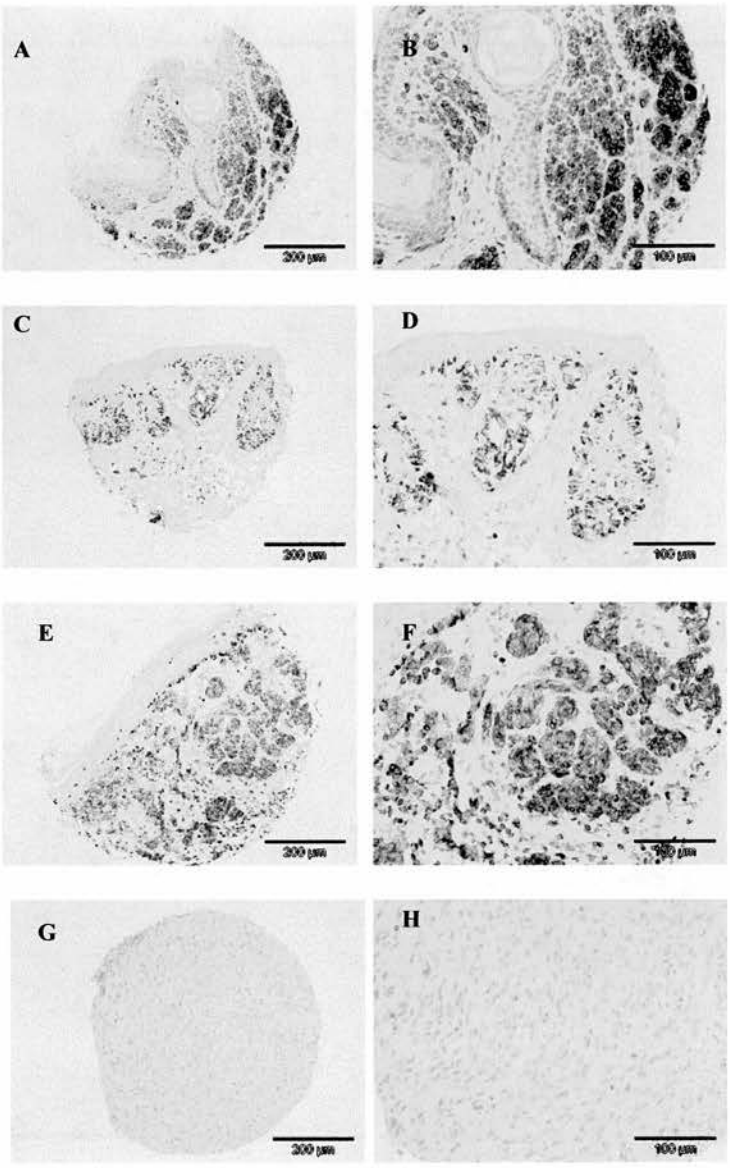

Figure 5.12. Bcl-2 immunohistochemistry. Representative images of bcl-2 immnunohistochemical staining in human melanocytic lesions. **(A)** and **(B)** Naevus showing strong cytoplasmic staining, **(C)** and **(D)** Dysplastic naevus showing moderate cytoplasmic staining, **(E)** and **(F)** Primary melanoma showing moderate cytoplasmic staining, **(G)** and **(H)** Metastatic melanoma showing negative staining. Magnification is x200 for **(A), (C), (E)** and **(G)** and x400 for **(B), (D), (F)** and **(H).**

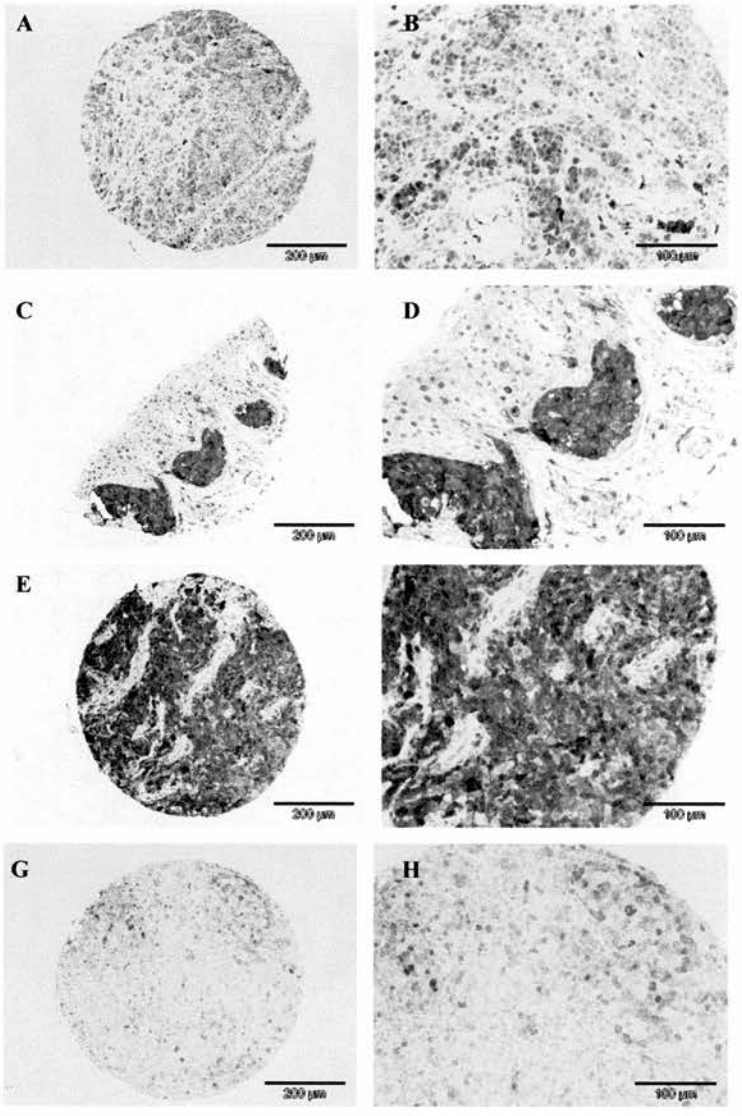

Figure 5.13 Galectin-3 immunohistochemistry. Representative images of galectin-3 immnunohistochemical staining in human melanocytic lesions. **(A)** and **(B)** Naevus showing strong nuclear and moderate cytoplasmic staining, **(C)** and **(D)** Dysplastic naevus showing strong cytoplasmic and nuclear staining, **(E)** and **(F)** Primary melanoma showing strong nuclear and cytoplasmic staining, **(G)** and **(H)** Metastatic melanoma showing weak nuclear staining. Magnification is x200 for **(A)**, **(C)**, **(E)** and **(G)** and x400 for **(B)**, **(D)**, **(F)** and **(H)**.

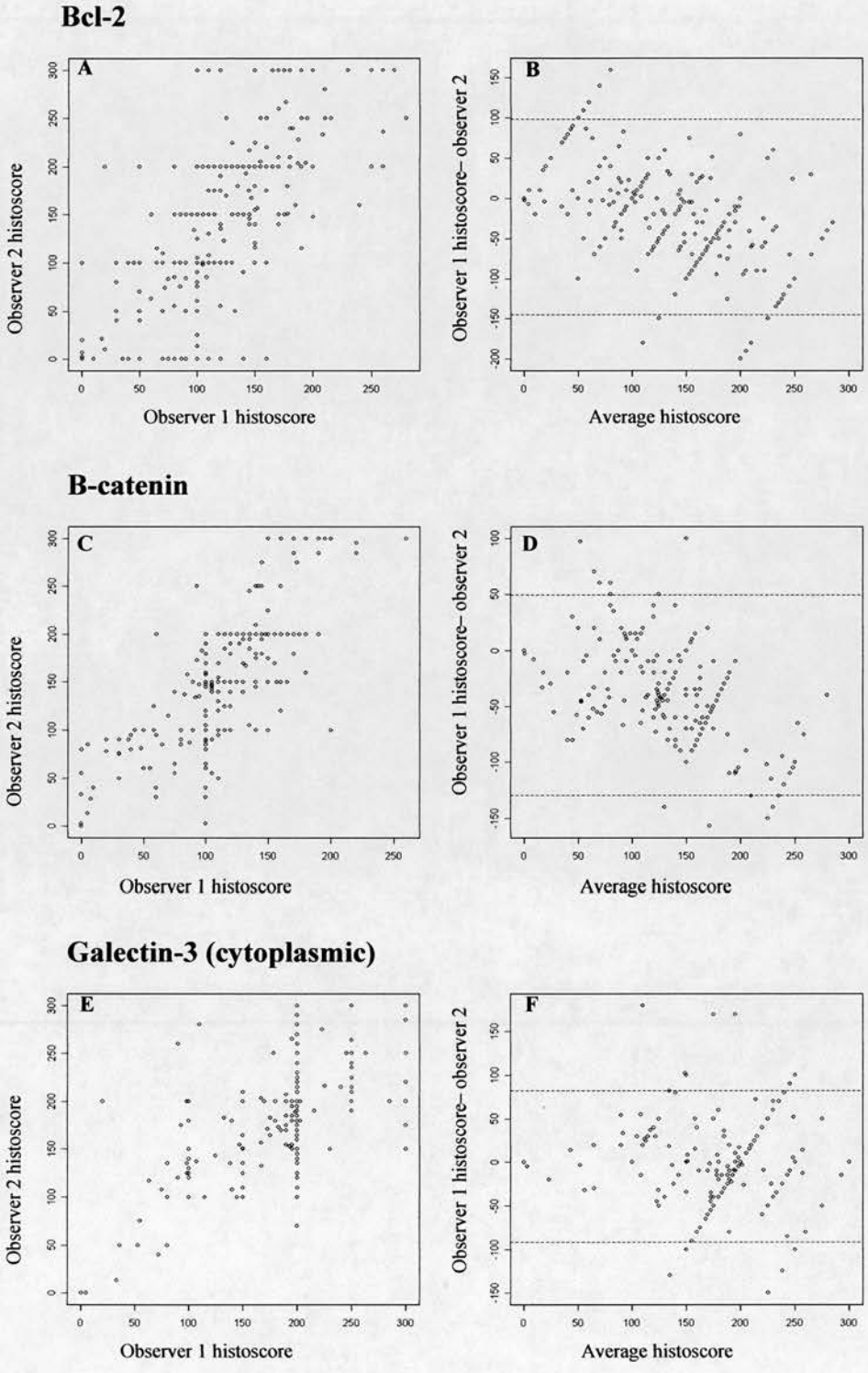

Figure 5.14. Correlation of immunohistochemistry scoring between observer 1 and observer 2. **(A), (C)** and **(E)** Scatter plots showing scores given by observer 1 versus observer 2 for each primary melanoma case for each of the 3 antibodies. **(B), (D)** and **(F)** Bland-Altman plots showing differences in scores between observers plotted against histoscore for each of the 3 antibodies. The dotted lines represent +2 and -2 standard deviation of the difference between observer 1 and observer 2.

5.3.4.4. Expression of B-catenin, Bcl-2 and galectin-3 during melanoma progression

Levels of B-catenin, bcl-2 and galectin-3 immunostaining were assessed in normal naevi, dysplastic naevi, in-situ melanomas, primary melanomas and metastatic melanomas (Figure 5.15).

The expression of B-catenin was low in normal naevi, higher in dysplastic naevi, in-situ melanomas and primary melanomas and then lower again in metastatic melanomas. There were significant differences in histoscore between normal naevi and dysplastic naevi ($p<0.0005$) and between primary and metastatic melanomas ($p<0.0005$) respectively.

The expression of bcl-2 was similar in normal naevi and dysplastic naevi, lower in in-situ melanomas and primary melanomas and lower again in metastatic melanomas There were significant differences in histoscore between dysplastic naevi and in-situ melanomas ($p=0.009$) and primary and metastatic melanomas ($p<0.0005$) respectively.

The expression of galectin-3 (cytoplasmic) was low in normal naevi, higher in dysplastic naevi, in-situ melanomas and primary melanomas lower again in metastatic melanomas. There were significant differences in histoscore between normal naevi and dysplastic naevi ($p<0.0005$) and between primary and metastatic melanomas ($p<0.0005$) respectively. Expression of galectin-3 (nuclear) showed a similar pattern although there were no statistically significant differences between adjacent groups on the progression pathway.

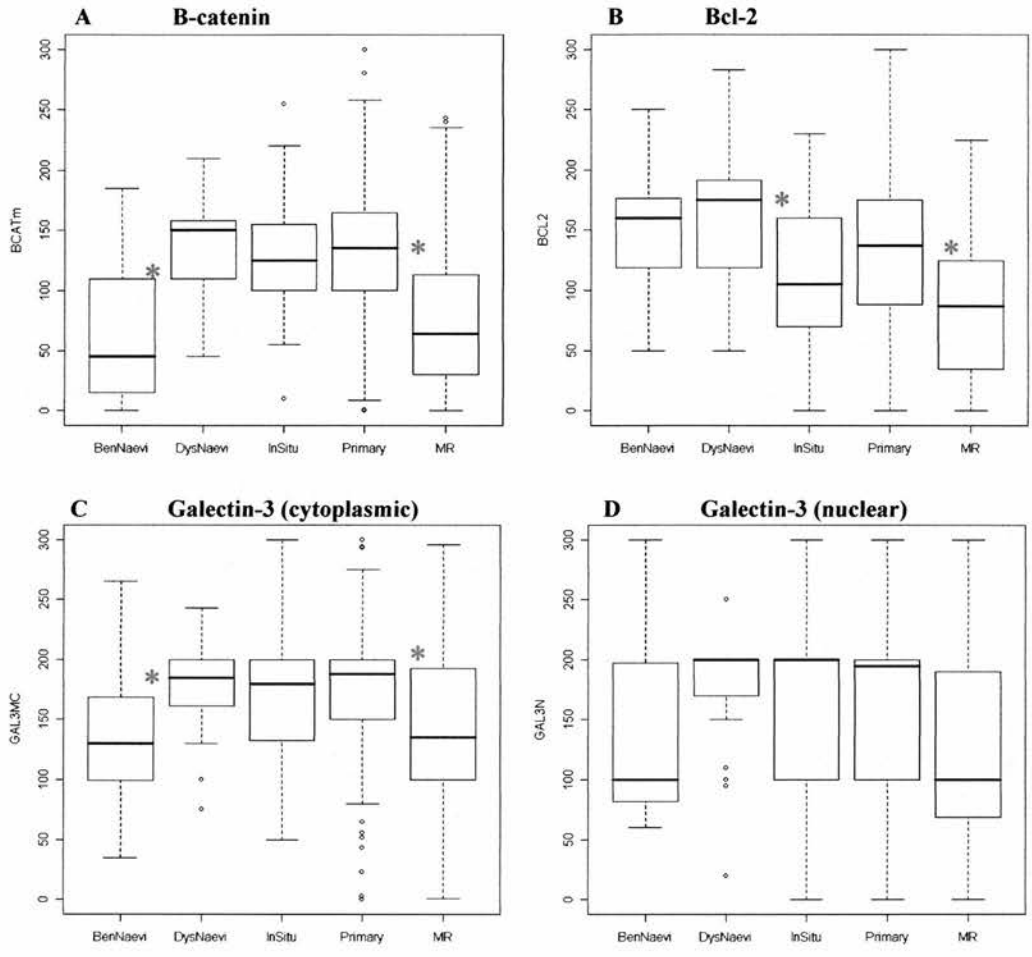

Figure 5.15. Expression of B-catenin, bcl-2 or galectin-3 during melanoma progression. (A) B-catenin, **(B)** bcl-2, **(C)** cytoplasmic galectin-3, **(D)** nuclear galectin-3. For each antibody the 5 groups along the x-axis are benign naevi, dysplastic naevi, in-situ melanomas, primary melanomas and mets/recurrences. Each box represents the interquartile range (1st quartile to 3rd quartile), the median value is marked with a bold line, the dotted lines represent the extent of 1.5 x the interquartile range and other points are marked as outliers. * indicates a significant change is seen between adjacent steps on the progression pathway.

5.3.4.6 Survival Analysis

To evaluate whether staining of B-catenin, bcl-2 or galectin-3 correlated with prognosis in patients with primary melanoma, Kaplan-Meier survival curves were constructed using overall and melanoma-specific survival. Histoscores were divided into quartiles for each antibody (Figures 5.16 and 5.17).

Patients with low expression of B-catenin had a significantly worse overall survival than other patients (log-rank test p=0.01). This result did not reach statistical significance for melanoma-specific survival (log-rank p=0.07). Bcl-2 expression was found to have no correlation with overall or melanoma-specific survival. Although cytoplasmic galectin-3 expression had no association with survival (log-rank test p=0.4 for both overall and melanoma-specific survival), low expression of nuclear galectin-3 correlated with worse overall survival (log-rank test p=0.0004) and melanoma-specific survival (log-rank p=0.0007).

A multifactorial Cox regression analysis was performed in order to assess whether B-catenin or nuclear galectin-3 expression were independent prognostic markers for melanoma (Table 5.4). The multifactorial analysis included age, sex, Breslow, ulceration and presence of elastosis. The results indicated that nuclear galectin-3 reached borderline significance for predicting overall survival independently of other clinicopathologic parameters (p=0.05). The risk ratio for death for patients with low (bottom quartile) compared to high (top quartile) nuclear galectin-3 was 8.00. This was considerably higher than risk ratios for established prognostic factors such as Breslow or presence of ulceration (see Table 5.4) although it should be noted that confidence intervals for nuclear galectin-3 were wide (1.02-62.89). Significance for melanoma-specific survival was not reached (p=0.12). In contrast, B-catenin was found to be an independent prognostic marker for melanoma specific survival (risk ratio 7.02, p=0.04) but not for overall survival (p=0.47). Other independent prognostic markers for worse overall survival were increasing age (p=0.02) and presence of ulceration (p=0.02). Independent prognostic markers for worse

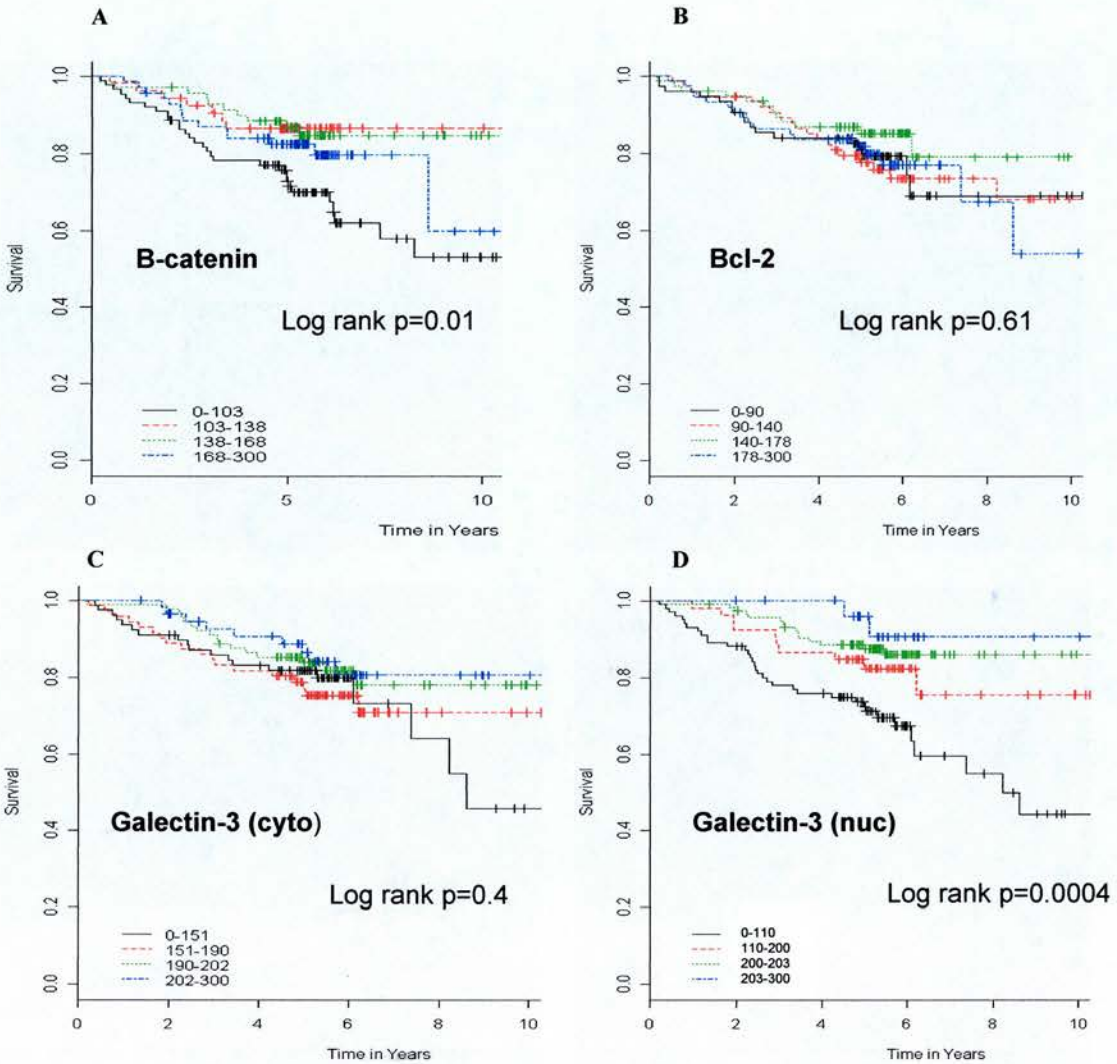

Figure 5.16. Kaplan-Meier analysis of overall survival according to expression of B-catenin, bcl-2 or galectin-3. **(A)** B-catenin, **(B)** bcl-2, **(C)** cytoplasmic galectin-3, **(D)** nuclear galectin-3. The histoscores for each antibody are divided into quartiles. The range for each quartile is indicated in the bottom left hand corner of each graph.

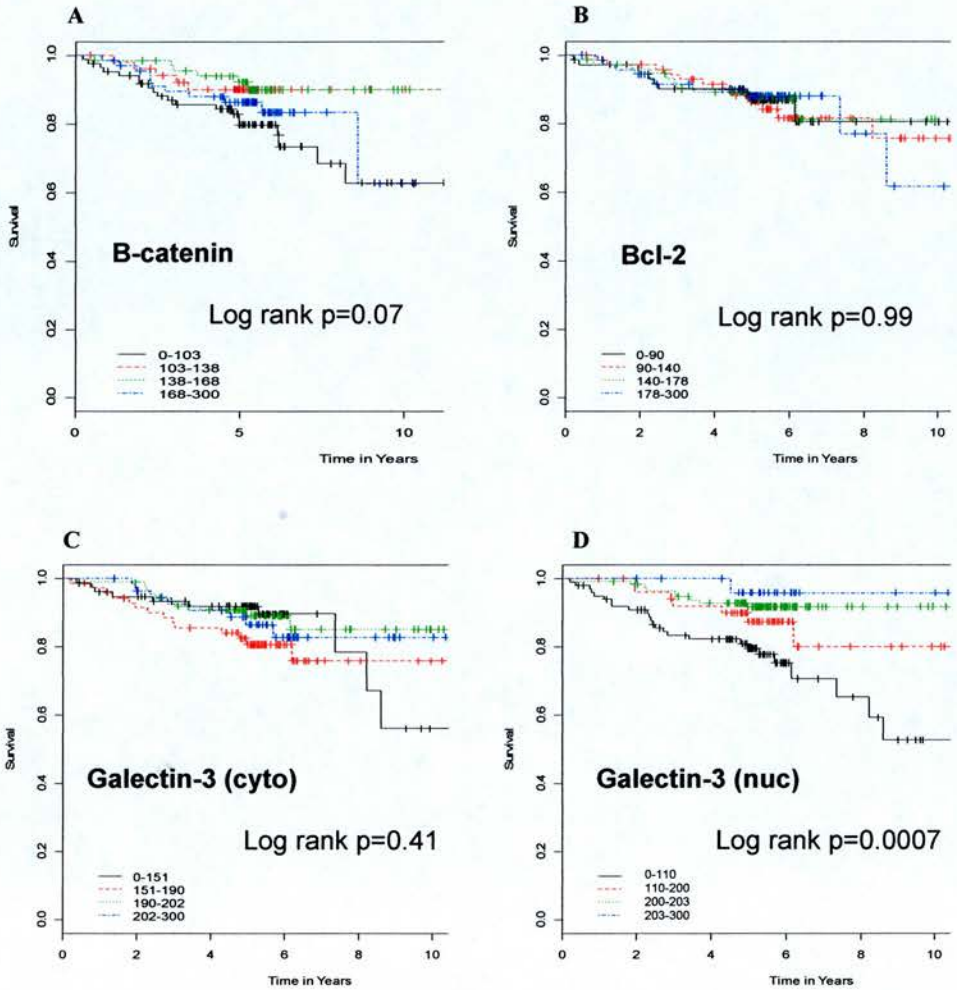

Figure 5.17. Kaplan-Meier analysis of melanoma-specific survival according to expression of B-catenin, bcl-2 or galectin-3. **(A)** B-catenin, **(B)** bcl-2, **(C)** cytoplasmic galectin-3, **(D)** nuclear galectin-3. The histoscores for each antibody are divided into quartiles. The range for each quartile is indicated in the bottom left hand corner of each graph.

A

	Overall survival			Melanoma-specific survival		
Variable	**Risk ratio**	**95% CI**	**p**	**Risk ratio**	**95% CI**	**p**
Galectin-3	8.00	1.02-62.89	0.05	5.49	0.66-46.0	0.12
Age	1.03	1.00-1.05	0.02	1.02	0.99-1.04	0.19
Sex	1.46	0.77-2.78	0.25	2.94	1.28-6.75	0.01
Ulceration	3.49	1.26-9.65	0.02	4.03	1.19-13.6	0.03
Breslow	2.46	0.61-9.81	0.20	5.24	0.80-34.4	0.09
Elastosis	1.14	0.98-1.32	0.09	1.32	1.06-1.65	0.02

B

	Overall survival			Melanoma-specific survival		
Variable	**Risk ratio**	**95% CI**	**p**	**Risk ratio**	**95% CI**	**p**
B-catenin	1.37	0.58-3.28	0.47	3.05	1.07-8.70	0.04
Age	1.03	1.01-1.06	0.01	1.02	0.99-1.05	0.14
Sex	1.37	0.70-2.66	0.36	2.79	1.19-6.55	0.02
Ulceration	3.35	1.23-9.12	0.02	3.45	1.02-11.61	0.05
Breslow	2.16	0.57-8.21	0.26	7.02	1.21-40.80	0.03
Elastosis	1.17	1.00-1.36	0.06	1.33	1.05-1.69	0.02

Table 5.4. Cox regression analysis of the impact of various factors on overall and melanoma-specific survival. A, Nuclear galectin-3. **B**, B-catenin. Coding of variable; nuclear galectin-3 was coded as 1, histoscore in top quartile, 2 histoscore in bottom quartile. Sex was coded as 1, female and 2, male. Ulceration was coded as 1, absent and 2 present. Breslow was coded as 1, <4mm versus 2, >4mm. Age and elastosis were included as continuous variables; risk ratio is per 1 unit decrease in elastosis score or 1 year increase in age, B-catenin was scored as 1, histoscore in top quartile, 2 histoscore in bottom quartile. Risk ratios represent the comparison of variable 2 versus 1.

melanoma-specific survival were Male sex (p=0.01), ulceration (p=0.03), Breslow >4mm (p=0.03) and absence of marked elastosis (p=0.02).

5.4 Discussion

A number of approaches to investigate novel prognostic markers in melanoma have been used. Gene expression microarray on frozen samples of melanoma has identified characteristic gene expression differences distinguishing different classes of metastatic melanoma from one another and from primary and premalignant lesions. These studies have been limited by unavailability of fresh primary material which is usually fixed in its entirety for diagnostic purposes. One recent study analysed gene expression in 83 frozen primary melanoma samples collected over a 20 year period (Winnepenninckx et al, 2006). 254 genes were identified that were associated with a good prognosis. However, when this set of genes were used to classify a validation set, only 11 out of 17 patients had clinical outcome predicted correctly. Indeed, mathematical modelling predicts that gene expression profiles of several thousand patients are needed to generate a robust gene set for predicting cancer outcome (Dai et al, 2005). Obtaining such large numbers of frozen primary melanomas is impossible, making it necessary to explore other ways to investigate gene expression changes in melanoma.

An alternative is protein expression profiling on tissue microarray (TMA), which allows investigation of a number of proteins in up to 1000 specimens on the same array. The advantages of this method include firstly, it uses fixed material and so opens the melanoma archive for study. Secondly, it employs immunohistochemistry which allows investigation of protein expression rather than expression of mRNA transcripts. Thirdly, it allows simultaneously assessment of protein expression from a number of different types of lesion including primaries and metastases. This may give an insight into key changes that occur during cancer development. Disadvantages of the TMA method include firstly, the limited number of biomarkers

that can be investigated due to the requirement for separate antibodies for each protein and secondly, the potential for tissue heterogeneity to result in unrepresentative cores of tumour being analysed.

The pilot immunohistochemistry study confirmed that differences in expression of 3 proteins could be found in melanoma specimens of a suitable age and confirmed the utility of the 'histoscore' as a method of quantifying staining. Construction of the 'practice TMA' allowed the assessment of various IHC conditions to try and improve the quality and interpretation of staining. Azure blue was found to stain melanin granules green-blue and allowed easier contrast with DAB but its inferiority as a counterstain and the instability of colour over time meant it was not used in the main TMA study. Alternative methods of aiding detection such as bleaching with potassium permanganate were not considered as there is evidence that tissue damage and loss of cytological detail may occur during the bleaching process (Kligora et al, 1999). Use of an alternative detection system such as 'permanent red' showed more potential but would require further assessment before being taken taken forward in future studies. From the limited assessment of alternative thickness of sections that was made on the practice TMAs it appeared that using sections that were thinner than 3μm had no deleterious effect on overall staining. In order to distinguish between pigment and IHC staining in heavily pigmented cores it was necessary to have an H&E slide of the corresponding TMA section available for comparison.

A method was developed to detect V600E BRAF mutations in cores of melanoma tissue in order to relate results of protein expression by IHC with presence of BRAF mutations. This was thought to be of value in order to allow classification of melanomas both according to history of sun exposure and presence of BRAF mutations and was of particular relevance to ongoing studies which aim to investigate expression of several proteins on the BRAF/MEK/ERK pathway. The first method that was used to detect V600E BRAF mutations (Bts1) gave clear-cut results using DNA isolated from cell lines but was more problematic when used with DNA isolated from melanoma tissue cores. The main problem was that it was

difficult to determine whether uncut DNA was due to the presence of a mutation or was due to incomplete digestion of wild-type DNA. The second method (Xba1) offered an improvement to the assay in that it only digested the PCR product in the presence of the mutation. The sensitivity of the assay was found however, to be approx 25% which suggested that false negative results may occur when a large proportion of DNA isolated from the tissue cores was from normal tissue or from stroma. Although the Xba1 method was effective in determining the presence of V600E BRAF mutations in cell lines it was evident that results from melanoma tissue DNA were more difficult to interpret due to the low abundance of the PCR products. This was improved by the use of nested primers. A further improvement to the method described above for determining V600E BRAF mutation status may have been possible if larger quantities of melanoma tissue that had a low risk of contamination by non-tumour DNA had been obtained using laser-capture microdissection from whole melanoma sections. Unfortunately this was not possible due to insufficient amounts of tissue being available.

Both the practice TMA and the melanoma TMAs were constructed using 0.6mm tissue cores. Although other studies have used larger cores it was felt that for thinner melanomas the use of the smaller core size would allow duplicate cores to be taken from a greater number of cases whilst ensuring that there was sufficient residual material for clinical purposes. For TMA studies in other cancer types one to four 0.6mm cores have been shown to yield as much information as standard tissue sections (Torhost et al, 2001). The optimum size and number of cores for melanoma TMAs has not been established (Becker et al, 2006). As this was a retrospective study on routinely collected pathology specimens there was no opportunity to ensure consistent fixation methods were used for all specimens. All specimens however underwent similar fixation protocols according to the standard of the time.

Although a number of melanoma TMA studies have been published some have been limited by inadequate archival tissue collections and unavailability of prospectively recorded clinical information. In particular there have been no large studies

published to date that included collections of dysplastic naevi and in-situ melanomas, important steps in the melanoma progression model. This study offers significant advantages compared to previous studies in that it combines a large collection of melanocytic lesions, it has a high percentage of thin melanomas and has high quality prospectively collected clinical data.

In the design of this TMA study it was felt important to follow the recommendations for tumour marker prognostic studies (REMARK) published by a working group set up by the National Cancer Institute-European Organisation for Research and Treatment of Cancer (NCI-EORTC). The guidelines include detailed recommendations on study design, statistical analysis, interpretation of data and presentation and aim to encourage transparent and complete reporting so that others will be able to judge the usefulness of the data and understand the context in which the conclusions apply (McShane et al, 2005).

One of the aims of the design of this study was to try and ensure that the samples included in the TMAs were representative of the melanoma population as a whole for the region. Previous melanoma TMAs (Pacifico et al, 2005, Prieto et al, 2006, Dai et al, 2005, Rangel et al, 2006) generally included a much higher proportion of thick melanomas, presumably due to availability of tissue rather than for scientific reasons. The comparison of the primary melanoma cases in this study that were included in the final analysis with those excluded confirmed there was little systematic bias in the set-up of the melanoma TMAs. This makes it more likely that any results obtained could be extrapolated to the wider population. Although it was hoped that there would be few cases that would be excluded from the TMAs due to uninsuitability the 66% inclusion rate (Table 5.2) compares favourably with the 55% that was seen in the only other study for which this information was provided (Pacifico et al, 2005).

Given the histological complexity of the lesions that were being scored (including the small number of melanocytes or melanoma cells and the presence of pigment in some cores) it is perhaps unsurprising that the comparison of IHC scoring between observer 1 and observer 2 revealed a correlation that was inferior to that shown in studies of breast cancer (Tovey et al, 2005). There were however no melanoma studies with which these results could be compared as previous studies that used 2 observers scored the slides simultaneously and came to a 'consensus' score whereas other studies simply used a single observer. For future scoring of the TMA an improved inter-observer correlation may be achieved if the observers undergo a more extensive period of training. Alternative scoring systems such as the use of automated systems could also be considered (Camp et al, 2002). Another criticism of the scoring is the 'granular' nature of the scoring which is best illustrated in Figure 5.14. It is clearly seen that there is a tendency for observers to score a large number of cores as either 200 or 100 rather than values in between.

The main aims of this study were to investigate changes in expression of B-catenin, bcl-2 and galectin-3 during melanoma progression and to identify whether any of these proteins have prognostic value in primary melanoma. B-catenin is a multi-functional protein that controls a number of cell activities in both the membrane and the nucleus (Peifer et al, 2000). It binds to the cytoplasmic tail of E-cadherin and therefore has an important role in cell adhesion. The Wnt/B-catenin signalling pathway affects a number of cellular activities including proliferation, migration and differentiation (Peifer and Polakis, 2000). Activation of the pathway triggers a cascade of events within the cell resulting in stabilization of the free cytoplasmic pool of B-catenin and the translocation of this protein to the nucleus where it regulates gene transcription (Larue and Delmas 2006). Loss of B-catenin membrane expression has been associated with increased cell invasiveness although the differential expression of B-catenin during melanoma progression is controversial (Bachman et al, 2005). In this study a significant increase in membranous B-catenin expression was seen between benign naevi compared to dysplastic naevi, in-situ melanomas and primary melanomas. This is consistent with a previous study that

suggested an increase in expression between naevi and primary melanoma (Bachmann et al, 2005). The fall in expression of membranous B-catenin between primary melanomas and metastatic melanomas has not previously been described. Low membranous B-catenin expression appeared to be associated with worse outcome in this study and was an independent prognostic marker for melanoma-specific survival. These results suggest that reduced membranous expression of B-catenin may be associated with more invasive behaviour perhaps through loss of cell adhesion. It should be noted however that unlike a previous study where nuclear B-catenin was found to be prognostic (Bachmann et al, 2005) nuclear expression of B-catenin was only seen in a small number of metastatic melanomas and was absent in all other lesions. The difference in findings between these studies may in part be explained by the use of a different antibody.

Bcl-2 oncoprotein is an inhibitor of apoptotic death that is involved in the control of the intrinsic apoptotic pathway. It is thought to function principally by binding and sequestering activators of apoptosis (Letai et al, 2007). It is highly expressed in melanocytes and melanomas although its contribution to chemoresistance and prognosis is controversial (Lomuto et al, 2004). Pharmacologic reduction or targeted inactivation of bcl-2 amplifies apoptotic responses to chemotherapy in multiple *in vivo* models (Jansen et al, 1998). The fall in bcl-2 expression between primary melanomas and metastatic melanomas supports findings from previous studies (Alonso et al, 2004, Fecker et al, 2006). As a number of drugs that target bcl-2 are in advanced stages of clinical development (Letai et al, 2007) it could be argued that these therapies may be ineffective if their target is not expressed at sufficiently high levels. Interestingly, no assessment of bcl-2 expression was made prior to treatment of metastatic melanoma patients with bcl-2 antisense therapy (Bedikian et al, 2006). Our results also confirmed previous work which showed that bcl-2 has no prognostic value in patients with primary melanoma (Mikhail et al, 2005, Fecker et al, 2006).

Galectins constitute a family of widely distributed carbohydrate-binding proteins characterised by their high affinity for β-galactoside sugars and share certain

conserved elements (Vereecken et al, 2005). Galectin-3 is a chimeric molecule consisting of both carbohydrate recognition and collagen-like domains (Krzeslak et al, 2004). It is predominantly localised in the cytoplasm although may translocate to the nucleus or be secreted from the cell by ectocytosis. It has been reported to be expressed by monocytes, macrophages, and several epithelial tissues including mammary, colonic and kidney tissue and has been found to be overexpressed in several pathological conditions including human athereosclerosis and cancer (Liu and Rabinovich, 2005). Galectin-3 plays an important role in several key aspects of cancer biology including adhesion, proliferation, differentiation, angiogenesis and metastasis. (Nakahar et al, 2005). Increased expression of galectin-3 has been correlated in some studies with tumour stage and both pro- and anti- apoptotic activities of galectin-3 have been found depending on the type of tumour studied (van den Brule et al, 2004). The anti-apoptotic activity of galectin-3 is not completely understood but it is thought that it may block changes in mitochondrial potential through an effect on other apoptosis regulators including bcl-2 (Liu and Rabinovich 2005).

In this chapter, the finding of lower expression of galectin-3 in naevi compared to dysplastic naevi, in-situ melanoma and primary melanomas is consistent with a previous TMA study which suggested that galectin-3 expression may be associated with tumour progression (Prieto et al, 2006). The reduced expression of galectin-3 in metastatic melanomas also confirmed results of a previous immunohistochemistry study (Vereecken et al, 2005). The survival analysis which revealed that high nuclear galectin-3 expression is associated with an improved overall survival suggests that sequestering of galectin-3 in the nucleus may be associated with a less malignant phenotype. This finding is consistent with the requirement of export of galectin-3 from the nucleus into the cytoplasm being required for anti-apoptotic activity (Yu et al, 2002). In summary, these results suggest that galectin-3 may have an important role in melanoma pathogenesis, is an independent marker of progression and prognosis in primary melanoma and is worthy of further investigation as a potential therapeutic target.

Chapter 6 Summary

The aim of the work presented in this thesis was to conduct a number of studies that would add to our understanding of melanoma biology. An improved understanding of the molecular pathogenesis of melanoma is required in order to develop more effective prevention strategies, define new prognostic markers and to identify new molecular targets for therapy. The work in chapter 3 explored the role of MC1R in cutaneous melanoma, chapter 4 established and characterised a novel melanoma cell line and chapter 5 studied markers of melanoma progression and prognosis with newly designed melanoma TMAs.

MC1R is established as a therapeutic target in melanoma prevention (D'Orazio et al, 2006) and has been used for delivery of radiolabelled isotopes for imaging and therapy in melanoma (Raposinho et al, 2008). Recent studies have also suggested a potential role of MC1R in the response to DNA damage-induced apoptosis in melanocytes (Bohm et al, 2005, Kadekaro et al, 2005). If an 'anti-apoptotic' role of MC1R is retained by melanoma cells it could be of great relevance to cancer therapeutics as alterations to components of the apoptotic pathways are amongst the most widely recognised drug resistance mechanisms described in melanoma cells. I investigated the MC1R pathway in melanoma cell lines and explored whether manipulation of MC1R could alter the susceptibility of melanoma cells to DNA damage-induced apoptosis. Results confirmed that MC1R mRNA was expressed by all melanoma cell lines and was low or absent in non-melanoma cancer cell lines. Manipulation of MC1R with antibody, α-MSH or siRNA had no effect on melanoma proliferation or of susceptibility to DNA damage-induced apoptosis. However, the information obtained from this work did have limitations including the modest knockdown of MC1R mRNA that was seen in the siRNA studies and the lack of confirmation of knock-down at the protein level. Although MC1R has a key role in melanoma susceptibility the evidence for an important role in the control of proliferation and apoptosis in melanoma remains less convincing.

Melanoma cell lines are widely used in melanoma research although the clinical relevance of any findings can be limited by the accumulation of multiple genetic changes during growth in culture and the lack of clinical information with which to correlate findings. In this study a novel melanoma cell line was isolated and characterised. It was found that Edmel 3 displayed several properties in culture that were similar to the parent tissue from which it was derived. The relatively slow growth, the lack of pigment and the presence of two morphologically distinct populations of cells were retained by Edmel 3 both in culture and following growth as xenografts in SCID mice. It is hoped that the knowledge gained from the isolation of melanoma cells from metastatic samples will be of value if future attempts to obtain fresh primary melanoma samples can be made.

A series of tissue microarrays were designed, constructed and optimised and subsequently used for investigation of melanoma progression and prognosis. To my knowledge this is the most comprehensive melanoma TMA project undertaken to date and the first to attempt to include a cohort of primary melanoma samples that are representative of the population as a whole. The main aspects of melanoma biology that the TMA project aims to address include changes in expression of key proteins during melanoma progression and identification of novel prognostic markers. Clearly, there are a number of approaches that could be taken in deciding which proteins to investigate on the TMAs. These include focusing on key pathways, validating results on established markers and investigating novel proteins that have been implicated in other studies such as gene expression microarray. The approach that was chosen was to further investigate an established therapeutic target (bcl-2) and a marker of progression (B-catenin) and to investigate a more novel protein that has recently been implicated in melanoma pathogenesis and prognosis (galectin-3).

A number of goals have been achieved in the TMA study. Firstly, a series of TMAs have been designed and constructed that include all stages of melanoma progression. Secondly, a large number of primary melanoma samples have been included that are representative of the melanoma population as a whole. Thirdly, changes in the

expression of several key proteins (bcl-2, B-catenin and galectin-3) have been found during melanoma progression. Fourthly, a novel prognostic marker (nuclear galectin-3) has been identified in primary cutaneous melanoma.

An improvement in our ability to predict outcome from primary melanoma would be beneficial in terms of improved patient counselling, therapeutic decision-making and the design and interpretation of clinical trials. It should be recognised however that in order to be of clinical use the findings from this study would have to be validated in a separate study, a feat that it is seldom achieved in research into novel molecular markers (Becker et al, 2006). Furthermore, a number of statistical concerns have to be considered (Reviewed in McShane et al, 2005) including the use of a more stringent cut-off for level of significance given that multiple proteins are being tested. Although the association of nuclear galectin-3 expression and clinical outcome is of interest greater benefit may be derived from novel hypotheses that are generated from this study such as the investigation of nuclear galectin-3 as a potential therapeutic target.

The comprehensive nature of the design of the TMAs in this study is ideally suited to set up collaborative projects with other melanoma investigators such as the investigation of the importance of BRAF mutations in melanoma pathogenesis and the identification of biomarkers of response to MEK inhibitors in cutaneous melanoma. The characterisation of BRAF mutations in cores of melanoma tissue has not proven to be straightforward but it is hoped that ongoing improvements in the assay may lead to the successful characterisation of V600E mutations in the majority of melanoma samples. This could provide the foundation to explore in detail the relationship between the presence of BRAF mutations and activation of downstream members of the pathway including ERK and MEK with a view to identifying the best marker of pathway activation and/or response to MEK inhibition.

In conclusion, it is hoped that the work presented in this thesis combined with the results of ongoing studies may lead to an improved understanding of key molecular pathways in melanoma pathogenesis. There is great hope that an increased understanding of melanoma progression and prognosis will ultimately lead to the timely development of novel therapeutics that are desperately required for this disease.

References

Ackerman AB. Mythology and numerology in the sphere of melanoma. *Cancer* 2000; **88** (3): 491-6.

Adachi S, Nakano T, Vliagoftis H, Metcalfe DD. Receptor-mediated modulation of murine mast cell function by alpha-melanocyte stimulating hormone. *Journal of Immunology* 1999; **163** (6): 3363-3368.

AIHW (Australian Institute of Health and Welfare, Australian Association of Cancer Registries (AACR) 2003. Cancer in Australia 2000. Canberra: *AIHW* (Cancer Series no. 23).

Aitken J, Welch J, Duffy D, Milligan A, Green A, Martin N, Hayward N. CDKN2A variants in a population-based sample of Queensland families with melanoma. *Journal of the National Cancer Institute* 1999; **91** (5): 446-452.

Akslen LA, Angelini S, Straume O, Bachmann IM, Molven A, Hemminki A, Kumar R. BRAF and NRAS mutations are frequent in nodular melanoma but are not associated with tumor cell proliferation or patient survival. *The Journal of Investigative Dermatology* 2005; **125**: 312-317.

Albino AP, Vidal MJ, McNutt NS, Shea CR, Prieto VG, Nanus DM, Palmer JM, Hayward NK. Mutation and expression of the p53 gene in human malignant melanoma. *Melanoma Research* 1994; **4**: 35-45.

Alonso SR, Ortiz P, Pollan M, Rodriguez-Peralto JL. Progression in cutaneous malignant melanoma is associated with distinct expression profiles. *American Journal of Pathology* 2004; **165**: 193-203.

Amiri KI, Richmond A. Role of nuclear factor kB in melanoma. *Cancer and Metastasis Review* 2005; **24**: 301-303.

Armstrong BK, Kricker A. The epidemiology of UV induced skin cancer. *Journal of Photochemistry Photobiology B* 2001; **63**: 8-18.

Autier P. Cutaneous malignant melanoma. Facts about sunbeds and sunscreens. *Expert Review of Anticancer Therapy* 2005; **5**: 881-83.

Bachmann IM, Straume O, Puntervoll HE, Kalvenes MB, Akslen LA. Importance of P-cadherin, beta-catenin, and Wnt5a/frizzled for progression of melanocytic tumors

and prognosis in cutaneous melanoma. *Clinical Cancer Research* 2005; **11** (24): 8606-8614.

Balch CM. Cutaneous melanoma: prognosis and treatment results worldwide. *Seminars in Surgical Oncology* 1992; **8**: 400-414.

Balch CM, Buzaid AC, Atkins MB, Cascinelli N, Coit DG, Fleming ID, Houghton A Jr, Kirkwood JM, Mihm MF, Morton DL, Reintgen D, Ross MI, Sober A, Soong SJ, Thompson JA, Thompson JF, Gershenwald JE, McMasters KM. A new American Joint Committee on cancer staging system for cutaneous melanoma. *Cancer* 2000; **88**: 1484-1491.

Banerjee SS, Harris M. Morphological and immunophenotypic variations in malignant melanoma. *Histopathology* 2000; **36**: 387-402.

Barsh G, Gunn T, He L, Schlossman S, Duke-Cohan J. Biochemical and genetic studies of pigment-type switching. *Pigment Cell Research* 2000; **13** (Supp. 8): 48-53.

Becker D, Mihm M, Hewitt S, Sondak VK, Fountain JW, Thurin M. Markers and tissue resources for melanoma: meeting report. *CancerResearch* 2006; **66** (22): 10652-10657.

Beddingfield FC 3rd. The melanoma epidemic: res ipsa loquitur. *Oncologist* 2003; **8**: 459-465.

Bedikian AY, Millward M, Pehamberger H, Conry R, Gore M, Trefzer U, Pavlick AC, DeConti R, Hersh EM, Hersey P, Kirkwood JM, Haluska FG. Bcl-2 antisense (oblimersen sodium) plus dacarbazine in patients with advanced melanoma: The Oblimersen Melanoma Study Group. *Journal of Clinical Oncology* 2006; **24**: 4738-4745.

Ben-Porath I and Weinberg RA. When cells get stressed: an integrative view of cellular senescence. *Cell* 2004; **113**: 8-13.

Berger AJ, Davis DW, Tellez C, Prieto VG, Gershenwald JE, Johnson MM, Rimm DL, Bar-Eli M. Automated quantitative analysis of activator protein-2a sub cellular expression in melanoma tissue micro arrays correlates with survival prediction. *Cancer Research* 2005: **65** (23): 11185-11192.

Bertolinin A and Gessa GL. Behavioural effects of ACTH and MSH peptides. *Journal of Endocrinological Investigation* 1981; **4**: 241-251.

Berwick M, Halpern A. Melanoma epidemiology. *Current Opinion in Oncology* 1997; **9**: 178-182.

Beuret l, Flori E, Denoyelle C, Bille K, Busca R, Picardo M, Bertolotto C, Ballotti R. Upregulation of MET expression by alpha-melanocyte-stimulating hormone and MITF allows hepatocyte growth factor to protect melanocytes and melanoma cells from apoptosis. *Journal of Biological Chemistry* 2007; **282** (19): 14140-7.

Bhardwaj R, Becher E, Mahnke K, Hartmeyer M, Schwarz T, Scholzen T, Luger TA. Evidence for the differential expression of the functional alpha-melanocyte-stimulating hormone receptor MC-1 on human monocytes. *Journal of Immunology* 1997; **158** (7): 3378-3384.

Bliss JM, Ford D, Swerdlow AJ, Armstrong BK, Cristofolini M, Elmwood JM, Green A, Hollyu EA, Mack T, MacKie RM. Risk of cutaneous melanoma associated with pigmentation characteristics and freckling: systematic overview of 10 case-controlled studies. The International Melanoma Analysis Group (IMAGE). *International Journal of Cancer* 1995; **62**: 367-76.

Bohm M, Metze D, Schulte U, Becher E, Luger TA, Brzoska T. Detection of melanocortin-1 receptor antigenicity on human skin cells in culture and in situ. *Experimental Dermatology* 1999; **8** (6): 453-461.

Bohm M, Schiller M, Stander S, Seltmann H, Li Z, Brzoska T, Metze D, Schioth HB, Skottner A, Seiffert K, Zouboulis CC, Luger TA. Evidence for expression of melanocortin-1 receptor in human sebocytes in vitro and in situ. *Journal of Investigational Dermatology* 2002; **118** (3): 533-539.

Bohm M, Wolff I, Scholzen TE, Robinson SJ, Healy E, Luger TA, Schwarz T, Schwarz A. Alpha-melanocyte-stimulating hormone protects from ultraviolet radiation-induced apoptosis and DNA damage. *Journal of Biological Chemistry* 2005; **280** (7): 5795-5802.

Box NF, Duffy DL, Chen W, Stark M, Martin NG, Sturm RA. MC1R genotype modifies risk of melanoma in families segregating CDKN2A mutations. *American Journal of Human Genetics* 2001; **69** (4): 765-773.

Breslow A. Thickness, cross-sectional areas, and depth of invasion in the prognosis of cutaneous melanoma. *Annals of Surgery* 1970; **172**: 902.8.

Brown CK, Kirkwood JM. Medical management of melanoma. *Surgical Clinics of North America* 2003; **83** (2):283-322, viii.

Busca R, Berra E, Gaggioli C, Khaled M, Bille K, Marchetti B, Thyss R, Fitsialos G, Larribere L, Bertolotto C, Virolle T, Barbry P, Pouyssegur J, Ponzio G, Ballotti R. Hypoxia-inducible factor 1α is a new target of micropthalmia-associated transcription factor (MITF) in melanoma cells. *Journal of Cell Biology* 2005; **170**; 49-59.

Camp RL, Chung GG, Rimm DL. Automated subcellular localization and quantification of protein expression in tissue microarrays. *Nature Medicine* 2002; **8**: 1323-7.

Cancer Research UK cancer stats 2006. *info.cancerresearchuk.org/cancerstats*.

Castro MG, Morrison E. Post-translational processing of proopiomelanocortin in the pituitary and in the brain. *Critical Reviews in Neurobiology* 1997; **11** (1): 35-57.

Chamberlain AJ, Fritshci L, Kelly JW. Nodular melanoma: patients' perceptions of presenting features and implications for earlier detection. *Journal of the American Academy of Dermatology* 2003; **48**: 694-701.

Chen YT, Stockert E, Jungbluth A, Tsang S, Coplan KA, Scanlan MJ, Old LJ. Serological analysis of Melan-A (MART-1), a melanocyte-specific protein homogeneously expressed in human melanomas. *Proceedings of the National Academy of Science* 1996; **93**: 5915-9.

Chung KW, Yang SK, Lee GK, Kim EY, Kwon S, Lee SH, Park do J, Lee HS, Cho BY, Lee HS, Kim SW. Detection of BRAF V600E mutations in FNA specimens of thyroid nodule refines cyto-pathology diagnosis, especially in BRAF V600E mutation-prevalent area. *Clinical Endocrinology* 2006; **65** (5): 660-6.

Clark WH Jnr, Elder DE. A study of tumour progression: the precursor lesions of superficial spreading and nodular melanoma. *Human Pathology* 1984; **15**; 1147-1165.

Cone RD, Lu D, Koppula S, Vage DI, Klungland H, Boston B, Chen W, Orth DN, Pouton C, Kesterson RA. The melanocortin receptors: agonists, antagonists, and the hormonal control of pigmentation. *Recent Progress in Hormone Research* 1996; **51**: 287-317.

Covell DG, Huang R, Wallqvist A. Anticancer medicines in development: assessment of bioactivity profiles within the National Cancer Institute anticancer screening data. *Molecular Cancer Therapy* 2007; **6** (8): 2261-70.

Cui R, Widland H, Feige E, Lin JY, Wilensky DL, Igras VE, D'Orazio J, Fung CY, Schanbacher CF, Granter SR, Fisher DE. Central role for p53 in the suntan response and pathologic hyperpigmentation. *Cell* 2007; **128** (5): 853-864.

Curtin JA, Busam K, Pinkel D, Bastian BC. Somatic activation of KIT in distinct subtypes of melanoma. *Journal of Clinical Oncology* 2006; **24** (26): 4340-4346.

Curtin JA, Fridlyand J, Kageshita T, Patel HN, Busam KJ, Kutzner H, Cho KH, Aiba S, Brocker EB, LeBoit PE, Pinkel D, Bastian BC. Distinct sets of genetic alterations in melanoma. *New England Journal of Medicine* 2005; **353** (20): 2135-2147.

Dai DL, Martinka M, Li G. Prognostic significance of activated Akt expression in melanoma: A clinicopathologic study of 292 cases. *Journal of Clinical Oncology* 2005; **23** (7):1473-1482.

Damsma GE, Alt A, Brueckner F, Carell T, Cramer P. Mechanism of transcriptional stalling at cisplatin-damaged DNA. *Nature Structural and molecular biology* 2007; 1127-1133.

Davies H, Bignell GR, Cox C, Stephens P, Edkins S, Clegg S, Teague J, Woffendin H, Garnett MJ, Bottomley W, Davis N, Dicks E, Ewing R, Floyd Y, Gray K, Hall S, Hawes R, Hughes J, Kosmidou V, Menzies A, Mould C, Parker A, Stevens C, Watt S, Hooper S, Wilson R, Jayatilake H, Gusterson BA, Cooper C, Shipley J, Hargrave D, Pritchard-Jones K, Maitland N, Chenevix-Trench G, Riggins GJ, Bigner DD, Palmieri G, Cossu A, Flanagan A, Nicholson A, Ho JW, Leung SY, Yuen ST, Weber

BL, Seigler HF, Darrow TL, Paterson H, Marais R, Marshall CJ, Wooster R, Stratton MR, Futreal PA. Mutations of the BRAF gene in human cancer. *Nature* 2002; **27** (41): 949-54.

de Kogel CE, Schellens JH. Imatinib. *Oncologist* 2007; **12** (12): 1390-4.

D'Orazio JA, Nobuhisa T, Cui R, Ayra M, Spry M, Wakamatsu K, Igras V, Kunisada T, Granter SR, Nishimura EK, Ito S, Fisher DE. Topical drug rescue strategy and skin protection based on the role of Mc1r in UV-induced tanning. *Nature* 2006; **443** (21): 340-344.

Doherty V. Melanoma in Scotland. Abstracts from Sun, sex and skin cancer symposium. *Royal College of Physicians of Edinburgh* 7th April 2006.

Dumaz N, Hayward R, Martin J, Ogilvie L, Hedley D, Curtin JA, Bastian BC, Springer C, Marais R. In melanoma, RAS mutations are accompanied by switching signaling from CRAF to BRAF and altered cAMP signaling. *Cancer Research* 2006; 1; **66** (19): 9483-91.

Duval C, Regnier M, Schmidt R. Distinct melanogenic response of human melanocytes in mono-culture, in co-culture with keratinocytes and in reconstructed epidermis, to UV exposure. *Pigment Cell Research* 2001; **14** (5): 348-355.

Eggermont AM, Kirkwood JM. Re-evaluating the role of dacarbazine in metastatic melanoma: what have we learned in 30 years? *European Journal of Cancer* 2004; **40** (12): 1825-1836

Eisen T, Ahmad T, Flaherty K, Gore M, Kaye S, Marais S, Gibbens I, Hackett S, James M, Schuchter LM, Nathanson KL, Xia C, Simantov R, Schwartz B, Poulin-Costello M, O'Dwyer PJ, Ratain MJ. Sorafenib in advanced melanoma. *British Journal of Cancer* 2006; **95**: 581-586.

Elliott RJ, Szabo M, Wagner MJ, Kemp EH, MacNeil S, Haycock JW. alpha-Melanocyte-stimulating hormone, MSH 11-13 KPV and adrenocorticotropic hormone signalling in human keratinocyte cells. *Journal of Investigative Dermatology* 2004; **122** (4): 1010-1019.

Eves P, Haycock J, Layton C, Wagner M, Kemp H, Szabo, Morandini R, Ghanem G, Garcia-Borron JC, Jiminez-Cervantes C, MacNeil S. Anti-inflammatory and anti-invasive effects of alpha-melanocyte-stimulating hormone in human melanoma cells. *British Journal of Cancer* 2003; **89** (10): 2004-2015.

Eves P, MacNeil S, Haycock J. Alpha-melanocyte stimulating hormone, inflammation and human melanoma. *Peptides* 2005; **27** (2): 444-52.

Fecher LA, Cummings SD, Keefe MJ, Alani RM. Toward a molecular classification of melanoma. *Journal of Clinical Oncology* 2007; **25** (12): 1606-1620.

Fecker LF, Geilen CC, Tchernev G, Trefzer U, Assaf C, Kurbanov BM, Schwarz C, Daniel PT, Eberle J. Loss of proapoptotic Bcl-2-related multidomain proteins in primary melanomas is associated with poor prognosis. *Journal of Investigational Dermatology* 2006; **126**: 1366-1371.

Flanagan N, Healy E, Ray A, Philips S, Todd C, Jackson IJ, Birch-Machin MA, Rees JL. Pleiotropic effects of the melanocortin 1 receptor (MC1R) gene on human pigmentation. *Human Molecular Genetics* 2000; **9** (17): 2531-2537.

Frandberg PA, Doufexis M, Kapas S, Chhajlani V. Human pigmentation phenotype: a point mutation generates nonfunctional MSH receptor. *Biochemical and Biophysical Research Communications* 1998; **245** (2): 490-492.

Fredholm BB, Hokfelt T, Milligan G. G-protein coupled receptors: an update. *Acta Physiology* 2007; **190** (1): 3-7.

Friedman RJ, Rigel DS, Kopf AW. Early detection of malignant melanoma: the role of physician examination and self-examination of the skin. *CA: A Cancer Journal for Clinicians* 1985; **35**: 130-151.

Gandini S, Sera F, Cattaruzza MS, Pasquini P, Albeni D, Boyle P. Meta-analysis of risk factors for cutaneous melanoma. 1. Common and atypical naevi. *European Journal of Cancer* 2005b; **41**: 28-34.

Garraway LA, Widlund HR, Rubin MA, Getz G, Berger AJ, Ramaswamy S, Beroukhim R, Milner DA, Granter SA, Du J, Lee C, Wagner SN, Li C, Golub TR, Rimm DL, Meyerson ML, Fisher DE, Sellers WR. Integrative genomic analysis

identify MITF as a lineage survival oncogene amplified in malignant melanoma. *Nature* 2005; **436**: 117-122.

Getting SJ. Targeting melanocortin receptors as potential novel therapeutics. *Pharmacology and Therapeutics* 2006; **111** (1): 1-15.

Gilchrest BA, Eller MS, Geller AC, Yaar M. The pathogenesis of melanoma induced by ultraviolet radiation. *New England Journal of Medicine* 1999; **340**: 1341-8.

Giltnane JM, Molinaro A, Cheng H, Robinson A, Turbin D, Gelmon K, Huntsman D, Rimm DL. Comparison of quantitative immunofluorescence with conventional methods for HER2/neu testing with respect to trastuzumab therapy in metastatic breast cancer. *Archives of Pathological Laboratory Methods* 2008; **132** (10): 135-47.

Goldstein AM, Landi MT, Tsang S, Fraser MC, Munroe DJ, Tucker MA. Association of MC1R variants and risk of melanoma in melanoma prone families with CDKN2A mutations. *Cancer Epidemiology Biomarkers and Prevention* 2005; **14** (9): 2208-12.

Gordon PR, Mansur CP, Gilchrest BA. Regulation of human melanocyte growth, dendricity, and melanization by keratinocyte derived factors. *Journal of Investigational Dermatology* 1989; **92** (4): 565-572.

Hamilton A, Baulcombe D. A species of small antisense RNA in posttranscriptional gene silencing in plants. *Science* 1999; **286** (5441): 950-2.

Haqq C, Nosrati M, Sudilovsky D, Crothers J, Khodabakhsh D, Pulliam BL, Federman SW, Miller JR 3rd, Allen RE, Singer MI, Leong SP, Ljung BM, Sagebiel RW, Kashani-Sabet M. The gene expression signatures of melanoma progression. *Proceeding of the National Academy of Sciences USA* 2005; **102**: 6092-6097.

Hayward NK. Genetics of melanoma predisposition. *Oncogene* 2003; **22**: 3053-3062.

Healy E. Melanocortin 1 receptor variants, pigmentation, and skin cancer susceptibility. *Photodermatology Photoimmunology and Photomedicine* 2004; **20**: 283-288.

Healy E, Jordan SA, Budd PS, Suffolk R, Rees JL, Jackson IJ. Functional variation of MC1R alleles from red-haired individuals. *Human Molecular Genetics* 2001; **10** (21): 2397-402.

Hersey P. Adjuvant therapy for high risk primary and resected metastatic melanoma. *International Medical Journal* 2003; **33**: 33-43.

Hirobe T. Control of melanocyte proliferation and differentiation in the mouse epidermis. *Pigment Cell Research* 1992; **5**: 1-11.

Hill HZ, Hill GJ. UVA, pheomelanin and th carcinogenesis of melanoma. *Pigment Cell Research* 2000; **13** (Supplement 8): 140-144.

Hodgkinson CA, Moore KJ, Nakayama A, Steingrimsson E, Copeland NG, Jenkins NA, Arnheiter H. Mutations at the mouse microphthalmia locus are associated with defects in a gene encoding a novel basic-helix-loop-helix-zipper protein. *Cell* 1993; **74**: 395-404.

Holly EA, Aston DA, Cress RD, Ahn DK, Kristiansen JJ. Cutaneous melanoma in women. 1. Exposure to sunlight, ability to tan, and other risk factors related to ultraviolet light. *American Journal of Epidemiology* 1995; **141**: 923-33.

Hsu MY, Meier M, Herlyn M. Melanoma development and progression: a conspiracy between tumor and host. *Differentiation* 2002; **70**: 522-536.

Jansen B, Schlagbauer-Wadl H, Brown BD, Bryan RN, van Elsas A, Muller M, Wolff K, Eichler HG, Pehamberger H. bcl-2 antisense therapy chemosensitizes human melanoma in SCID mice. *Nature Medicine* 1998; **4**: 232-234.

Jhappan C, Noonan FP, Merlino G. Ultraviolet radiation and cutaneous malignant melanoma. *Oncogene* 2003; **22** (20): 3099-3112.

Kadekaro AL, Kavanagh RJ, Kanto H, Terzieva S, Hauser J, Kobayashi N, Schwemberger S, Cornelius J, Babcock G, Shertzer HG, Scott G, Abdel-Malek ZA. anti-Melanocortin and endothelin-1 activate antiapoptotic pathway and reduce DNA damage in human melanocytes. *Cancer Research* 2005; **15**: 65 (10): 4292-9.

Kadekaro AL, Kavanagh RJ, Wakamatsu K, Ito S, Pipitone MA, Abdel-Malek ZA. Cutaneous photobiology. The melanocyte vs. the sun: who will win the final round? *Pigment Cell Research* 2003; **16** (5): 434-447.

Kamangar F, Dores GM, Anderson WF. Patterns of cancer incidence, mortality, and prevelance across five continents: defining priorities to reduce cancer disparities in different geographic regions of the world. *Journal of Clinical Oncology* 2006; **10**; 24(14): 2137-2150.

Kamb A, Shattuck-Eidens D, Eeles R, Liu Q, Gruis NA, Ding W, Hussey C, Tran T, Miki Y, Weaver-Feldhaus J. Analysis of the p16 gene (CDKN2A) as a candidate for the chromosome 9p melanoma susceptibility locus. *Nature Genetics* 1994: **8** (1): 23-36.

Karasarides M, Chiloeches A, Hayward R, Niculescu-Duvaz D, Scanlon I, Friedlos F, Ogilvie L, Hedley D, Martin J, Marshall CJ, Springer CJ, Marais R. B-RAF is a therapeutic target in melanoma. *Oncogene* 2004; **23** (37); 6292-6298.

Karst AM, Dai DL, Martinka M, Li G. PUMA expression is significantly reduced in human cutaneous melanomas. *Oncogene* 2005; **24**: 1111-1116.

Kim M, Gans JD, Nogueira C, Wang A, Paik JH, Feng B, Brennan C, Hahn WC, Cordon-Cardo C, Wagner SN, Flotte TJ, Duncan LM, Granter SC, Chin L. Comparative oncogenomics identifies NEDD9 as a melanoma metastasis gene. *Cell* 2006; **125** (7): 1269-1281.

Kirkwood JM, Manola J, Ibrahim J, Sondak V, Ernstoff MS, Rao U. A pooled analysis of Eastern cooperative oncology group and intergroup trials of high-dose inteferon for melanoma. *Clinical Cancer Research* 2004; **10**: 1670-77.

Kligora CJ, Fair KP, Clem MS, Patterson JW. A comparison of melanin bleaching and azure blue counterstaining in the immunohistochemical diagnosis of malignant melanoma. *Modern Pathology* 1999; **12** (12): 1143-7.

Kluger HM, McCarthy M. XIAP is highly expressed in melanoma and is associated with chemotherapy resistance. *Journal of Clinical Oncology* 2006 ASCO Annual Meeting Proc. **24**; 18S: 8008.

Kononen J, Bubendorf L, Kallioniemi A, Barlund M, Schraml P, Leighton S, Torhorst J, Mihatsch MJ, Sauter G, Kallioniemi OP: Tissue microarrays for high-throughput molecular profiling of tumor specimens. *Nature Medicine* 1998; **4**: 844-847.

Kowalczuk CI, Priestner MC, Pearson AJ, Saunders RD, Bouffler SD. Wavelength dependence of cellular responses in human melanocytes and melanoma cells following exposure to ultraviolet radiation. *International Journal of Radiation Biology* 2006; **82** (11): 781-92.

Kraemer KH, Lee MK, Andrews AD, Lambert WC. The role of sunlight and DNA repair in melanoma and nonmelanoma skin cancer. The xeroderma pigmentosum paradox. *Archives of Dermatology* 1994; **130**: 1018-21.

Krzeslak A, Lipinska A. Galectin-3 as a multifunctional protein (Review). *Cellular and Molecular Biology Letters* 2004; **9**: 305-28.

Land EJ and Reiley PA. Spontaneous redox reactions of dopaquinone and the balance between the eumelanic and phaeomelanic pathways. *Pigment Cell Research* 2000; **13**: 273-77.

Landi MT, Bauer J, Pfeiffer RM, Elder DE, Hulley B, Minghetti P, Calista D, Kanetsky PA, Pinkel D, Bastian BC. MC1R germline variants confer risk for BRAF-mutant melanoma. *Science* 2006; **313**: 521-522.

Larue L and Delmas V. The WNT/Beta-catenin pathway in melanoma. *Frontiers of Bioscience* 2006; **11**: 733-742.

Levene A. On the histological diagnosis and prognosis of malignant melanoma. *Journal of Clinical Pathology* 1980; **22**: 101-124.

Letai AG. Diagnosing and exploiting cancer's addiction to blocks in apoptosis. *Nature reviews cancer* 2008; **8**: 121-132.

Levy C, Khaled M, Fisher DE. MITF: master regulator of melanocyte development and melanoma oncogene. *Trends in Molecular Medicine* 2006; **12** (9): 406-414.

Lin JY, Fisher DE. Melanocyte biology and skin pigmentation. *Nature* 2007; **445** (22): 843-850.

Liu FT, Rabinovich GA. Galectins as modulators of tumour progression. *Nature reviews cancer* 2005; **5**: 29-41.

Lomuto M, Calabrese P, Giuliani A. Prognostic signs in melanoma: state of the art. *Journal of the European Academy of Dermatology and Venereology* 2004; **18**: 291-300.

MacKie RM, Bray CA, Hole DJ, Morris A, Nicolson M, Evans A, Doherty V, Vestey J. Incidence of and survival from malignant melanoma in Scotland: an epidemiological study. *Lancet* 2002; **360** (9333): 587-591.

Maldonado JL, Fridlyand J, Patel H, Jain AN, Busam K, Kageshita T, Ono T, Albertson DG, Pinkel D, Bastian BC. Determinants of BRAF mutations in primary melanomas. *Journal of the National Cancer Institute* 2003; **95**; 1878-1890.

Marrett LD, King WD, Walter SD, From L. Use of host factors to identify people at high risk for cutaneous melanoma. *Canadian Medical Association Journal* 1992; **147**: 445-53.

Mayer TC. The migratory pathway of neural crest cells into the skin of mouse embryos. *Developmental Biology* 1973; **34**: 39-46.

McHugh B, Krause SA, Yu B, Deans AM, Heasman S, McLaughlin P, Heck MM. Invadolysin: a novel, conserved metalloprotease links mitotic structural rearrangements with cell migration. *Journal of Cell Biology* 2004; **167** (4): 673-686.

McShane LM, Altman D, Sauerbrei W, Taube SE, Gion M, Clark GM. Reporting recommendations for tumour marker prognostic studies. *Journal of the National Cancer Institute* 2005; **97** (16): 1180-1184.

Menon IA, Persad S, Ranadive NS, Haberman HF. Effects of ultraviolet-visible irradiation in the presence of melanin isolated from human black or red hair upon Ehrlich ascites carcinoma cells. *Cancer Research* 1983; **43** (7): 3165-3169.

Meyskens FL, Farmer PJ, Anton-Culver H. Etiologic pathogenesis of melanoma: a unifying hypothesis for the missing attributable risk. *Clinical Cancer Research* 2004; **10**: 2581-83.

Michell DL, Jen J, Cleaver JE. Relative induction of cyclobutane dimers and cytosine photohydrates in DNA irradiated in vitro and in vivo with ultraviolet-C and ultraviolet-B light. *Journal of Photochemistry and Photobiology* 1991; **54**; 741-746.

Mikhail M, Velaquez E, Shapiro R, Berman R, Pavlick A, Sorhaindo L, Spira J, Mir C, Panageas KS, Polsky D, Osman I. PTEN expression in melanoma: Relationship with patient survival, bcl-2 expression and proliferation. *Clinical Cancer Research* 2005; **11** (14): 5153-5157.

Miller AJ, Mihm MC. Melanoma. *New England Journal of Medicine* 2006; **355**: 51-65.

Millward MJ, Bedikian AY, Coury RM. Randomized multinational phase 3 trial of dacarbazine (DTIC) with or without Bcl-2 antisense (oblimersen sodium) in patients with advanced malignant melanoma: Analysis of long-term survival. New Orleans: *ASCO*, 2004: **708** (abstr 7505).

Mogil JS, Ritchie J, Smith SB, Strasburg K, Kaplan L, Wallace MR, Romberg RR, Bijl H, Sarton EY, Fillingim RB, Dahan A. Melanocortin-1 receptor gene variants affect pain and mu-opioid analgesia in mice and humans. *Journal of Medical Genetics* 2005; **42** (7): 583-587.

Morton DL, Wen DR, Wong JH, Economou JS, Cagle LA, Storm FK, Foshag LJ, Cochran AJ. Technical details of intraoperative lymphatic mapping for early stage melanoma. *Archives of Surgery* 1992; **127** (4): 392-9.

Mountjoy KG, Robbins LS, Mortrud MT, Cone RD. The cloning of a family of genes that encode the melanocortin receptors. *Science* 1992; **257**: 1248-1251.

Murata H, Ashida A, Takata M, Yamaura M, Bastian BC, Saida T. Establishment of a novel melanoma cell line SMYM-PRGP showing cytogenetic and biological charcteristics of the radial growth phase of acral melanomas. *Cancer Science* 2007; **98**; 7: 958-963.

Nakahara S, Oka N, Raz A. On the role of galectin-3 in cancer apoptosis. *Apoptosis* 2005; **10**: 267-75.

NCI (National Cancer Institute). Surveillance epidemiology and end results. http://seer.cancer.gov/faststats/selections.php. 2008.

Nelson MA, Reynolds SH, Rao UN, Goulet AC, Feng Y, Beas A, Honchak B, Averill J, Lowry DT, Senft JR, Jefferson AM, Jophnson RC, Sargent LM. Increased copy number of the transcription factor E2F1 in malignant melanoma. *Cancer Biology and Therapy* 2006; **5**; 407-412.

Newton Bishop JA, Gruis NA. Genetics: what advice for patients who present with a family history of melanoma? *Seminars in Oncology* 2007; **34**: 452-9.

Oetting WS, Fryer JP, Shriram S, King RA. Occulocutaneous albinism type 1; the last 100 years. *Pigment Cell Research.* **16**; 307-311.

Orchard GE. Comparison of immunohistochemical labelling of melanocyte differentiation antibodies melan-A, tyrosinase and HMB 45 with NKIC3 and S100 protein in the evaluation of benign naevi and malignant melanoma. *Histochemistry Journal* 2000; **32**: 475-81.

Pacifico MD, Grover R, Richman PI, Daley FM, Buffa F, Wilson GD. CD44v3 levels in primary cutaneous melanoma are predictive of prognosis: assessment by the use of tissue microarray. *International Journal of Cancer* 2006; **118** (6): 1460-4.

Pacifico MD, Grover R, Richman PI, Buffa F, Daley FM, Wilson GD. nm23 as a prognostic marker in primary cutaneous melanoma: evaluation using tissue microarray in a patient group with long-term follow-up. *Melanoma Research* 2005; **15** (5): 435-40.

Pacifico MD, Grover R, Richman PI, Daley FM, Buffa F, Wilson GD. Development of a tissue array for primary melanoma with long-term follow-up: discovering melanoma cell adhesion molecule as an important prognostic marker. *Plastic and Reconstructive Surgery* 2005; **115** (2): 367-375.

Packer L, Pavey S, Parker A, Stark M, Johansson P, Clarke B, Pollock P, Ringner M, Hayward N. Osteopontin is a downstream effector of the PI3-kinase pathway in melanomas that is inversely correlated with functional PTEN. *Carcinogenesis* 2006; **209**: 1-36.

Palmer JS, Duffy DL, Box NF, Aitken JF, O'Gorman LE, Green AC, Hayward NK, Martin NG, Sturm RA. Melanocortin-1 receptor polymorphisms and risk of melanoma: is the association explained solely by pigmentation phenotype? *American Journal of Human Genetics* 2000; **66**(1): 176-186.

Panka DJ, Atkins MB, Mier JW. Targeting the mitogen-activated protein kinase pathway in the treatment of malignant melanoma. *Clinical Cancer Research* 2006; **12**: 2371-2375.

Pelfer M and Polakis P. Wnt signalling in oncogenesis and embryogenesis – a look outside the nucleus. *Science* 2000; **287**: 1606-1609.

Plattenberg A, Ballaun C, Pammer J, Mildner M, Strunk D, Weininger W, Tschachier E. Human melanocytes and melanoma cells constitutively express the Bcl-2 proto-oncogene in situ and in cell culture. *American Journal of Pathology* 1995; **146** (3): 51-9.

Polska D, Bastian BC, Hazan C, Meizer K, Pack J, Houghton A, Busam K, Cordon-Cardo C, Osman I. HDM2 protein overexpression, but not gene amplification, is related to tumorigenesis of cutaneous melanoma. *Cancer Research* 2001; **61**: 7642-7646.

Povey JE, Darakhshan F, Robertson K, Bisset Y, Mekky M, Rees J, Doherty V, Kavanagh G, Anderson N, Campbell H, MacKie RM, Melton DW. DNA repair gene polymorphisms and genetic predisposition to cutaneous melanoma. *Carcinogenesis* 2007; **28** (5): 1087-93.

Prieto VG, Mourad-Zeidan AA, Melinikova V, Johnson MM, Lopez A, Diwan AH, Lazar AJ, Shen SS, Zhang PS, Reed JA, Gershenwald JE, Raz A, Bar-Eli M. Galectin-3 expression is associated wuth tumor progression and pattern of sun exposure in melanoma. *Clinical Cancer Research.* 2006; **15**; 12 (22): 6709-15.

Prota G. Melanins, melanogenesis and melanocytes: looking at their functional significance from the chemist's viewpoint. *Pigment Cell Research* 2000; **13**: 283-293.

Raposinho PD, Correia JD, Alves S, Botelho MF, Santos AC, Santos I. A (99m)Tc(CO)(3)-labeled pyrazoyl-alpha-MSH analog conjugate for melanoma targeting. *Nuclear Medicine and Biology* 2008; **35** (1): 91-9.

Rana BK. High polymorphism at the human melanocortin-1receptor locus. *Genetics* 1999; **151**: 1547-1557.

Rangel J, Nosrati M, Shaikh L, Leong SP, Haqq C, Miller JR 3rd, Sagebiel RW, Kashani-Sabet M. Osteopontin as a molecular prognostic marker for melanoma. *Cancer* 2008; **112**: 144-150.

Rangel J, Torabian S, Shaikh L, Leong SP, Haqq C, Miller JR 3rd, Sagebiel RW, Kashani-Sabet M. Prognostic significance of nuclear receptor over expression in primary cutaneous melanoma. *Journal of Clinical Oncology* 2006; **2** (28): 4565-569.

Robbins LS, Nadeau JH, Johnson KR, Kelly MA, Roselli-Rehfuss L, Baack E, Mountjoy KG, Cone RD. Pigmentation phenotypes of variant extension locus alleles result from point mutations that alter MSH receptor function. *Cell* 1993; **72** (6): 827-834.

Roberts DL, Anstey AV, Barlow RJ, Cox NH, Newton Bishop JA, Corrie PG. UK guidelines for the management of cutaneous melanoma. *British Journal of Dermatology* 2002; **146**: 7-17.

Robinson SJ, Healy E. Human melanocortin 1 receptor (MC1R) gene variants alter melanoma cell growth and adhesion to extracellular matrix. *Oncogene* 2002; **21** (52): 8037-8046.

Rodolfo M, Daniotti M, Vallacchi V. Genetic progression of metastatic melanoma. *Cancer letters* 2004; **214**: 133-147.

Rouzaud F, Annereau JP, Valencia JC, Costin GE, Hearing VJ. Regulation of melanocortin 1 receptor expression at the mRNA and protein levels by its natural agonist and antagonist. *FASEB Journal* 2003; **17** (14): 2154-6.

Royal College of Pathologists. Standards and minimum datasets for reporting skin cancers. 2002. www.rcpath.org/resources/pdf/skincancers2802.pdf

Runger TM, Vergilis I, Sarkar P, DePinho RA, Sharpless NE. How disruption of cell cycle regulating genes might predispose to sun-induced skin cancer. *Cell Cycle* 2005; **4**; 5: 643-645.

Salazar-Onfray F, Lopez M, Lundqvist A, Aguirre A, Escobar A, Serrano A, Korenblit C, Petersson M, Chhajiani V, Larsson O, Kiessling R. Tissue distribution and differential expression of melanocortin 1 receptor, a malignant melanoma marker. *British Journal of Cancer* 2002; **87** (4): 414-422.

Sanchez Mas J, Olivares Sanchez C, Ghanem G, Haycock J, Teruel JA, Garcia-Borron JC, Jiminez-Cervantes C. Loss-of-function variants of the human melanocortin-1 receptor gene in melanoma cells define structural determinants of receptor function. *European Journal of Biochemistry* 2002; **269**: 6133-6141.

Sarkar-Agrawal P, Vergilis I, Sharpless NE, DePinho RA, Runger TM. Impaired processing of DNA photoproducts and ultraviolet hypermutability with loss of p16INK4a or p19ARF. *Journal of the National Cancer Institute* 2004; **96**: 1790-1793.

Sauter ER, Yeo UC, von Stemm A, Zhu W, Litwin S, Tichansky DS, Pistritto G, Nesbit M, Pinkel D, Herlyn M, Bastian BC. Cyclin D1 is a candidate ongogene in cutnaeous melanoma. *Cancer Research* 2002; **62**: 3200-3206.

Schauer E. Proopiomelanocortin-derived peptides are synthesized and released by human keratinocytes. *Journal of Clinical Investigation* 1994; **93**: 2258-2262.

Schioth HB, Phillips S, Rudzish R, Birch-Machin M, Wikberg J, Rees JL. Loss of function mutations of the human melanocortin-1 receptor are common and associated with red hair. *Biochemical and Biophysical research Communications* 1999; **260**: 488-491.

Scott MC, Wakamatsu K, Ito S, Kadekaro AL, Kobayashi N, Groden J, Kavanagh R, Takakuwa T, Virador V, Hearing VJ, Abdel-Malek ZA. Human melanocortin 1 receptor variants, receptor function and melanocyte response to ultraviolet radiation. *Journal of Cell Science* 2002; **115**: 2349-2355.

Schmitt CA, Rosenthal CT, Lowe SW. Genetic analysis of chemoresistance in primary murine melanomas. *Nature Medicine* 2000; **6**: 1029-35.

Scott MC, Suzuki I, Abdel-Malek ZA. Regulation of the human melanocortin-1 receptor expression in epidermal melanocytes by paracrine and endocrine factors and by ultraviolet raqdiation. *Pigment Cell Research* 2002; **15**: 433-439.

Sequist LV, Bell DW, Lynch TJ, Haber DA. Molecular predictors of response to epidermal growth factor receptor antagonists in non-small-cell lung cancer. *Journal of Clinical Oncology* 2007; **25** (5): 587-95.

Serrone L, Hersey P. The chemoresistance of human malignant melanoma: an update. *Melanoma Research.* 1999; **9**: 51-58.

Singluff CL, Seigler HF. 'Thin' malignant melanoma: risk factors and clinical management. *Annals of Plastic Surgery* 1992; **28**: 89-94.

Smalley K, Eisen T. The involvement of p38 mitogen-activated protein kinase in the alpha-melanocyte stimulating hormone (alpha-MSH)-induced melanogenic and anti-proliferative effects in B16 murine melanoma cells. *FEBS Letters* 2000; **476** (3): 198-202.

Soengas MS, Capodieci P, Polsky D, Mora J, Esteller M, Opitz-Araya X, McCombie R, Herman JG, Gerald WL, Lazebnik YA, Cordón-Cardó C, Lowe SW. Inactivation of the apoptosis effector Apaf-1 in malignant melanoma. *Nature* 2001; **409**: 207-11.

Soengas MS, Lowe S. Apoptosis and melanoma chemoresistance. *Oncogene* 2003; **22**: 3138-3151.

Stander S, Bohm M, Brzoska T, Zimmer KP, Luger T, Metze D. Expression of melanocortin-1 receptor in normal, malformed and neoplastic skin glands and hair follicles. *Experimental Dermatology* 2002; **11** (1): 42-51.

Sturm RA. Skin colour and skin cancer - MC1R, the genetic link. *Melanoma Research* 2002; **12** (5): 405-416.

Sundram U, Harvell JD, Rouse RV. Expresion of the B-cell proliferation marker MUM1 by melanocytic lesions and comparison with S100, gp100 (HMB45), and Melan A. *Modern Pathology* 2003; **16**: 802-810.

Takeuchi S, Zhang W, Wakamatsu K, Ito S, Hearing VJ, Kraemer KH, Brash DE. Melanin acts as a potent UVB photosensitizer to cause an atypical mode of cell death

in murine skin. *Proceedings of the National Academy of Sciences* 2004; **101** (42): 15076-81.

Thomas NE, Berwick M, Cordeiro-Stone M. Could BRAF mutations in melanocytic lesions arise from DNA damage induced by ultraviolet radiation? *Journal of Investgative Dermatology* 2006; **126**: 1693-1696.

Thompson JF, Scolyer RA, Kefford RF. Cutaneous Melanoma. *The Lancet* 2005; **365**: 687-700.

Torhost J, Bucher C, Kononen J, Haas P, Zuber M, Kochli ORE, Mross F, Dieterich H, Moch H, Mihatsch M, Kallioniemi OP, Sauter G. Tissue microarrays for rapid linking of molecular changes to clinical endpoints. *American Journal of Pathology* 2001; **159**: 2249-2256.

Tovey S, Dunne B, Witton CJ, Forsyth A, Cooke TG, Bartlett JM. Can molecular markers predict when to implement treatment with aromatase inhibitors in invasive breast cancer. *Clinical Cancer Research* 2005; **11** (13): 4835-4841.

Tsao H, Atkins MB, Sober AJ. Management of cutaneous melanoma. *New England Journal of Medicine* 2004; **351** (10): 998-1012.

Tsavachidou D, Coleman ML, Athanasiadis G, Li S, Licht JD, Olson MF, Weber BL. SPRY2 is an inhibitor of the ras/extracellular signal-regulated kinase pathway in melanocytes and melanoma cells with wild-type BRAF but not with the V599E mutant. *Cancer Research* 2004; **64**: 5556-5559.

Uribe P, Andrade L, Gonzalez S. Lack of association between BRAF mutation and MAPK ERK activation in melanocytic naevi. *Journal of Investigative Dermatology* 2006; **126**: 1561-166.

Van den Brule F, Califice SW, Castronovo V. Expression of galectins in cancer: a critical review. *Glycoconjugate journal* 2004; **19**: 537-542.

Vereecken P, Debray C, Petein M, Awada A, Lalmand MC, Laporte M, Van Den Heule B, Verhest A, Pochet R, Heenen M. Expression of galectin-3 in primary and metastatic melanoma: immunohistochemical studies on human lesions and nude mice xenograft tumours. *Archives of Dermatological Research* 2005; **296**: 353-358.

Voisey J, Carrol L, van Daal A. Melanocortins and their receptors and antagonists. *Current Drug Targets* 2003; **4**: 586-597.

Wei ML. Hermansky-Pudlak syndrome: a disease of protein trafficking and organelle function. *Pigment Cell Research.* 2006; **16**: 19-42.

Wei Q, Lee JE, Gershenwald JE, Ross MI, Mansfield PF, Strom SS, Wang LE, Guo Z, Qiao Y, Amos CI, Spitz MR, Duvic M. Repair of UV light-induced DNA damage and risk of cutaneous malignant melanoma. *Journal of the National Cancer Institute.* 2003; **95**: 308-315.

Westerdahl J, Olsson H, Masback A, Ingvar C, Jonsson N, Brandt L. Use of sunbeds or sunlamps and malignant melanoma in southern Sweden. *American Journal of Epidemiology* 1994; **140**: 691-9.

Wheatley K. Interferon-alpha as adjuvant therapy for melanoma: an individual patient meta-analysis of randomised trials [abstract]. *Journal of Clinical Oncology* 2007; **25**: (18S): 8526.

Whiteman DC, Whiteman CA, Green AC. Childhood sun exposure as a risk factor for melanoma: a systematic review of epidemiological studies. *Cancer Causes Control* 2001; **12**: 69-82.

Wilberg JE, Muceniece R, Mandika I, Prusis P, Lindblom J, Post C, Skottner A. New aspects of the melanocortins and their receptors. *Pharmacology Research* 2000; **42**: 393-420.

Winnepenninckx V, Lazar V, Michiels S, Dessen P, Stas M, Alonso SR, Avril MF, Ortiz Romero PL, Robert T, Balacescu O, Eggermont AM, Lenoir G, Sarasin A, Tursz T, van den Oord JJ, Spatz A. Gene expression profiling of primary cutaneous melanoma and clinical outcome. *Journal of the National Cancer Institute* 2006; **98** (7): 472-482.

Wolfel T, Hauer M, Schneider J, Serrano M, Wolfel C, Kiehmann-Hieb E, De Plaen E, Hankeln T, Meyer zum Buschenfelde KH, Beach D. A p16INK4a-insensitive CDK4 mutant targeted by cytolytic T lymphocytes in a human melanoma. *Science* 1995; **269**: 1281-1284.

Wu H, Goel V, Haluska FG. PTEN signalling pathways in melanoma. *Oncogene* 2003; **22**: 3113-3122.

Xia Y, Wikberg JE, Chhajlani V. Expression of melanocortin 1 receptor in periaqueductal gray matter. *Neuroreport* 1995; **6** (16): 2193-2196.

Xu L, Begum S, Hearn JD, Hynes RO. GPR56, an atypical G protein-coupled receptor, binds tissue transglutaminase, TG2, and inhibits melanoma tumour growth and metastasis. *Proceedings of the National Academy of Sciences USA* 2006; **103** (24): 9023-9028.

Yu F, Finley RL, Razz A, Kim HR. Galectin-3 translocates to the perinuclear membrane and inhibits cytochrome c release from the mitochondria. A role for synexin in galectin-3 translocation. *Journal of Biological Chemistry* 2002; **277**: 15819-15827.

Zhu N, Lalla R, Eves P, Brown TL, King A, Kemp EH, Haycock JW, MacNeil S. Melanoma cell migration is upregulated by tumour necrosis factor-alpha and suppressed by alpha-melanocyte-stimulating hormone. *British Journal of Cancer* 2004; **90** (7): 1457-63.

Zuo L, Weger J, Yang Q, Goldstein AM, Tucker MA, Walker GJ, Hayward N, Dracopoli NC. Germline mutations in the p16INK4a binding domain of CDK4 in familial melanoma. *Nature Genetics* 1996; **12** (1): 97-99.